

UNCLASSIFIED

AD 407 071

DEFENSE DOCUMENTATION CENTER

FOR

SCIENTIFIC AND TECHNICAL INFORMATION

CAMERON STATION, ALEXANDRIA, VIRGINIA



UNCLASSIFIED

NOTICE: When government or other drawings, specifications or other data are used for any purpose other than in connection with a definitely related government procurement operation, the U. S. Government thereby incurs no responsibility, nor any obligation whatsoever; and the fact that the Government may have formulated, furnished, or in any way supplied the said drawings, specifications, or other data is not to be regarded by implication or otherwise as in any manner licensing the holder or any other person or corporation, or conveying any rights or permission to manufacture, use or sell any patented invention that may in any way be related thereto.

407 071

INSTITUTE OF AEROPHYSICS

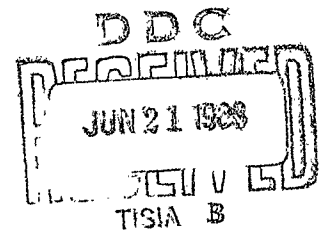
UNIVERSITY OF TORONTO

AN INVESTIGATION OF THE FATIGUE OF ALUMINUM ALLOY
DUE TO RANDOM LOADING

by

S. R. Swanson

CATALOGED BY DDC
AS AD No. 407071



FEBRUARY, 1963

UTIA REPORT NO. 84

AN INVESTIGATION OF THE FATIGUE OF ALUMINUM ALLOY
DUE TO RANDOM LOADING

by

S. R. Swanson

FEBRUARY, 1963

UTIA REPORT NO. 84

ACKNOWLEDGEMENT

The opportunity to carry out this research was generously extended to the author by the Director of the Institute, Dr. G. N. Patterson.

The continuous and valuable supervision given by Professor E. D. Poppleton, now at the University of Sydney, Australia, is heartily acknowledged.

The author also wishes to thank Professor H. S. Ribner, for his guidance and review of the final manuscript.

This project was supported by the United States Air Force Office of Scientific Research of the Air Research and Development Command under Contract No. AF 49(638)-548.

The author is deeply grateful to the deHavilland Aircraft of Canada Limited for financial assistance throughout the period of the project, and to various members of this firm who were responsible for this gesture and to those who have since helped with the many different aspects of the program.

SUMMARY

A study of the aluminum alloy 2024-T4 under random and constant amplitude axial fatigue loading was undertaken using 1500 unnotched extruded bar specimens. In the constant amplitude test series, it was discovered that the stress amplitude - endurance (S-N) relation is well represented by two separate failure distributions such that, as the stress amplitude is lowered, the one distribution recedes while the other distribution becomes predominant. The knee of the S-N curve is then considered as a transition from endurances predominantly of the one distribution to endurances predominantly of the other.

A series of two-level "single-jump" constant amplitude tests were also carried out. It was found that for the low pre-stress - high test stress tests, the linear rule of cumulative damage could be used, while for the high pre-stress - low 'runout' stress tests, the ideas of Corten and Dolan appear to work well.

In order to apply random amplitude loads to specimens, a fatigue machine was specially designed, having a 600 lb electromagnetic shaker driven by random noise as its prime mover. By placing a lever between the shaker and the gripping jaws for the specimen, it was possible to apply large Rayleigh peak distribution fatigue loadings to the specimens.

When the test results were compared with various cumulative damage theories, it was found that the linear rule of cumulative damage was entirely inadequate and unsafe. The best representations of the Rayleigh endurance curve were obtained using Freudenthal's rule and Fuller's rule. An attempt to obtain a Rayleigh prediction from the application of the linear law to the two distribution interpretation of the S-N curve was only partially successful.

By adding a second lever to the machine, it was possible to test using the complex wave obtained when two degrees of freedom are randomly excited. Fuller's rule, modified to some extent, gave reasonable predictions of the resulting endurance at the intermediate RMS levels.

After the above series of fatigue tests were carried out, with the RMS stress level held constant to failure, a number of single degree-of-freedom tests were performed using a "program" of RMS levels obtained from random numbers. These test histories were called Quasi-Stationary Random Fatigue. While most of these tests were performed using a rectangular distribution of RMS stress, a few tests were performed using truncated Gaussian and truncated Exponential distributions. Fuller's method, suitably modified, resulted in a fairly good prediction of the test results, while Freudenthal's rule and the linear law were quite unconservative. A new technique for prediction based on a linear summation of "cycle ratios" of RMS stress, and using the experimental Rayleigh endurance relation is

suggested, and this gives fair results for programmed RMS tests of this type.

An interesting series of tests were conducted to obtain the constant amplitude S-N relation with specimens having fixed amounts of random preloading. In all cases the random preloading resulted in a uniform translation, at all but the lowest stress levels, of the virgin S-N curve to lower endurance.

A significant observation from the random load tests has been the appearance of visible secondary cracks on the unnotched axially-loaded specimens. The number of these cracks increases by orders of magnitude as the RMS level increases for a given load configuration. Also the number of cracks other than the failure crack is greater with complex-wave (two-lever) loading than with the single lever, and greatest with the quasi-stationary type of loading. This effect was not found to any appreciable extent in any constant amplitude tests except in a small series of specimens tested with a very large fluctuating compression loading. It was not determined if the secondary cracking was from the same mechanism in the fluctuating compression tests, as in the random tests.

TABLE OF CONTENTS

	<u>Page</u>
NOTATION	vii
I. INTRODUCTION	1
II. ANALYSIS OF THE CONSTANT AMPLITUDE FATIGUE DATA	2
2.1 Introduction	2
2.2 Regression of Test Results	3
2.3 Comparison with Other Sources	4
2.4 The log-log Slope Parameter δ	5
2.5 The 'Bimodal' Phenomenon	5
III. STATIONARY RANDOM (RAYLEIGH) TESTS	10
3.1 Introduction	10
3.2 Test Results	11
3.3 The Linear Law of Damage Accumulation	13
3.3.1 Log-Log Presentation	13
3.3.2 Linear Damage Accumulation with Two Distributions	13
3.4 Freudenthal's Prediction of Endurance	16
3.5 Fuller's Predicted Endurance Line	17
IV. STATIONARY RANDOM (COMPLEX WAVE) FATIGUE	19
4.1 Introduction	19
4.2 Evaluation of Spectral Quantities	20
4.3 Test Results	25
4.4 Application of Cumulative Damage Laws	26
4.4.1 The Linear Law	26
4.4.2 Fuller's Technique	28
4.4.3 Results of Cumulative Damage Analyses	28
V. QUASI STATIONARY RANDOM AMPLITUDE FATIGUE	28
5.1 Introduction	28
5.2 The Rectangular Distribution	30
5.3 Test Results - Rectangular Distribution	32
5.4 Cumulative Damage - Rectangular Distribution	32
5.4.1 The Linear or Miner Law	32
5.4.2 Fuller's Method	33
5.4.3 Freudenthal's Method	34
5.4.4 Life Prediction Using Units of RMS Stress	35
5.5 Tests with Other Distributions	35
5.5.1 Transformations to Other Distributions	35
5.5.2 Tests with the Truncated Gaussian and Truncated Exponential QS Distribution	36
5.5.3 Arbitrary Distribution of RMS Levels	37

	<u>Page</u>
VI. ENDURANCE BEHAVIOR WITH CONSTANT AND RANDOM AMPLITUDE PRELOAD	39
6.1 Introduction	39
6.2 Endurance Behavior with Constant Amplitude Preload	39
6.2.1 Low Prestress - High Test Stress Results	40
6.2.2 High Prestress - Low Test Stress Results	41
6.3 Constant Amplitude Endurance Behaviour with Random Preload	43
6.3.1 Introduction	43
6.3.2 Evaluation of the Maximum Stress Peak S_1 from the Slope of the $S_2 - N$ Curve	44
6.3.3 Intuitive Values of S_1 from the Probability of Occurrences	48
6.4 Discussion of Partial Damage Results	50
VII. CONCLUDING REMARKS	51
REFERENCES	55
APPENDIX A - The Random Load Fatigue Machine	60
APPENDIX B - Discussion of Principles and Terminology Used in the Report	68
TABLES	
FIGURES	

NOTATION

T. N. 35	UTIA Technical Note No. 35, which contains a substantial amount of the constant amplitude test data used in this report (Ref. 1).
ANC-5	"Strength of Metal Aircraft Elements", used jointly by the U. S. Departments of the Air Force, the Navy and Commerce, March, 1955.
kcs	thousands of cycles (fatigue)
ksi	thousands of pounds per square inch (unit of stress)
CG	centre of gravity
CA	constant stress amplitude
RA	random stress amplitude
VA	variable stress amplitude
CD	cumulative fatigue damage
QS	Quasi.- stationary (random process)
S-N	general expression used to denote the stress-amplitude, logarithm-of-endurance relation in fatigue
RMS	root mean square
UTS	ultimate tensile strength
STF	short term fatigue (Section 2.5)
LTF	long term fatigue (Section 2.5)
a	exponent governing rate of increase of crack propagation with number of cycles (Section VI); also distance from lever fulcrum to specimen axis on the fatigue machine (Appendix A), inches
b	curve-fitting constant in expression for STF line (Section II)
c	curve-fitting factor for expression used to define LTF line (Section II); also cycles

d	slope parameter of fictitious S-N curve used in the Corten-Dolan hypothesis, i. e, change in log N divided by (-change in log S); also curve-fitting constant in exponent of expression for LTF line (Section II)
e	base of natural logs (2.7183)
f	frequency, cps (Section IV)
f_1, f_2	number of degrees of freedom, used in comparing two stochastically independent sets of observations containing n_1 and n_2 items respectively (Ref. 48, page, 395)
g	gravity units of acceleration
g, h	parameters used in assessing linear cumulative damage with two semilog-linear endurance relations, for a Rayleigh loading spectrum (Section III)
i	statistical order number in ranked data
k_d, k_{sp}, k_h	stiffness, pounds per inch (Appendix A), of the driver coil, the specimens and the gripping jaws respectively.
k_f	effective stiffness of the single-lever configuration of the fatigue machine for purposes of specifying resonance (Appendix A).
m	slope of straight line obtained by a linear regression analysis of data by least squares (Section II); also number of initial active crack nuclei formed in a fatigue process (Section VI).
n	number of specimens in a sample; also number of fatigue cycles endured
p, p_i	probability density function, and proportion of test time spent at a given RMS stress level (Section V), respectively.
r	coefficient of crack propagation, modified by the occurrence of a maximum stress peak during crack initiation (Section VI). Also correlation coefficient for least squares linear regression analysis (Section II), and proportion of negative-valued maxima in a stress history (Section IV).
r_d, r_f	damping constants for the driver coil and shaker table flexures - see Ref. 50
s	seconds (time)

t_1	duration of preload fatigue cycles (Section VI), minutes
w	power spectral density function (Section IV)
x	symbol used to denote a variable integration limit
x_T	displacement at the shaker table, inches (Appendix A)
D	fatigue damage parameter used in Section VI
F_{sp}	force or load, lb, applied to the specimen in the fatigue machine (Appendix A)
G	maximum permissible shaker table acceleration in meter/sec/sec (Appendix A)
I_d	current, amperes, applied to the shaker driven coil (constant amplitude) - see Appendix A
K, K_t	factor used to obtain equivalent truncated distributions from asymptotic distributions (Section V); also number of turns in an electro-mechanical transformer representing the shaker (Appendix A); theoretical stress concentration factor, respectively
K_v	slope of line representing a variable amplitude endurance relation, using a semilog (S-logN) plot
K_{SN}	slope of basic S-N (Stress-log endurance) relation in Fuller's hypothesis.
K_σ or K_{RMS}	slope of line representing Fuller's prediction of VA endurance using the semilog (σ -log N) plot
K_{σ_p}	Fuller's slope for the line predicting fatigue endurance using the semilog (σ_p - log N) grid
$K(g, \sigma),$ $K(g^1, \sigma)$	terms used in the application of the linear cumulative damage law to two distributions (STF and LTF) (Section III)
L	distance from shaker table axis to lever fulcrum, inches
L_1, L_2	First (main) lever, second lever
M	equivalent mass of mechanical system under vibration, for purposes of defining resonance (Appendix A)
N	number of observations (Section II), also number of cycles to failure

N_f, N_g	total number of cycles to failure in a fatigue test
N_{ge}, N_{gt}	cycles to failure of specimen under variable amplitude loading obtained experimentally, and the theoretical prediction, respectively, in the Corten-Dolan hypothesis (Section VI).
N_{fr}	Number of cycles to failure using random amplitude loading
N_{O+}	number of zero crossings with positive slope for a stress history per second, on the average
N_1	number of peaks in a stress history per second, on the average
P, P_i	cumulative probability function (general), and specifically for the i^{th} item to fail, respectively.
$R, R^{1/a}$	irregularity factor (N_{O+} / N_1) used in Section IV, and the Corten-Dolan stress interaction parameter used in Section VI, respectively
$R(b, \sigma)$	term used to denote the analytical endurance relation obtained when the linear cumulative damage rule is applied to the STF endurance line (Section III)
S, S_a, S_m	stress amplitude ksi, alternating stress amplitude, and mean stress amplitude respectively
S_0, S_1, S_2	datum stress amplitude, peak or maximum stress amplitude achieved, and runout stress amplitude respectively (Section VI)
$T, T_{\text{exp}}, T_F, T_F^1$	life or duration of a fatigue test in seconds; actual, experimental, predicted by the linear law, and predicted by Freudenthal's theory respectively
V_d	voltage applied to the shaker driven coil (peak, constant amplitude)
α	weighting factor for two-distribution cumulative damage analysis (Section III); also proportion of preload cycles in a two-step test (Section VI)
β	Fuller's distribution parameter in VA cumulative damage analysis, also factor in exponent used in the expression for the weighting function α .
δ, ν	slope of the straight line used to represent the log S-logN relation, measured similarly to d

ϵ	complex wave spectrum-width parameter (Section IV)
η	non-dimensional peak stress amplitude (Section IV)
μ	crack nucleii parameter discussed in Section VI and Ref. 34.
ρ	Slope of straight line suggested by Freudenthal for endurance under Rayleigh loading (Section III); also derived crack growth rate parameter used in Section VI.
σ	RMS stress amplitude, ksi
σ_p	RMS stress peaks, ksi
σ', σ''	first and second derivatives of RMS stress respectively, with time
ω	Freudenthal's stress interaction parameter
Γ, Γ_x	the complete, and incomplete gamma function, respectively.
Δ	damage function discussed in Section VI and Ref. 34.
Σ	symbol used to denote summation
$\psi_0, \psi_0'', \psi_0^{(4)}$	Rice's notation (Ref. 39) for the spectral distribution functions defined in Section IV. Note that $\psi_0^{1/2} = \sigma$

Subscripts

a	alternating
mean	mean value
p	peak or maximum

Superscripts

\wedge	hat symbol is used to denote peak values
$\bar{}$	bar symbol is used to denote mean values
"	inches

I. INTRODUCTION

This report describes an investigation into the nature of fatigue damage when a typical metal is subjected to random loading. It is now becoming increasingly evident that actual service loadings for a wide variety of structures - aircraft, engines, turbines, farm machinery, road vehicles, railway rolling stock etc. - can be simulated satisfactorily by random-process - generated load histories. In the past there seems to have been no real effort made to simulate such loadings in themselves, but rather to rely on theoretical estimates of what effect varying load amplitudes would have on the fatigue life of a structural member.

It is absurd, however, to speculate on a cumulative fatigue damage law to apply to variable amplitude loadings without having at least some accurate fatigue data on this type of loading. All commercial fatigue machines presently available employ principles of operation which make it extremely difficult to test under random or even variable amplitude conditions. As a result, they are unable to prove or disprove any practical cumulative damage rule, since the crucial test must lie in accurate simulation of actual operating conditions. For the most part, these operating conditions are the outcome of random processes disturbing the structure under consideration.

It is demonstrated in this report that such simulation of random loadings is not only feasible, but can be carefully controlled to supply fundamental fatigue data pertaining to a wide variety of operations involving repeated loads. In Appendix A, it will be shown that a large electromagnetic shaker driven by amplified random noise can be integrated into a testing system capable of applying carefully controlled random fatigue loads to test specimens and structural components. Using this axial load apparatus, shown in Fig. 1, a study of both constant and random amplitude fatigue was undertaken, with unnotched 2024-T4 Aluminium Alloy extruded bar specimens (Fig. 2). Nearly all tests in this investigation were carried out using a tensile mean stress of 16,000 psi. This choice was based on factoring the Ultimate Tensile Strength of 86 ksi (Ref. 1) for these specimens by the ultimate load factor of 5.25 typical of utility aircraft which use this material in great quantities.

The random amplitude tests discussed in Section III were performed using a Stationary Random Process; i. e., the statistical mean values (such as the RMS stress) remained constant throughout the test to failure. For the majority of the Random Amplitude tests, the machine was used in its simplest configuration - a lightly damped single-degree-of-freedom system utilizing a single lever, so that the stress output at the specimen constituted almost a pure Rayleigh density distribution of stress peaks. (Figure 28).

The only exception to the above was the program of tests described in Section IV, in which a second lever was attached by a spring to the first, resulting in a two-degree-of-freedom system. The density distribution of stress peaks now becomes a combined Rayleigh-Gaussian form described in Section IV.

As a further attempt to simulate ideally the service conditions existing for fatigue-sensitive structures, a series of tests were performed using a manually-produced Quasi-Stationary Random process. The results of these tests are discussed in Section V. They arise essentially from discrete-value random programming of the RMS level of the stationary random process used in the previous sections.

To investigate certain features of Cumulative Fatigue Damage, a series of tests were performed in which fixed amounts of Stationary random amplitude preload cycles were applied to the specimens before they were used to obtain constant amplitude endurance curves. These tests provided additional insight into the distinction between nucleation and propagation of fatigue cracks (see Section VI).

Due to the fact that the data obtained in this program constitute the results of the first experimental fatigue program in which random loads were applied using a uniform stress field (unnotched axial loading) with a non-zero mean stress, their effect on existing cumulative damage theories is discussed throughout the report.

Nearly all cumulative damage theories put forward thus far require the establishment of constant amplitude parameters for the given material. In a preliminary program described in the first section and Ref. 1, about 1000 specimens of the original population of about 1400 specimens from the same melt were tested under constant amplitude conditions, the majority of these tests being carried out using an Amsler Vibrophore. The remaining 400 test specimens (representing about 250 million test cycles) were used in the Random Load Fatigue machine to obtain the data for the main body of this report.

In Appendix B, an attempt has been made to clarify the concepts and terminology used in this report, as they apply to fatigue analysis for both constant and random amplitude loadings. This appendix is intended for readers perhaps unfamiliar with the statistical and metallurgical terms currently in vogue in fatigue analysis.

II. ANALYSIS OF THE CONSTANT AMPLITUDE FATIGUE DATA

2.1 Introduction

In any development of fatigue parameters, the problem of statistical scatter in the individual test results presents itself. The approach followed throughout this report has been to use a reasonably large number of tests (usually at least 6) to assess the mean value for any given test condition, and to establish the general nature of the underlying population (e. g. approximately log-normal or 2-distribution). Then linear or exponential regression techniques were employed to obtain the most objective values of the overall fatigue parameters necessary for the study of cumulative damage. Where significant discrepancies were observed between the assumptions used in such

'smoothing' procedures, and the test results, these were then discussed in detail. The most significant discrepancy consists of a distinct bimodal behavior in the specimen endurance distributions at low constant amplitude stress levels, and the associated appearance of a discontinuity in the constant amplitude S-N relation immediately above these stress levels.

The log-normal distribution can be shown to be a natural one for fatigue behavior since such failure is a gradual phenomenon (Laurent, Ref. 2). The plotting procedure used for all results presented on log-normal probability paper was

$$P_i = \frac{i - 3/8}{n + 1/4} \quad (1)$$

This rule is suggested by Weibull (Ref. 3) as the best rule for obtaining unbiased estimates of the standard deviation from the slope of the test result line. The rule used in Reference 1, $P_i = i/(n + 1)$ results in a slight overestimate of the standard deviation. This difference in plotting procedures does not, of course, affect the qualitative ideas first developed in Reference 4 and discussed in this section.

2.2 Regression of Test Results

Assessment of the Constant Amplitude parameters necessary for certain cumulative damage theories requires that the data be plotted on Log S - Log N coordinates. However the bulk of S-N data (with which a comparison may be made with the S-N curve obtained in this project) has been presented on the semilog plot; i. e. S-log N. Therefore the regression analysis described below, which assumes the underlying process is log S - log N linear, is presented without intending to imply that the fatigue mechanism has been established to be log S - log N linear. In this analysis two further assumptions are made:

- a) Each endurance mean value has equal weight
- b) Values of log S are more "accurate" than values of log N_f

The slope of the straight line yielding the least squares for the residuals (i. e., the regression line) is

$$m = \frac{N \sum xy - \sum x \sum y}{N \sum x^2 - (\sum x)^2} \quad (2)$$

Where $x = \log_{10}$ (Stress Amplitude)

$y = \log_{10}(N_{fail})$

N = total number of observations

Normally if there are no other restrictions on the position of the regression

line, it will pass through the "centre of gravity" defined by

$$\bar{x} = \frac{\sum x}{N} \quad \bar{y} = \frac{\sum y}{N} \quad (3)$$

In order to assess the degree to which the data correlate with the above straight line representation, a correlation coefficient can be derived as follows:

$$r = \frac{N \sum xy - \sum x \sum y}{\left[[N \sum x^2 - (\sum x)^2] [N \sum y^2 - (\sum y)^2] \right]^{1/2}} \quad (4)$$

For a given set of test data the above quantities can be used to define the least squares straight line by obtaining the C. G. and the slope m . The correlation coefficient r then is a measure of the quality of this representation.

Weibull, (Page 201 of Ref. 3) discussing Least Squares states "This principle can be justified if it is assumed that the measures are normally distributed, which is very often a dubious assumption". Here we use the logarithms of lives which are assumed normally distributed. Figures 3 and 19 show this assumption to be justified. A more comprehensive technique described by Weibull in this reference uses an analysis giving minimum variance (method of linear estimates), and leads to exactly the same equations if the observations are independent of one another. This also is a reasonable assumption in the present work.

2.3 Comparison with Other Sources

In order to confirm that the Constant Amplitude S-N curve obtained in the present study is a reasonably accurate one for the material a brief literature survey revealed four other sources of data, for axially loaded unnotched 2024-T4 extruded bar specimens. The results are presented below:

Reference	Diameter of Specimens	Fatigue Strength S_a at		
		10^5 cycles	10^6 cycles	10^7 cycles
Present study (T. N. 35)	.282"	33.0 ksi	23.5 ksi	18.0 ksi
Items 212, 213, P. 326 Ref. 5	.30"	36.8 ksi	26.1 ksi	20.7 ksi
Items 216 - 223, P. 326 327, Ref. 5	.20"	28.7 ksi	22.9 ksi	17.9 ksi
Ref. 6, Fig. 7	.285"	31.0 ksi	21.7 ksi	19.5 ksi
Ref. 7 (also in Table 3.112(d) ANC-5)	.20"	31.8 ksi	24.0 ksi	18.8 ksi

In each case, the source data were used to interpolate graphically for values at a mean stress of 16 ksi (tension). In general the present results compare well with previous data.

2.4 The log-log Slope Parameter δ

The sample test data from TN 35 for the single level endurance have been used to obtain the slope parameter by the method of least squares. This parameter, $\delta = 5.54$ with a regression correlation coefficient of 98.5%. The resulting least squares straight line representation of the data is given by the equation

$$N = \left(\frac{2.64}{S} \right)^{5.54} \quad (5)$$

This value compares with 5.4 obtained by Liu and Corten in Ref. 8, and 5.73 obtained by D'Amato in Ref. 9. Due to the 2-Distribution behavior at low stress levels, only the top twelve stress levels ($24 \text{ ksi} \leq S \leq 52 \text{ ksi}$) were used to determine this parameter.

The corresponding Constant Amplitude tests using the Random load fatigue machine are presented in Table 1. These tests were carried out to check if any variation in the Constant Amplitude parameters established by the Vibrophore occurred due to the change in testing machines. The results obtained are illustrated in Fig. 3 which shows the ranked results plotted on log-normal probability paper. The slope of the lines on these graphs is a measure of the standard deviation of the sample, and in general, at high stresses, the dispersion of the UTIA results is somewhat less than those obtained on the Vibrophore (Ref. 1).

At low stresses, where the distributions are bimodal, the difference in standard deviation is less noticeable, particularly in the component distribution having the shorter mean life. Due to the presence of both the discontinuity effect and the "bimodal" effect, the results using the Random Load fatigue machine were not regressed in themselves to obtain a separate value of δ but their mean values are shown in Fig. 4 with the TN 35 values. They show that within the accuracy possible at present with statistical scatter, there is no reason to believe a significant difference in the 'machine-factor' exists.

2.5 The 'Bimodal' Phenomenon

It was found that for stress amplitudes above about 20 ksi (with a mean stress of 16 ksi) the test endurance were well represented by the single symmetrical log-normal distribution. However, as the stress amplitude was lowered, the endurance data departed from linearity when plotted on log-normal probability paper, and, if assumed to be the result of a single mechanism or population, the dispersion increased in the manner shown in Fig. 5. This is a common observation in constant amplitude fatigue testing.

At first, an attempt was made to fit these data to the (skew) extreme value distribution. While a reasonable fit was usually obtained, the method appeared to yield little fundamental insight into the action of fatigue at the knee of the curve. Since the distribution of ranked test results on log-normal probability paper deviated in a manner vaguely like that which one would obtain if a separate distribution were to intrude upon the first (unsuspected by the analyst) and finally become predominant, this line of reasoning was pursued. By grouping the data visually into the two distributions suggested from the shapes of the curves of ranked data on log-normal probability paper, a logical pattern developed over the stress range (Fig. 6).

The distributions usually exhibiting the smaller standard deviations (steeper slope in Fig. 6) were found to be the logical linear continuation of the intermediate stress distributions. These are called Short Term Fatigue, STF. The distributions with the larger standard deviations seemed to indicate the emergence of the line of the single distributions characteristic of stress levels well below the knee of the S-N curve. These distributions are called Long Term Fatigue LTF.

This 2-distribution interpretation was thus used with the data of Ref. 1, and rather than rely on a visual estimation of the mean life positions, a least squares exponential regression was carried out with the aid of an IBM 650 Computer on the 15 sample means, using the expression $N = a e^{-bS} + c e^{-dS}$ where N are the cycles to failure, S is the stress amplitude, and, a, b, c, d curve-fitting constants obtained by iteration to a Least Squares minimum.* The resulting S-log N curve (Fig. 4) is not only an excellent fit of the test data over a greatly enlarged range of stress amplitude, but it was possible to identify the first term $a e^{-bS}$ as passing through the STF means and the intermediate stress means, while the second term $c e^{-dS}$ was representative of the LTF and low stress means (Fig. 6).

While the data used by the author involved the testing of only 9 specimens at each of 15 levels of stress amplitude, the test results of References 10 and 11 have been similarly re-examined, having sample sizes of approximately 20 and 100 specimens, respectively. These data give striking confirmation of this behavior. (See Reference 4 for typical distribution shapes.) The increase in sample size (especially for $\pm 40,000$ and $\pm 35,000$ in Reference 11) allows one to suspect that both the LTF and STF distributions appear to follow a log-normal probability of failure. Also it is apparent that this behavior is unaffected qualitatively by the type of loading, the mean stress or the presence of notches. At present these observations appear limited to materials with no well-defined endurance limit.

* The author is greatly indebted to Dr. B. Worsley of the University of Toronto Computation Centre and to Dr. L. Lax for generous assistance in this phase of the work. The program, developed for the field of medicine, is described in Reference 12.

In general, the ends of the distributions seem to fade rapidly and the STF and LTF lines terminate within the transition region. Possibly a great deal of the usual jaggedness of the line joining the endurance means near the knee of the curve would be removed if a metallurgical and/or statistical study were to separate single endurances arising from the non-zero probability of second-distribution failures.

It is possible of course, to obtain component distributions as the result of inaccuracies in amplitude setting and "inherent scatter". However the standard deviations are usually quite similar, and the distributions overlap within the sample range of probabilities. In the separation of the data of References 1, 10 and 11 no overlap occurred, and there was an obvious difference (by a factor of about 3 in Reference 1) in the standard deviations of the component distributions. Also the means were separated by as much as one cycle (or more) of log N requiring an amplitude error far too great to be resolved by inaccuracies. Inaccuracies in settings would result in a random arrangement of distributions rather than the orderly continuation of straight line segments observed here. Nevertheless, the sequence of events in the transition from one distribution to another occurs in an extremely small interval of stress amplitude (6 ksi in Reference 1).

While a great number of specimens in the present study were used in the preparation of Reference 1, a small number of specimens from the same melt of material were set aside to be tested on the Random Load Fatigue Machine to explore further the bimodal behavior of fatigue endurances at low stress levels. By careful choice of stress amplitude it was possible to obtain a wide separation between the two test result groups at a given stress level (notably 19.5 ksi. See Fig. 3). This was a significant finding since it follows that representation of the results at such a stress level by a single-mode distribution of any type would be erroneous.

One of the earliest thorough statistical studies emphasizing the dual mode behavior of endurances at low stress levels is reported in Reference 13. In this program 216 unnotched extruded steel specimens were tested from one billet at about 15 tons per square inch stress amplitude, while the U. T. S. for the material was about 34 tons (mean stress zero). The resulting distribution of failures plotted against the logarithm of the cycles to failure was described as a double-humped skew distribution with the major peak at approximately 1.2 million cycles and the minor peak at about 20 million cycles. Possibly this level of stress represents a level at which the STF mechanism is just beginning to decrease in prominence while the LTF mechanism has increased to be responsible for a significant proportion of the endurances. The authors quote earlier evidence of this behavior given by R. R. Moore in Vol. 23 Part II of the ASTM Proceedings, June 1923.

The plotting of the ranked data obtained from five studies (Refs. 1, 10, 11, 14 and the present tests) shows that both distributions appear linear on log-normal probability paper. While this is not conclusive evidence that both distributions are indeed log-normal, it shows that such an assumption would be adequate to describe the results at the present time.

Webber and Levy, in Reference 15, present normal probability plots of rotating beam constant amplitude endurance data for the British Aluminum Alloy DTD683, at three different stress levels (their Figure 13(b)). A study of these three curves shows that the 50 ksi level is probably 100% STF, while the specimens tested at 40 ksi are STF to 532,700 cycles and then LTF for the remaining 42% of specimens tested at that level. At the lowest level, 35 ksi, the first 10% of the results can be considered STF with the remaining results exhibiting the increased standard deviation characteristic of the LTF family. The authors identified the fractures as being of two types:

- a) side-type - single-point crack propagation, with the final break to one side of the cross-section
- b) ring-type - multiple circumferential crack nuclei surrounding the final central break

The ring type was found predominant at the 40 ksi level and above.

The test data taken from Ref. 14 is also of particular interest due to the extensive statistical coverage of the low and intermediate stress levels. Forty-eight tests were performed at each of 12 stress levels for the Hard Temper Phosphor Bronze Strip, with 48 tests at each of 8 stress levels for the Spring Temper strip. The means obtained are shown in Fig. 7 and appear to follow the trends indicated in Fig. 6. Figure 8 of Ref. 14 shows the results of considering the data as arising from a single distribution. The authors state that "neither the log-normal nor the extreme value distribution fits the data for the $\pm .300$ inch deflection level". An attempt was made to fit these and other low stress level data into log-log normal distributions. This of course results in a more linear grouping of data, but it is felt that this is due more to the lack of sensitivity of the distribution than to a real understanding of the basic patterns of behavior.

In the present work, all the specimens tested in the random load machine were coated with an inert grease to prevent further exposure to the atmosphere past the date of greasing. This presents specimens to the machine with approximately identical periods of corrosion. The similarity in the results at 19.5 ksi and 22.5 ksi given in Figure 3 with the results at 20 ksi and 22 ksi given in Reference 1 shows that this factor is probably not a significant one for the existence of the "bimodal" phenomenon.

Little mention was made in Reference 4 of the possible differences in fatigue mechanisms which could cause the two-distribution behavior aside from the suggestion that the STF mechanism may consist of the creation of a great number of crack nuclei with the development of more than one final crack, while the LTF mechanism may consist of the exclusive propagation of a single crack as indirectly suggested by Webber and Levy. In the STF mechanism, nucleation may be so fast that the development of fatigue areas occurs in a relatively spontaneous manner, while the LTF mechanism required the development of localized stress concentrations ahead of a single crack nucleus for its growth.

While metallurgical examination of the specimens in the present study has been inconclusive, there does appear to be a transition of this kind over a wide range of stress (45 ksi to 19 ksi). Further research on this point is presently being carried out at the Institute of Aerophysics. However, the statistical duality of the fatigue mechanism as exhibited by Constant Amplitude test results below the 'plasticity' range can be considered consistent with metallurgical observations of two fatigue processes discussed by Freudenthal (Ref. 16), Wood (Ref. 17) and Lazan (Ref. 18).

Feltner and Morrow, in Reference 19 discuss the two-mechanism phenomenon in terms of hysteresis energy conversion. In the low-stress region this energy is due to "anelastic dissipating mechanisms" which are essentially non-damaging such as magneto-elastic coupling and atomic diffusion. The presence of this anelastic hysteresis energy in this region is apparently the reason why very large amounts of total energy may be measured. In the high-stress region the hysteresis energy is due to plastic deformation which is damaging in a fatigue sense. They state that between these two distinct regions (near the fatigue limit), a transition zone exists in which the energy per cycle is composed of both anelastic and plastic hysteresis energy. These workers then describe the identical (qualitative) behavior in the stress-inelastic strain relation, and relate this behavior with fatigue performance correlating the high stress fatigue region to the region of predominant plastic strain, and the low stress region to an area of predominant "anelastic" strain. For stresses near the fatigue limit, the authors state that the two may be combined to form the curved (transition zone) portion of the stress-strain curve. The present study relates this behavior to the fatigue endurance curve in like manner.

Figure 4 shows the sample means for the endurances obtained in the construction of the semilog S-N relation for the subject material. Note that the endurances at 34 ksi and 32 ksi are both greater than the endurance at 30 ksi. Similar behavior has been noted by Williams using L65 Aluminum Alloy (Ref. 20) and V. I. Shabalin (Ref. 21) using 'Dural' specimens. In the latter work the discontinuity was observed at cycling such that the maximum stress was 32 kg/mm^2 (45.5 ksi). Assuming 30 ksi as the position of the discontinuity in Figure 4 this corresponds to a maximum stress of $16 + 30 = 46$ ksi. Also the endurance at which this phenomenon occurs is roughly 100,000 cycles, which corresponds to the life obtained with the second set of Dural specimens (Fig. 2, Ref. 21). The Russian report then concludes: "A suggested explanation of the form of the curve lies in the theory of crystal dislocation, which points to a difference in the mechanism of fatigue failure in the cases of high and low stress. Above the yield point, the major failure mechanism is the coagulation of vacancies on the planes of maximum shear stress, while for lower stresses the build-up of vacancies occurs on planes of maximum normal stress". While the Dural specimens were tested up to their yield point (which was given as $33.4 \text{ kg/mm}^2 = 47.5$ ksi), the yield point for the 2024-T4 alloy (0.2% Proof Stress) is about 68.5 ksi (Reference 1) so that the correlation in Stress levels may not be so simply explained.

The L65 material used by Williams, reveals the discontinuity between 21 and 22 tons/sq. inch with zero mean stress i. e. , 47 ksi to 49 ksi. This correlates well with the two previous values. The rotating cantilever specimens show a change in fracture appearance from a crescent-shaped fatigue crack path below the discontinuity to a concentric path above the discontinuity, i. e. , single-crack to multi-crack propagation.

In the present study it was found that for amplitudes above the discontinuity the distribution of the log-endurances was approximately normal, while the endurances below this stress level were essentially of the 2-distribution type discussed earlier. The "discontinuity" described above can be explained logically using the two distributions of endurances, if one considers the effect of the continuation of the LTF line ahead of the STF family (level b of Figure 6). When this occurs, the single mean of the two distributions will shift to lower endurances than for the all-STF populations immediately above this level. At still lower stress levels, this single mean will move through the intersection of the two distribution lines and its position will become more and more dictated by the LTF distribution. An interesting result of this approach is that it provides a logical explanation for the 6 test results rejected by Weibull (Figure 4 in Reference 10). When plotted log-normally as a second component distribution, the standard deviation was found to be greater than that of the main distribution while the mean life was less. It thus appears that the LTF line of distributions can extend across the STF line and yield a small LTF distribution preceding the STF or intermediate stress distribution.

All the UTIA Specimens used in the complete test program were inspected at failure for cracks using the Dye Penetrant technique specified in the American Military Specification MIL-I-6866 A (ASG) Type II (nonfluorescent Methods). This technique involves the application of a penetrating red dye solution to the cleaned specimen with a brush, and a 20 minute immersion period before excess dye is removed with a wash and the specimen dried with a clean cloth. The specimen is then painted evenly with a thin coat of developer solution, a white solution. After a period of at least 5 minutes, the developer will cause the dye in the cracks to come to its surface and reveal defects as red markings on a chalky-white background. It was found that, for all constant amplitude tests with tensile mean stress, failure of the constant amplitude specimens usually proceeded uniformly from a single crack as can be seen in Figure 11, which shows typical UTIA specimens tested at 16 ksi \pm 34 ksi.

III. STATIONARY RANDOM (RAYLEIGH) TESTS

3.1 Introduction

Ideal simulation of most service fatigue loads involves a close study of the process forming the disturbance. An investigation of the random process responsible for most of the fatigue loading of aircraft (Ref. 22) reveals that a given patch of turbulence has a marked similarity with random noise as obtained from a thyratron in a magnetic field, when observed as a continuous trace. Examination of short time traces of either process reveals that the

distribution of vibration amplitudes is roughly Gaussian, and neither process shows periodicity in the input exciting function. That is, while the instantaneous values of the functions are unpredictable, both processes have the same statistical property, that they possess a close approximation to a Gaussian or Normal distribution of probable values.

The distribution of peak values in the structural response time history is of prime importance if the general analysis objective is the prediction of structural fatigue life. With a Gaussian noise source, a linear system will respond with a strain peak distribution which may range from Gaussian to Rayleigh with all possible combinations in between, depending on the number of modes which are excited to a significant degree. When the random load fatigue machine used in this project is in the single-lever configuration, there is a single mode of vibration with a peak centred at the resonant frequency (in this case about 45 to 50 cps).

The analytical form of the Rayleigh Distribution of peaks is, of course, the exact formulation only for an ideal case where the bandwidth at the resonant frequency is negligible. It was necessary early in the testing program with the machine to assess the degree to which the strain history was of the Rayleigh type. The simplest experimental procedure was to take sample traces at various RMS strain levels and determine experimentally the sample irregularity ratio R by actually obtaining the ratio of zero crossings to peaks. This resulted in an average value of $R = .96$ for samples involving about 250 cycles. Then the individual peak strains were tabulated, ranked and plotted on Rayleigh Probability Paper. This paper was constructed using the procedure described on Page 22-12 of Ref. 54. It was found that, for the trace samples studied, no appreciable falling off or "clipping" in the strain peak distribution occurred up to almost $3.6 \times \text{RMS}$, as shown in Figure 8. This clipping implies that all values of stress peak greater than 3.6 rms will be given the value 3.6 rms . Considering the probability of all such peaks, this error is considered negligible in the assumption of a Rayleigh Peak distribution.

3.2 Test Results

The simplest utilization of a Fatigue Machine employing a Gaussian Noise input is to test at constant RMS stress (i. e. , a Stationary Random Process) to failure and thus obtain a Random Fatigue Curve of RMS Stress versus endurance. Since the test machine in the single-lever configuration is lightly damped, the output stress history has been shown to be well represented by the Rayleigh density distribution of peak stresses. It is therefore possible to use the resulting test curve to check damage accumulation with Rayleigh density distributions of stress peaks. As in the case of Constant Amplitude testing the endurance have inherent statistical scatter (see Fig. 9) so that it is necessary to test a similar number of specimens to obtain a mean endurance under Random Amplitude conditions, as it was under Constant Amplitude conditions, to obtain meaningful correlations.

The 'Rayleigh' endurance curve was obtained by testing, to failure, at least 6 specimens at each of seven RMS levels. These endurance data appear in Table 2. A linear regression was performed on all the test data, in the $\log \sigma_p - \log N$ form with the following results:

$$(6) \quad N = \left(\frac{276.3}{\sigma_p} \right)^{4.22} \quad S_m = 16 \text{ ksi}$$

Comparing this equation with the least squares straight line from the Constant Amplitude tests

$$(5) \quad N = \left(\frac{264}{S} \right)^{5.54} \quad S_m = 16 \text{ ksi}$$

it is interesting to note that the application of Rayleigh variable load history results in a clockwise rotation of the Constant Amplitude line about a cycle value of approximately unity. This experimentally-obtained 'rotation' of the endurance curve has been observed by Fuller in Ref. 23, and Schjelderup and Galef in Ref. 24. It also agrees with the ideas of Corten and Dolan and Freudenthal in that extensive damage occurs below the Constant Amplitude endurance limit from prior load history above the endurance limits resulting in finite lifetimes well below the Constant Amplitude endurance limit. It supports the general finding that a linear accumulation of damage based on the fraction of cycles endured at a given level compared with the available Constant Amplitude cycles, cannot account for the Random Amplitude curve since it will be shown that no rotation of the straight line would occur on the log-log plot when deriving the Random Amplitude line from Constant Amplitude line. Also the Random Amplitude line will not exhibit endurance limit effects due to the asymptotic nature of the Rayleigh distribution, due to the presence of some probable loads above the endurance limit, which would give the low stresses nuclei to work on.

A dye-penetrant study of the unnotched specimens used in the determination of the experimental Random Amplitude curve revealed a significant change in the accumulation of fatigue damage. Figure 10 shows representative specimens tested at $\sigma_p = 18$ ksi. The presence of a great number of small cracks on these specimens when tested at higher values of σ_p , and which were manufactured identically to those used for the Constant Amplitude tests (Figure 11) was quite unexpected. Re-examination of the actual crack number was carried out and the results included in Table 2. The variation of visible crack nuclei with endurance at a given σ_p appears random; however, the variation with RMS stress level is quite marked. Figure 12 shows the variation in mean crack number with RMS level for these tests.

It appears that, while the Constant Amplitude specimens and Random Amplitude specimens were randomly taken from a population of identically-manufactured specimens, the numerous cracks found under high-level Random Amplitude testing do show a preference to occur at surface irregularities resulting from the turning down of the waisted sections. Random sample specimens of the UTIA test series were examined to determine the RMS micro-inches roughness in this waisted portion of the specimen. This

was accomplished using a commercial apparatus known as the Profilometer, manufactured by Micrometrical of Ann Arbor. The results of these tests indicated that the RMS micro-inches roughness varied only slightly (15 to 30 Micro-inches). The specimens therefore had a uniform RMS roughness of fair manufacturing quality.

3.3 The Linear Law of Damage Accumulation

3.3.1 Log-Log Presentation

The Rayleigh distribution is given by Equation 16, page 41, Ref. 25.

$$p(s) = \frac{s}{\sigma^2} e^{-s^2/2\sigma^2} \quad (7)$$

where $p(s)$ is the probable number of stress peaks between s and $s + ds$.

Considering the linear accumulation of damage with a Rayleigh distribution of stress cycles, the equation for Random Amplitude endurance is given by the expression for the number of random peaks to failure:

$$N_{fr} = N_f T = \left[\int_0^\infty \frac{s}{\sigma^2} \frac{e^{-s^2/2\sigma^2}}{N(s)} ds \right]^{-1} \quad (8)$$

where

$$N(s) = (s_0/s)^\delta$$

$$\therefore N_{fr}^{-1} = \frac{1}{\sigma^2} \int_0^\infty \frac{s^{s+1}}{s_0^\delta} e^{-s^2/2\sigma^2} ds = \left(\frac{s_0}{\sigma}\right)^{-\delta} \Gamma(1 + \delta/2) \quad (9)$$

For the present value of the Constant Amplitude line $\delta = 5.54$

$$\therefore N_{fr} = .22 \left(\frac{264}{\sigma}\right)^{5.54} \quad (10)$$

Thus for linear damage accumulation we obtain a straight line parallel to the Constant Amplitude line, but below the Constant Amplitude line such that

$$N_{fr} = .22 (N_f)_{CA} \quad \text{for a given stress level. This line is}$$

plotted as a curve on the semilog presentation of data in Figure 4. It must be remembered that the Constant Amplitude line used is the straight line passing through to the endurance above 22 ksi, and as such, it is quite inaccurate in the low stress region. A numerical integration at these levels might be better, but would yield endurance even greater than those obtained from the above equation.

3.3.2 Linear Damage Accumulation with Two Distributions

Consider the accumulation of fatigue damage under the action of two semilog-linear (S-Log N) damage relations $N = ae^{-bS} + ce^{-dS}$ as discussed in Section II.

a) If the STF mechanism were the predominant fatigue mechanism with the LTF effect negligible, and Short Term Fatigue were effective throughout the stress range (from zero to, say, $\sigma_p = 20$ ksi) then, for a Rayleigh peak distribution,

$$N_{fr}^{-1} = \int_0^{\infty} \frac{s}{\sigma^2} N_{STF} e^{-s^2/2\sigma^2} ds \quad (11)$$

from which

$$\begin{aligned} a N_{fr}^{-1} &= 1 + \sigma b \sqrt{\frac{\pi}{2}} e^{\frac{\sigma^2 b^2}{2}} \left(1 + \operatorname{erf} \frac{\sigma b}{\sqrt{2}} \right) \\ &\equiv R(b, \sigma) \end{aligned} \quad (12)$$

b) If the STF and LTF mechanisms both contribute to the accumulation of damage, and each contributes according to a weighting function α such that at a given stress level

$$N_{\text{mean}} = (1 - \alpha) N_{STF} + \alpha N_{LTF} \quad (13)$$

then a more complex expression will result for the Rayleigh Life,

$$N_{fr}^{-1} = \int_0^{\infty} \frac{s}{\sigma^2} e^{-s^2/2\sigma^2} \left(\frac{1-\alpha}{N_{STF}} + \frac{\alpha}{N_{LTF}} \right) ds \quad (14)$$

i) Assuming $\alpha = e^{-\beta s}$

$$N_{fr}^{-1} = \frac{1}{a} [R(b, \sigma) - R(h, \sigma)] + \frac{1}{c} [R(h', \sigma)] \quad (15)$$

where

$$R(h, \sigma) \equiv R(b, \sigma) \quad \text{with the substitution } h = b - \beta$$

and

$$R(h', \sigma) \equiv R(b, \sigma) \quad \text{with the substitution } h' = d - \beta$$

ii) Assuming $\alpha = e^{-\beta' s^2}$

$$N_{fr}^{-1} = \frac{1}{a} [R(b, \sigma) - K(q, \sigma)] + \frac{1}{c} [K(q', \sigma)] \quad (16)$$

where

$$K(q, \sigma) \equiv \frac{1}{1 + 2\beta' \sigma^2} + \frac{\sqrt{\pi} \sqrt{q} b e^{\frac{b^2 q}{4}}}{2(1 + 2\beta' \sigma^2)} \left(1 + \operatorname{erf} \frac{b \sqrt{q}}{2} \right) \quad (17)$$

and $K(q', \sigma) \equiv K(q, \sigma)$, substituting d for b

$$\text{and } q^{-1} = \frac{1}{2\sigma^2} + \beta'$$

Determination of α :

There are two ways to obtain α from the test results.

a) Use α as the proportion of test results which were designated as the LTF group at each of the four stress levels where the results were separated into 2 distributions.

This derivation of α will be called α_e .

b) Find α as the unknown in the equation:

$$N_{\text{mean}} = (1 - \alpha) N_{\text{STF}} + \alpha N_{\text{LTF}} \text{ and obtain}$$

N_{STF} and N_{LTF} from their "regressed" values from Ref. 1.

$$N_{\text{STF}} = 7.86 \times 10^6 e^{-.113 S}$$

$$N_{\text{LTF}} = 1.74 \times 10^{11} e^{-.532 S}$$

N_{mean} is the logarithmic mean of all test endurances at the given S. This derivation of α will be called α_t .

From these two sources we have:

S_{ksi}	α_e	β_e	β_e'	α_t	β_t	β_t'
18	1.000	0	0	.654	.024	.0013
19.5	.170	.091	.0047	.154	.096	.0049
20	.131	.102	.0051	.125	.104	.0052
22	.124	.095	.0043	.333	.050	.0023
22.5	.338	.048	.0021	.836	.080	.0004
28	0	∞	∞	.700	.013	.0005
30	0	∞	∞	.219	.051	.0017

$$\beta \text{ average} \doteq 0.1$$

$$\beta' \text{ average} \doteq .0023$$

The predictions of endurance are given below.

σ ksi	σ_p ksi	(N_{fr}) STF only	$(N_{fr})^{\beta} = .1$	$(N_{fr})^{\beta'} = .0023$
0	0	7.86×10^6	1.74×10^{11}	1.74×10^{11}
2	2.83	5.55×10^6	2.38×10^7	2.65×10^8
4	5.66	3.78×10^6	8.77×10^6	3.96×10^7
6	8.48	2.48×10^6	4.18×10^6	1.09×10^7
8	11.31	1.57×10^6	2.09×10^6	3.44×10^6
10	14.14	$.942 \times 10^6$	639,280	771,000
12	17.00	$.541 \times 10^6$	18,879	96,500
14	19.80	$.295 \times 10^6$	130	10,900

Comparison with test results (Fig. 4) shows that the evaluation of the Rayleigh curve with the STF line only is a very poor prediction, while the use of β appears quite promising. The use of β' is less promising possibly due to the scatter of the values of α_T which formed the basis for its use.

Like Fuller's rule discussed in Section 3.5, these methods are invariably unrealistic at low stress levels since they are restricted to the zero stress intercept of the distribution lines.

An examination of the 2-Distribution linear cumulative damage rule just developed reveals that the good agreement at high stress levels is almost entirely due to the contribution to N_{fr}^{-1} from the LTF distribution. While it was noted in Section II that an instance has occurred where the LTF distribution has appeared ahead of the STF results (as indicated at level b of Fig. 6) this agreement is probably spurious since it has already been observed that the high stress level Rayleigh results contain a significant proportion of stress peaks exceeding the upper limit of the STF or "macro-elastic" stress region.

3.4 Freudenthal's Prediction of Endurance

Experiments by Freudenthal and Heller (Ref. 26) have indicated that the linear CD rule is unconservative and that a safe life would be one-tenth that indicated by the linear theory. Smith and Malme (Ref. 27) and Fralich (Ref. 28 and 29) report similar results. Their findings are therefore in agreement with the author's. It is noteworthy that the loading used by Freudenthal and Heller is essentially multilevel (Randomly applied) programmed Constant Amplitude, rather than a random-process-generated loading.

In their theory of cumulative damage, the total cycles to failure

$$N_{fr}^{-1} = \sum \frac{\alpha_i \omega_i}{N_i} \quad (18)$$

where α_i is the relative frequency of cycles at stress S_i

and ω_i is a stress interaction factor for the given stress level, determined from experiment, and dependent on the load spectrum and the material.

In Reference 30, Freudenthal illustrated how his Rayleigh curve with stress interaction can be obtained from the Rayleigh-Miner line by the ratio

$$\frac{T_F'}{T_F} = \left(\frac{RMS}{S_1} \right)^{\delta - \rho} \frac{\Gamma(1 + \delta/2)}{\Gamma(1 + \rho/2)} \quad (19)$$

Freudenthal suggests the slope for the Rayleigh curve will be $\rho = 4$ from rotating bending data. This agrees well with the present axial data (4.22) and 4.0 will be used in the evaluation of the above ratio. Smith and Malme, in Ref. 27 obtain $\rho = 3.9$ for random tests using bending cantilever specimens. Thus

$$T_F' = 2.26 \left(\frac{RMS}{S_1} \right)^{1.54} T_F \quad (20)$$

If we use $S_1 = 51$ ksi, the stress amplitude for 10^4 cycles, as suggested by Freudenthal in Ref. 26 we obtain:

$$T_F' = .0053 \sigma^{1.54} T_F \quad (21)$$

The accurate selection of a unique maximum stress level as a demarcation between fatigue and alternating plasticity is quite difficult, and wide variations in life can be obtained from relatively small variations in stress level. However, agreement with test results (Fig. 4) is quite good when one considers the usual test scatter.

3.5 Fuller's Predicted Endurance Line

The principal advocate for Cumulative Damage to be studied using semilog (S-logN) format has been Fuller (Ref. 23). In this reference he outlines the application of his method to cases where the load pattern is purely Rayleigh. The crux of his method lies in the observation that the slopes of Constant Amplitude endurance curves, and those arising from programmed Constant Amplitude testing exhibit slopes which are only a function of the load distribution and not of the magnitudes of the loading parameters. Using his nomenclature, the distribution coefficient $\beta = K_{SN}/K_V$ is a function only of load pattern where K_{SN} is the slope of the S-N curve, and K_V is the slope of the maximum stress VA curve. Both of these parameters are based on the semilog slopes. If, for instance, the values of the minimum stress amplitude in a programmed Constant Amplitude test are changed and a variety of maximum stress amplitudes is considered for each minimum stress amplitude having the same distribution, the result is a number of parallel straight lines for the Programmed Constant Amplitude endurance terminating at the respective minimum stress amplitude as given by the virgin S-N curve.

Fuller also found that for values of minimum stress amplitude (in a Programmed Constant Amplitude test) below the so-called fatigue limit,

the correct VA endurance lines could be obtained by extending the "sloped-leg" portion of the S-N diagram to the required value of minimum stress amplitude and drawing the VA line with slope K_V upwards from this point. It is interesting to note that in Levy's Cumulative Damage analysis (page 751 and Figure 3.136, Reference 18), Levy tried extrapolating the "falling portion" of the S-N curve to the minimum stress of the programmed Constant Amplitude test (in log-log presentation) after the manner of Fuller, and found surprisingly good agreement in endurance with experimentally obtained data for VA type loadings.

For reasons discussed in the preceding section of this report, this "sloped-leg" portion is assumed to be the STF endurance mechanism. From Ref. 1, the semilog equation for the STF distribution is $N_f = 7.86 \times 10^6 e^{-.133S}$. Thus the zero-S intercept is 7.86×10^6 cycles. This is point D in Fuller's notation. The slope of the STF line using the S-log N grid is $-.133 \times .4343 = -.0577$.

Now (β) Rayleigh = .667 when one arbitrarily uses the cumulative distribution of 1000 cycles. This is due to the ratio of the area of a parabola (formed by the cumulative probability function plotted logarithmically) to its enclosing rectangle being 2/3. Therefore the value of $K_V = -.0667 \times .0577$. This VA line passes through D with slope $-.0384$. In order to apply this VA line to the Rayleigh results it will be noted from Figure 8 that no appreciable 'clipping' of the Rayleigh signal occurs to at least 3.6 RMS. There is reason to believe however, that clipping does occur just above this level, from an examination of two long-term traces.

The operative Rayleigh line using Fuller's method is then a line with slope $-3.6 \times .0384 = -.138$ if the ordinate is the RMS stress, or $-.707 \times .138 = -.097$ if the ordinate is the RMS peak stress, with the line terminating at Point D. Figure 4 shows the representation of the Rayleigh results obtained with the Fuller method. The lack of correlation of high values of RMS peak stress can be expected from the assumption that the STF mechanism is the operative one, since in Constant Amplitude testing the STF is limited to the elastic fatigue range. RMS peak stresses above 16 ksi are considered to contain a non-negligible amount of alternating-plasticity cycles causing abnormally low endurance.

Fuller concludes that high cycles of stress are "not remembered" by the material if the probability of occurrence is less than .001 and this is his basis for the arbitrary selection of 1000 cycles.

The lowest RMS stress Rayleigh endurance was also used in an attempt to obtain a second line based on Fuller's technique using the equation for the LTF distribution

$$N_f = 1.74 \times 10^{11} e^{-.532S}$$

However the results did not correlate with the lower stresses of the Rayleigh curve. This lack of correlation is considered not due to lack of accuracy of LTF data (the test results follow the line well) but rather due to possible differences in damage accumulation with the LTF mechanism compared with the STF mechanism, if indeed the former has a cumulative damage mechanism at all.

IV. STATIONARY RANDOM (COMPLEX WAVE) FATIGUE

4.1 Introduction

The problem of fatigue behavior when a structure possesses multi-mode response to excitation, is one of extreme practical importance, since most structures experiencing fatigue are more or less flexible, and hence possess more than one degree of freedom. Fortunately, in many cases, a simple two-degree-of-freedom system is capable of simulating a wide range of structures, due to the fact that often fatigue stresses are developed to a significant extent in only one or two predominant modes of vibration. An aircraft wing is a good example of this, since it is usually excited to any extent in only the rigid body and fundamental wing bending mode. This is due to the spectral characteristics of the atmosphere, which result in a concentration of turbulent energy in the lower frequencies only. Recently the multi-mode vibration model has also been applied to nautical problems involving the pitching and rolling motion of a ship due to the action of sea waves (Ref. 31).

A logical extension of the single-lever fatigue testing of the previous section was to incorporate a second lever in the random load fatigue machine elastically attached to the first, and excite the first lever, as before, with wide-band random noise. It would then be possible to discover what differences in endurance ensue at the same RMS stress, with the resulting change in wave-form. The direct use of a multi-mode loading arrangement for the specimen carries with it the vital advantage that the fatigue loading is not restricted to the traditional concept of "cycle".

A fatigue cycle is only clearly defined when the response is Rayleigh or when the forcing function is a single sine-wave. Various workers, such as Schijve (Ref. 32) have examined the problem of equating complex wave-forms to equivalent fatigue cycles. It will be seen in this section that a more rational approach is to analyse the spectrum of the load and then to simulate this loading. The cumulative damage analysis can then be kept in terms of spectral quantities.

Cumulative damage theories which examine the non-cyclic character of truly random load-time histories are very rare. The work of Torbe (Ref. 33) and its extension by Poppleton (Ref. 34) appear to be the only serious analysis of this problem. Kowalewski, in Ref. 35, has carried out what appears to be the first instance of random load testing with broad-band excitation, using a shaker connected to a cantilever. A fixed configuration of a single complex cycle has been repeatedly applied to specimens (Ref. 36), but

no experiments have been carried out under conditions of a random input to a multi-degree-of-freedom system. Marco and Starkey (Ref. 36) applied a constant phase angle relation to failure in each test, using angles 0° and 90° . While this work was perhaps the first attempt to study complex-cycle fatigue, the complex and random load traces taken from aircraft show no such periodicity.

4.2 Evaluation of Spectral Quantities

An examination of a typical load trace resulting from a random noise excitation of the 2-lever configuration is shown in Figure 13. The RMS stress of the traces was obtained for a number of samples (see Table 3) by assuming the cumulative distribution of amplitude to be Gaussian (in contrast to the density distribution of maxima which is combined Rayleigh and Gaussian). Since the machine is linear in response, this is equivalent to assuming the input process to be Gaussian. The percentage of time the loading exceeds the given load level is then a function of the RMS, and can yield the function through the intermediate parameter, the normal deviate (using Table II of Ref. 37).

The basic power spectrum for the two-lever configuration of the fatigue machine used in the fatigue tests may be derived from Figure 14, which is the dimensional form of the frequency response function one obtains from sinusoidal excitation of the structure over the frequency spectrum. Figure 14 is only the power spectral density for the particular noise input used in carrying out this sweep.

The spectral density function arising from the energy distribution over the frequency domain will be used in this report, although it is of course possible to use the time domain and analyse the phenomenon using the auto-correlation function. Reference 38 discusses the relation between the two methods. The spectral density is defined as the mean square stress per unit bandwidth (whose units are ksi^2/cps). Sinusoidal excitation to include all significant values of spectral density, therefore allows determination of the fundamental and higher moments of the spectral density distribution about the zero frequency axis.

In order to obtain the spectral quantities necessary for load analysis, the second and fourth moments of this distribution must be evaluated. They are, using Rice's notation (Ref. 39):

His Eq. 3.1-2:
$$\psi_0 = \sigma^2 = \int_0^\infty \omega(f) df \quad (22)$$

$$\psi_0 = 680 \text{ ksi}^2 \quad \text{by integration of Figure 14}$$

His Eq. 3.3-14:

$$\begin{aligned}\Psi_0'' &= \sigma'^2 = -4\pi^2 \int_0^\infty f^2 \omega(f) df \\ &= -\frac{4}{3}\pi^2 \int_0^\infty \omega(f) df^3 \quad (23)\end{aligned}$$

$$\Psi_0'' = -16 \times 10^6 \text{ (ksi)}^2/\text{sec}^2$$

$$\begin{aligned}\Psi_0^{(4)} &= \sigma''^2 = 16\pi^4 \int_0^\infty f^4 \omega(f) df \\ &= \frac{16}{5}\pi^4 \int_0^\infty \omega(f) df^5 \quad (24)\end{aligned}$$

$$\Psi_0^{(4)} = 1.14 \times 10^{12} \text{ (ksi)}^2/\text{sec}^4$$

Some workers have expressed difficulty in 'closing' the integration of the moment distributions due to the frequency factor in the integration (Ref. 32). This problem is minimized by using the equivalent forms removing the frequency factor from the integrand as suggested to the author by Poppleton, for the graphical integration usually required. Almost invariably there is no simple analytical relation between the basic spectrum and its moments.

The experimental value of σ^2 is of course very large due to the method employed in obtaining Fig. 14 (a frequency sweep using an oscillator with constant output volts to drive the power amplifier and machine). It is only necessary to factor down this value to obtain the correct RMS stress levels in order to apply these quantities to the fatigue tests. Ψ_0'' and $\Psi_0^{(4)}$ are factored identically since the stress term is unchanged in the integrands.

In the following calculations it is assumed that the frequency characteristics of the input are 'white', i. e., uniform over the frequency range of operation for the fatigue machine.

<u>Configuration</u>	<u>RMS Stress</u>	<u>ψ_0</u>	<u>ψ_0''</u>	<u>$\psi_0^{(4)}$</u>
1-Lever	13.8 ksi	190.6	-17.84×10^6	1.793×10^{12}
2-Lever	10.4 ksi	108.6	-2.54×10^6	$.181 \times 10^{12}$
	8.8 ksi	77.4	-1.82×10^6	$.130 \times 10^{12}$
	7.9 ksi	62.4	-1.47×10^6	$.105 \times 10^{12}$

From Rice's paper two more quantities of interest are obtained from the basic spectral moment functions. They are:

a) Number of peaks (maxima) per second, (on the average)

His Eq. 3.6-6:

$$N_1 = \frac{1}{2\pi} \left(-\frac{\psi_0^{(4)}}{\psi_0''} \right)^{1/2} \quad (25)$$

= 50.6/sec. for 1-Lever configuration
= 42.5/sec. for 2-Lever configuration

b) Number of zero crossings with positive slope (on the average)

His Eq. 3.3-10

$$N_{0+} = \frac{1}{2\pi} \left(-\frac{\psi_0''}{\psi_0} \right)^{1/2} \quad (26)$$

$$N_{0+} = 48.7/\text{sec. for 1-Lever}$$

$$= 24.4/\text{sec. for 2-Lever}$$

From the ratio of these two quantities, two commonly-used spectral parameters are obtained:

a) The Irregularity factor R

$$R \equiv N_0 / N_1 = .96 \text{ for 1-Lever*}$$

$$= .57 \text{ for 2-Lever**}$$

*which is in agreement with the value obtained directly from the trace.
(Section III)

** With the power spectrum shown in Figure 14, the machine was used to obtain single-RMS endurences at three separate RMS levels. Oscillograph traces of the strain taken at each of these levels with about 300-400 peaks, were analyzed to obtain the ratio of zero crossings with positive slope to the total number of peaks. A portion of one of these traces is shown in Figure 13. The experimental results were (average from at least 3 samples) as follows:-

<u>RMS Level</u>	<u>IRREGULARITY FACTOR R</u>
10.4 ksi	.568
8.8 ksi	.573
7.9 ksi	.578

As expected there is no significant variation with stress level since this parameter has been shown to depend only on the power spectrum and its moments.

b) The Spectrum-width parameter ϵ .

$$\epsilon \equiv \sqrt{1 - R^2} = .28 \text{ for 1-Lever}$$

$$= .82 \text{ for 2-Lever}$$

Either the Irregularity factor or the spectrum width parameter, may be used in Rice's equation. Using ϵ , it becomes:

$$\left| \frac{p(s)}{N_1} \right| = \frac{\epsilon}{\psi_0^{1/2} \sqrt{2\pi}} e^{-\frac{s^2}{2\psi_0 \epsilon^2}} + \frac{\sqrt{1-\epsilon^2}}{2\psi_0} s e^{-\frac{s^2}{2\psi_0}} \left[1 + \text{erf} \left\{ \left(\frac{1-\epsilon^2}{2\psi_0} \right)^{1/2} \frac{s}{\epsilon} \right\} \right] \quad (27)$$

Since it is simpler to work with non-dimensional parameters, we define $\gamma \equiv s / \psi_0^{1/2}$ as employed in Ref. 31.

Then $p(\gamma) = \psi_0^{1/2} \left| \frac{p(s)}{N_1} \right|$ (Eq. 1.17, Ref. 31)

Thus

$$p(\eta) = \frac{\epsilon}{\sqrt{2\pi}} e^{-\frac{\eta^2}{2\epsilon^2}} + \frac{\sqrt{1-\epsilon^2}}{2} \eta e^{-\frac{\eta^2}{2}} \left[1 + \operatorname{erf}\left\{ \frac{\eta}{\epsilon} \left(\frac{1-\epsilon^2}{2} \right)^{\frac{1}{2}} \right\} \right] \quad (28)$$

i) Setting $\epsilon = 0$ ($R=1$)

$$p(\eta) = \frac{\eta}{2} e^{-\frac{\eta^2}{2}} (1 + \operatorname{erf} \infty) = \eta e^{-\frac{\eta^2}{2}}$$

which is the Rayleigh Distribution used in the previous section.

ii) Setting $\epsilon = 1$ ($R=0$) i. e., two spikes in the frequency spectrum with the ratio of the lower frequency to the higher approaching zero for equal energies at each.

$$p(\eta) = \frac{1}{\sqrt{2\pi}} e^{-\frac{\eta^2}{2}} \quad \text{which is the Gaussian Distribution}$$

Near $\epsilon = 1$, the trace will have about the same appearance as at $\epsilon = 0$ except for a very small high frequency ripple superimposed on the main low frequency fluctuating stress.

iii) For a flat frequency response (such as one obtains with a low-pass filter)

$$\epsilon = \frac{2}{3} = .667$$

One of the main differences in the distribution of peaks for the two-degree-of-freedom configuration, in contrast with the Rayleigh distribution, is the occurrence of negative-valued maxima. This can be seen to result from the introduction of the 'normal' component, which is symmetrical about zero peak stress (or the mean stress). The proportion of negative maxima, is given in Reference 31 (Eq. 3.4) as r .

where

$$r = \frac{1}{2} (1-R)$$

$r = 2\%$ for the 1-Lever case

$r = 21.5\%$ of the maxima for the 2-Lever case

In Reference 28, Fraich gives the equivalent peak RMS equation

as

$$\sigma_p = \sqrt{1+r^2} \psi_0^{1/2} = \sqrt{2} \psi_0^{1/2} \quad \text{if pure Rayleigh} \quad (29)$$

Thus

$$\begin{aligned} \sigma_p &= 1.39 \psi_0^{1/2} && \text{1-Lever} \\ &= 1.15 \psi_0^{1/2} && \text{2-Lever case} \end{aligned}$$

This peak RMS value occurs at the mode of the Rayleigh component distribution.

As pointed out in Reference 31, the distribution of minima is the reflection of Figure 15 about $\eta = 0$.

Using the non-dimensional stress parameter η with $R = .57$ (the two-lever case)

$$p(\eta) = .328 e^{-.74\eta^2} + .285 \eta e^{-.5\eta^2} (1 + \text{erf} .49\eta) \quad (30)$$

This relation is plotted in Figure 15,

4.3 Test Results

The single RMS (Stationary) fatigue endurance are given in Figure 9. The mean values in this plot are based on 50 cps as a reference frequency. See Table 3.

$\psi_0^{1/2}$ ksi	\bar{T}_{secs}	$(N_f)_{N_1}$	$(N_f)_{N_0+}$	$(N_f)_{50 cps}$
10.4	2,900	123,250	70,760	145,000
8.8	9,500	403,750	231,800	475,000
7.9	24,600	1,045,500	600,240	1,230,000

A crack detection study of the two-lever test specimens revealed crack nucleation similar to that observed with the single-lever Random Amplitude tests. Figure 16 shows the cracks on the specimens tested at the level ($\psi_0^{1/2} = 10.4$ ksi). The mean number of cracks for each of the three stress levels is shown with the corresponding stress level value from the single lever tests in Figure 12. It can be seen that the introduction of a second degree of freedom accelerates the nucleation process.

The discovery of visible crack nuclei on the specimens used in the random load tests led naturally to a re-examination of the specimens tested under Constant Amplitude conditions. All the Constant Amplitude specimens tested with the Random load machine exhibited negligible crack nuclei apart from the failure crack. A random sampling of the earlier Constant Amplitude test pieces tested in the Amsler Vibrophore confirmed this finding. From the proportion of negative maxima mentioned in this section, it appeared that possibly the value of the "oscillating mean stress" may affect the appearance of crack nuclei. Accordingly three widely-spaced values of mean stress were used to augment the data obtained with $S_m = 16$ ksi. For all these tests the Constant Amplitude alternating stress was 34 ksi. The results are given in Table 8. It can be seen that the number of crack nuclei is small for all mean stress levels except for the compressive mean stress case $S = -34$ ksi + 34 ksi, a fluctuating compression test. These tests revealed an astonishing

average crack nuclei of 15 per specimen. A sample of these specimens is shown in Figure 27. Unfortunately there were no tests performed between zero mean stress and this very high compressive mean stress. Certainly this would appear a worthwhile future project utilizing Constant Amplitude test equipment.

4.4 Application of Cumulative Damage Laws

4.4.1 The Linear Law

In order to apply the linear or Miner Law to the results from a flexible or multimode structure, it is necessary to obtain the cycle ratio at each level of stress. The number of stress peaks lying between s and ds is $\bar{T} p(s) ds$, where \bar{T} is the mean duration of the test in seconds, is:

$$\begin{aligned} dn(s) &= \bar{T} p(s) ds = \frac{\bar{T} N_1}{\psi_0^{1/2}} p(\eta) ds \\ &= \bar{T} p(\eta) d\eta = N_f p(\eta) d\eta \end{aligned} \quad (31)$$

Thus we have, for the three test points

$\psi_0^{1/2}$	$dn(s)/d\eta$
10.4 ksi	11,850 $p(\eta)$
8.8 ksi	45,880 $p(\eta)$
7.9 ksi	132,340 $p(\eta)$

The abscissa of Figure 15 is a stress parameter. For the linear rule, the S-N curve of the material is used to obtain the cycles to failure $N_f(s)$ for evaluation of the cycle ratio at all stress levels. From the S-N data for the material used in these tests, $N_f(s)$ is greater than 10 million for $s \leq 18$ ksi, or a value of $\eta = 1.8$ at least, for the test RMS levels considered. It can be seen from Figure 15 that as ϵ increases, a larger proportion of peaks will occur below the endurance limit, as the normal component increased in proportion for a given RMS stress level. Now at $\eta = 1.8$ for $\epsilon = .82$, the Rayleigh component is greater than 85% of the total distribution, and only peaks above this η level need be considered in the linear summation. Consider the Rayleigh term in the basic equation

$$[p(\eta)] = \frac{R}{2} \eta e^{-\eta^2/2} (1 + \text{erf } .49\eta) \quad (32)$$

Rayleigh

Note that if the error function term in brackets were replaced by unity at $\eta = 1.8$, the error would be a 12% increase. In other words, using the simplified expression

$$p(\eta) = R \eta e^{-\eta^2/2} \quad (33)$$

as the effective Rayleigh distribution for the 2-lever case, the error at $\eta = 1.8$ is only 4%, decreasing to zero as η increases. This equivalent Rayleigh distribution is also shown in Figure 15.

An analytical evaluation of the equivalent Rayleigh fatigue curve may now be carried out using the procedure of the previous section

$$p(s) = \frac{N_1}{\psi_0^{1/2}} R \frac{s}{\psi_0^{1/2}} e^{-s^2/2\psi_0} = N_{0+} \left(\frac{s}{\psi_0} e^{-s^2/2\psi_0} \right) \quad (34)$$

The mean time to failure, in seconds is

$$[\bar{T}] \equiv \left[\frac{\text{peaks/sec}}{\text{peaks or cycles}} \right]^{-1}$$

If we use the number of peaks N_1 to determine the cycles to failure:

$$\begin{aligned} N_{f_r}^{-1} &= [N_1 \bar{T}]^{-1} \\ &= N_1^{-1} \left[\frac{N_{0+}}{\psi_0} \int_0^{\infty} \frac{s e^{-s^2/2\psi_0}}{N(s)} ds \right] \end{aligned} \quad (35)$$

$$\begin{aligned} \therefore N_{f_r} &= \frac{1}{R} \left(\frac{S_0}{S} \right)^8 \frac{1}{\Gamma(1+1/2)} \\ &= \frac{.22}{R} (N_f)_{CA} \end{aligned} \quad (36)$$

While this results in an accurate representation only of the high values of η , at the expense of all but neglecting the lower stresses, it can be seen that the contributions to the linear summation at low stress levels is negligible. Since $\int_0^{\infty} p(\eta) d\eta = R$, we are omitting 100(1-R)% of the peaks from the calculation, which is quite a high percentage. An alternative procedure would be to use the exact $p(\eta)$, but the result would not be much different. Thus an equivalent Rayleigh distribution for $R < 1$ is obtained by dividing the Rayleigh line for $R = 1$ by $(R)_{\text{complex}}$.

When $R = .57$ this factor for the Rayleigh endurance is 1.75. Alternatively, the equivalent Rayleigh endurance will be exactly equal to the predicted cycles to fail from Section III, if the number of zero crossings with positive slope, N_{0+} is used to assess the cycles endured.

4.4.2 Fuller's Technique

As described in Ref. 23, the application of Fuller's cumulative damage rule involves the calculation of the cumulative probability.

$$P(\eta) = \int_x^{\infty} p(s) ds$$

For the present case $\beta \doteq .774$ for $\epsilon = .82$ and Fuller's endurance line can be found as before. This value of β was obtained by using the probability limits $P = .003$ and $P = .999$ in the analytical expression. The former value is dictated by the clipping limit (3.6). The latter occurs at about $\eta = -2.5$. Thus $k_v = .774 \times .0577$ and $k_{RMS} = -.160 = -.0446$

The resulting random load fatigue line is shown in Figure 4.

4.4.3 Results of Cumulative Damage Analyses

$\sigma_{P_{k_{s,i}}}$	$(N_f)_{N_1}$	$(N_f)_{N_1}^{Miner}$	$(N_f)_{Fuller}$
12.0	123,250	10.6×10^6	164,000
10.1	403,750	27.2×10^6	303,000
9.1	1,045,500	44.5×10^6	420,000

As in the single-lever case, Fuller does not predict the rapid increase in endurance at the lowest stress level. It would be interesting to test at different values of R to assess further the comparative merits of these two techniques.

V. QUASI STATIONARY RANDOM AMPLITUDE FATIGUE

5.1 Introduction

The importance of the assumption of stationarity in the random process being considered is clearly shown in the interesting discussion of the occurrence of very large peaks in ocean waves given in Ref. 40. It has been found that, while the wave peaks can be well represented by the Rayleigh distribution, the low frequency of the waves makes the problem of accurate assessment of the maximum peak difficult, due to violation of the requirement of stationarity for the 'sea' considered. The general statistical level of the waves usually changes before the rare values predicted by the Rayleigh probability law can occur. Longuet-Higgins gives a typical example where it takes $11\frac{1}{2}$ days for the (mean)occurrence of a peak at 3.5 RMS and concludes that it is unlikely that the sea state would be stationary for such long periods of time. It is, therefore, important to assess the statistical behavior of the mean intensity, to obtain the compound probability of the 'instantaneous' peak values at all levels.

A disadvantage to the use of stationary random noise to generate fatigue loads is that there is no control over the probability density of the maxima of the function. It will be demonstrated in this section that the application of programmed random loading not only overcomes the above restriction, by allowing almost any form of peak frequency distribution to be generated, but also is highly representative of the random load history actually encountered by such structures as aircraft wings.

Throughout the life history of an aircraft for instance, the structure experiences a discrete change in random load intensity when the pilot flies from one patch of turbulence (shown to be effectively stationary by the work of Ref. 22), and abruptly enters another path of turbulence, either of greater intensity or less. When the discrete nature of this transition from one stationary turbulence patch to another is appreciated, it can readily be seen that discrete programming of the RMS level of stress intensity with the random fatigue machine is not an approximation to an actually continuous variation (as Programmed Constant Amplitude tests are), but a satisfactory simulation of the actual service history. The gust history is then reduced to the specification of the probability distribution of the RMS gust velocity in each stationary section. It has also been found that, over the service life of a great many structures other than aircraft, the actual periods of use are discrete intervals, and as such the loadings in the long run can be represented by a Quasi-Stationary Random Process.

Two conditions are required to simulate such a Quasi-Stationary random process. They are:

1. Control over the 'patch' RMS level and avoidance of any appreciable non-stationary behavior in this quantity.
2. Control over the final distribution of patch RMS stress levels, so that the overall stress history closely resembles the desired one.

A knowledge of the service load distributions arising from a quasi-stationary load history is important to obtain not only the probability of occurrence of extreme values for static design considerations, but also the occurrence of the most probable (and therefore the most frequent) loadings for fatigue studies of both the structure and its occupants.

Considerable work has been done by the NASA to establish the distribution of RMS gusts. The results of their work (Ref. 41) have been incorporated into a military reliability specification (Ref. 42). The distribution agreed upon is a dual exponential distribution to include both 'storm' and 'non-storm' turbulence. In their notation:

$$f(\sigma_w) = P_1 \frac{1}{b_1} \sqrt{\frac{2}{\pi}} e^{-\frac{\sigma_w^2}{2b_1^2}} + P_2 \frac{1}{b_2} \sqrt{\frac{2}{\pi}} e^{-\frac{\sigma_w^2}{2b_2^2}} \quad (37)$$

where $\hat{f}(\sigma_w)$ is the probability density distribution of σ_w , the root-mean-square gust velocity and P_1, P_2 are parameters representing the proportion of time in non-storm and storm turbulence respectively. The scale-parameters b_1 and b_2 represent the relative scale for the individual probability distributions for the two types of turbulence.

In England, Raithby has described a similar dual exponential relation (Ref. 43) for discrete gusts in the form

$$F = 27.8 e^{-\frac{v}{2.916}} + .878 e^{-\frac{v}{4.803}} \quad (38)$$

where F is the number of gusts $\geq v$ for each gust ≥ 10 fps and v = gust velocity, fps.

In performing random programmed RMS Random Amplitude tests with the fatigue machine, it is also possible to simulate the change in RMS stress level which occurs dynamically on an aircraft wing when the aircraft abruptly enters a new patch of turbulence. This change is quite similar to the change in specimen stress history obtained when the RMS level of the machine is abruptly altered manually from one level to another. Figure 17 shows an example of manually increasing the true RMS level of the machine from 5.3 ksi to 11.0 ksi. The sample trace at the top of the figure was taken at slow speed (5 mm/sec) while the lower trace shows the continuous dynamic nature of the change in detail, by running the trace at high speed (625 mm/sec). Since no appreciable 'clipping' of the process occurs over the range of RMS levels considered, the variation of the single parameter, patch RMS stress level, is adequate to specify the changes in load history completely.

5.2 The Rectangular Distribution

As a preliminary step to the simulation of such a process, consider the application of a Quasi-Stationary process in which the frequency function of RMS Stresses is rectangular; i. e., every value of RMS stress in the range considered is equally probable. The endurance curve shown in Fig. 19 was arrived at by the application of successive RMS stress levels for one minute each, following the percent values given by Hald's Table of Random numbers (Table XIX, of Ref. 37 beginning on Page 93) and partially reproduced in Table 4.

One minute corresponds to about 3000 cycles during which, on the average, a stress of 3.6 RMS is exceeded once. Consequently the specimen is subjected to a good sample of the random process at each value of RMS.

Values were taken reading down the first column of numbers, then down the second column etc., until the specimen failed. The range of RMS stress levels was specified as $0 \leq \sigma \leq \hat{\sigma}_f$. Since the distribution used is rectangular, the Overall RMS depends only on the maximum RMS stress level in the range.

The overall RMS stress level for a Rectangular Distribution of RMS stresses ranging from zero to $\hat{\sigma}$, in terms of $\hat{\sigma}$:

$$\text{is } \frac{1}{\hat{\sigma}} \int_0^{\hat{\sigma}} \sigma^2 d\sigma = \frac{\hat{\sigma}^2}{3} \quad (39)$$

$$\text{Thus } \sqrt{\bar{\sigma}^2} = .577 \hat{\sigma}$$

The probability density of half-cycle stress peaks for this distribution can be obtained by assuming the Rayleigh distribution of peaks within a given patch of turbulence.

If N_f is the number of cycles to failure, then the number of cycles spent with a value of RMS between σ and $\sigma + \Delta\sigma$ is $N_f \Delta\sigma/\hat{\sigma}$. If this is a sufficiently large number to be fully representative of the process, then the number of cycles during which S has a maximum between S and $S + dS$ while σ lies between σ and $\sigma + \Delta\sigma$ is $N_f \frac{S}{\sigma^2} e^{-S^2/2\sigma^2} \frac{\Delta\sigma}{\hat{\sigma}}$.

Consequently, the number of cycles having a stress maximum between S and $S + dS$ during the lifetime is $N_f \frac{S}{\sigma^2} e^{-S^2/2\sigma^2} \frac{\Delta\sigma}{\hat{\sigma}}$.

and the probable density of stress maxima is thus:

$$\begin{aligned} p(S) &= \sum \frac{S}{\sigma^2} e^{-S^2/2\sigma^2} \frac{\Delta\sigma}{\hat{\sigma}} \\ &= \int_0^{\infty} \frac{S}{\sigma^2} e^{-S^2/2\sigma^2} \frac{d\sigma}{\hat{\sigma}} \quad (40) \end{aligned}$$

$$\text{then } p(S) = \frac{1}{\sqrt{2}\hat{\sigma}} \left[\Gamma\left(\frac{1}{2}\right) - \Gamma\left(\frac{S^2}{2\hat{\sigma}^2}, \left(\frac{1}{2}\right)\right) \right] \quad (41)$$

Where $\Gamma\left(\frac{S^2}{2\hat{\sigma}^2}, \left(\frac{1}{2}\right)\right)$ is the incomplete Gamma Function evaluated to $\frac{S^2}{2\hat{\sigma}^2}$. This can be carried out using Pearsons Tables (Ref. 44) by putting the above equation in the form

$$p\left(\frac{S}{\hat{\sigma}}\right) = \sqrt{\frac{\pi}{2}} \left[1 - I\left(\frac{S^2}{\sqrt{2}\hat{\sigma}^2}, -\frac{1}{2}\right) \right] \quad (42)$$

using Pearson's notation for I .

This distribution is shown in Fig. 18. The distribution contains an extremely large number of small half-cycle stress peaks, compared with the rare occurrence of high stress levels. The expression for the cumulative probability

$$P\left(\frac{S}{\hat{\sigma}} > \frac{S_0}{\hat{\sigma}}\right) = \sqrt{\frac{\pi}{2}} \left(3.6 \hat{\sigma} - S_0 \right) - \frac{1}{\sqrt{2}} \int_{S_0}^{3.6 \hat{\sigma}} \Gamma\left(\frac{S^2}{2\hat{\sigma}^2}, \left(\frac{1}{2}\right)\right) dS \quad (43)$$

where 3.6 is the clipping ratio for the signal. Since \hat{m} is not a simple analytical function of S , this integration would be difficult in an analytic form. Since it is required to obtain $n(s)$ for the Miner calculation in any event, the density distribution of stress will be evaluated instead, and a numerical cumulative integration carried out to obtain the Cumulative Probability needed for Fuller's treatment, using the logarithm of the cumulative probability function, as described in Section III.

5.3 Test Results - Rectangular Distribution

Test Results

The overall RMS achieved with a given range of stresses used will have a significant variation due to the fact that one specimen will have a different endurance than the next, and consequently experience a different duration of the random number sequence. For the tests described in this report the lives were sufficiently short (less than 400 minutes) for a calculation of overall RMS to be performed for each specimen endurance. It was found, as can be seen from Fig. 19, that this refinement greatly reduced the apparent scatter, since a pronounced correlation existed to yield high endurances for low overall RMS levels, and vice versa. Due to this effect, it was found that, by specifying only three values of $\hat{\sigma}$, 10 ksi, 10.8 and 11.7 ksi (with overall RMS $\sigma = 5.77, 6.24$ and 6.75 respectively) and testing about 4 specimens with each range, a continuous line of endurances was obtained over a wide range of overall RMS stress levels. See Table 5.

This endurance curve obtained for the rectangular Quasi-Stationary process using unnotched specimens, exhibited surprisingly low endurances when compared with the Rayleigh curve. Also the mean number of crack nuclei for the low overall RMS stress level is comparable with the highest RMS stress level results from the stationary random amplitude program (Fig. 12). It is interesting to speculate whether the great number of fatigue cracks found in aircraft structures in service is probably not entirely due to stress concentrations alone, but also due to the Quasi-Stationary nature of service loadings, since the specimens tested in this manner were unnotched. A sample of Rectangular Distribution specimens is shown in Fig. 20.

5.4 Cumulative Damage - Rectangular Distribution

5.4.1 The Linear or Miner Law

From inspection of Fig. 18, it can readily be seen that the vast majority of stress peaks for such a distribution lie below the S-N curve. For example, consider $\hat{\sigma} = 11.7$ ksi. From Table 3, Ref. 1, a stress level of 18 ksi represents a life of about 12 million cycles, so that all the stress peaks yielding significant cycle ratios will lie above $S/\hat{\sigma} = 1.5$. The area under the curve in Fig. 18 is Unity. One million cycles would therefore be distributed as tabulated below, for $\hat{\sigma} = 11.7$ ksi.

$S_{k\text{ksi}}$	$S_2-S_1\text{ksi}$	Cycles $\geq S_2$	Cycles in ΔS	$(N \text{ failure})_S$	$\frac{1}{N} \times 10^3$
18	17-19	80,000	25,000	12,704,000	1.97
20	19-21	55,000	19,000	4,682,900	4.06
22	21-23	36,000	13,000	1,845,900	7.04
24	23-25	23,000	8,700	813,400	10.70
26	25-27	14,300	5,300	416,000	12.74
28	27-29	9,000	3,700	247,300	14.96
30	29-31	5,300	2,200	164,800	13.35
32	31-33	3,100	1,370	117,800	11.63
34	33-35	1,730	830	87,300	9.50
36	35-37	900	450	65,900	6.83
38	37-39	450	250	50,100	4.99
40	39-41	200	146	38,300	3.81
Total $\sum \frac{1}{N} = 0.11$		(54 cycles ≥ 41 ksi)			

Now from Section IV, the number of maxima per second, $N_1 = 50.6/\text{second}$ for the single-lever configuration. Therefore 1 million cycles will take about 20,000 seconds or about 5 1/2 hours. From the above calculation the endurance for the quasi-stationary loading using the rectangular distribution ($\hat{\sigma} = 11.7$ ksi) will be of the order of 50 hours. The average endurance from Table 5 was about 1 1/2 hours. Clearly the linear rule is inadequate to predict life using realistic load distributions, since, aside from stress interaction, the calculation has ignored a very large number of cycles, viz. 92% of the total applied to the structure.

5.4.2 Fuller's Method

Replotting the distribution shown in Fig. 18 to obtain the cumulated distribution of peaks (on a logarithmic scale) versus the stress peak level, one obtains a value for Fuller's parameter ($\beta = .58$ when considering one thousand peaks. Using this value, and following the method outlined in previous sections, Fuller's line underestimates the intermediate stress level endurance.

A re-examination of Fuller's treatment for the stationary Rayleigh distribution suggests that possibly the criterion implied by the use of 1000 cycles may have been fortuitous, in that it gave the same result as one would obtain using an alternative criterion; i. e. that the Cumulative Probability function be plotted to the maximum stress peak value for the test. When this is done, one obtains $\beta = .665$. That is, plotting the cumulative probability distribution to $S = 3.6 \hat{\sigma}$ results in $\beta = .665$.

The ratio of maximum stress peak to the overall RMS will then be given from

$\hat{\sigma}$ ksi	\hat{S} ksi	Overall RMS = 0.577 $\hat{\sigma}$	Overall RMS peak
10.0	36.0	5.77 ksi	8.165 ksi
10.8	38.9	6.24 ksi	8.825 ksi
11.7	42.1	6.75 ksi	9.546 ksi

Thus $\hat{S} = 4.4$ (Overall RMS peak)

The slope of Fuller's line is thus (from Section III)

$$-4.4 \times 0.0384 = -0.169$$

This line is shown in Fig. 19 with the experimental data from Table 5. The result is in reasonable agreement with tests carried out at the intermediate levels of stress. The modification of Fuller's rule to depend on the occurrence of the maximum stress peak is anticipated by the theory proposed by Freudenthal, as described in the next sub-section.

5.4.3 Freudenthal's Method

Since each turbulence patch has the Rayleigh distribution

$$N_{fr}^{-1} = \int_0^{\infty} \frac{p(s)}{N(s)} ds = \int_0^{\infty} \frac{p(s)}{10^4} \left(\frac{s}{s_1}\right)^p ds \quad (44)$$

where

$$\left. \begin{array}{l} s_1 = 51 \text{ ksi} \\ p = 4.0 \end{array} \right\} \text{Section 3.4}$$

and

$$p(s) = \frac{1}{\sqrt{2} \sigma} \left[\Gamma\left(\frac{1}{2}\right) - \sqrt{\frac{s^2}{2} \sigma^2} \Gamma\left(\frac{1}{2}\right) \right] \quad (41)$$

(Page 31) Section 5.2

A numerical evaluation of the damage using Freudenthal's S-N equation

$$N_f = 10^4 \left(\frac{51}{s}\right)^4$$

can be carried out using the million-cycle load spectrum as shown in sub-section 5.4.1, but including the lower stress levels. The value for the summation $\sum \frac{1}{N}$ with a rectangular distribution was

$$\sum \frac{1}{N} = 0.44$$

For this value, the predicted endurance (from Section 5.4.1) is about 11.0 hours. While this is still a ten-fold increase over the observed value, it is certainly a better estimate than the linear rule.

5.4.4 Life Prediction Using Units of RMS Stress

Since we have the Stationary Rayleigh endurance curve (Fig. 4), it would be interesting to attempt a life prediction for the rectangular Quasi-Stationary tests, which are essentially a programming of discrete RMS levels, using a linear summation of cycles at a given RMS divided by the cycles to failure at that RMS, from the Stationary Rayleigh curve.

This procedure was carried out using a linear interpolation between the stationary Rayleigh mean endurance obtained from testing. These values are given in Section 5.5.3, where this technique was applied to an arbitrary RMS distribution. For the present case, the Rectangular distribution, the results were, using 1 minute (3,036 cycles) per RMS level:

$\frac{\Delta}{\sigma_{ksi}}$	<u>Time</u>	$\sum \frac{n}{N}$	<u>N_f predicted</u>
11.7	117 minutes	.364	974,550
10.8	108 minutes	.225	1,285,750
10.0	100 minutes	.186	1,630,330

It can be seen from Fig. 19, that this method is not very promising on the face of this example, which is probably an unsafe oversimplification of the effect of the Quasi-Stationary load spectrum. However, it does yield predictions which are closer than the more conventional techniques discussed elsewhere in this report.

5.5 Tests with Other Distributions

5.5.1 Transformations to Other Distributions

When considering the transformation of a rectangular distribution set of random numbers to another distribution whose form is asymptotic with increasing stress level, it is necessary to employ truncated distributions with the maximum RMS obtainable set at some realistic value, such as, say, the (static) limit load. The respective values of the rectangular distribution are then used to obtain random values of the upper limit in the cumulative probability function of the new distribution, as indicated in Ref. 45, i. e.

$$\int_{-\infty}^x p(x) dx = D \quad (45)$$

where D = random number in the rectangular distribution

and $p(x)$ = probability density function in the new distribution

5.5.2 Tests with the Truncated Gaussian and Truncated Exponential QS Distribution

a) Truncated Exponential QS Distribution

The integral of the truncated probability density between truncation points is

$$P(x) = \int_{-\hat{x}/\sigma}^{\hat{x}/\sigma} K e^{-\frac{|x|}{\sigma}} d\left(\frac{x}{\sigma}\right) = 1 \quad (46)$$

where K is the amplification factor applied to all values of the basic asymptotic distribution to obtain values in the truncated distribution. For the maximum value of the RMS, \hat{x} to be 1.7 times the overall RMS level (here denoted as σ), i. e., for $\hat{x}/\sigma = 1.7$, $K = 0.612$. The overall RMS level of the quasi-stationary process is obtained from the equation

$$S^2 = \frac{2K}{\sigma} \int_0^{\hat{x}} e^{-\frac{x}{\sigma}} x^2 dx = 2K \sigma^2 \int_0^{\frac{\hat{x}}{\sigma}} (3) \quad (47)$$

Thus $S = 0.7709 \sigma$ where σ is such that $1.7 \sigma = \hat{x}$, i. e., the overall RMS level for the truncated distribution is 77 percent the value for untruncated distribution. A sample set of random numbers obtained using the truncated exponential distribution is shown in Table 4.

b) The Truncated Normal Distribution

The cumulative distribution $P(x)$ for the truncated normal distribution is

$$P(x) = \frac{K}{\sqrt{2\pi}} \int_{-\infty}^{\hat{x}/\sigma} e^{-x^2/2\sigma^2} d\left(\frac{x}{\sigma}\right) - \frac{K}{\sqrt{2\pi}} \int_{-\infty}^{-\hat{x}/\sigma} e^{-x^2/2\sigma^2} d\left(\frac{x}{\sigma}\right) \quad (48)$$

The second term = 0.04457 when $\hat{x}/\sigma = -1.7$, as shown in Table II of Ref. 37, and the numbers are generated by evaluating the integral in the first term from Table II. A sample of these numbers is given in Table 4.

Unfortunately, it was not possible to test extensively with these two extremely interesting load histories. However, two specimens were used for each of these two quasi-stationary loadings and are shown in Table 5. If anything, these sparse results indicate lives of the same order of magnitude, or less, than obtained using the rectangular RMS distribution. This is not unexpected since an attempt was made to test at close to the same overall RMS for these distributions as for the rectangular, with similar values of maximum RMS, $\hat{\sigma}$. It is obvious that such restrictions result in severe truncation, with the distributions approaching the rectangular. A more interesting test would have been to use a lower RMS and hence obtain a greater contrast in distribution. (The final distribution of stress peaks for these loadings is shown in Fig. 18 for a test duration of 200 minutes each.)

However, the endurance line for these QS tests appears to be characteristically flat, and since the application of RMS levels was manual, this innovation was not attempted.

5.5.3 Arbitrary Distributions of RMS Levels

In order to obtain the distribution of stress peaks from a given arbitrary Quasi Stationary Distribution of RMS levels, a computer program was developed which obtained the proportion of stress peaks at each of a large number of stress levels, assuming 100% Rayleigh distribution for a given RMS level. These proportions were then obtained for all RMS levels desired. By storing this information, all that is required is the relative proportion of time spent at each RMS level for a summation to be carried out yielding the final stress peak density distribution. That is;

$$p(s) = \sum_{\sigma_i} p_i \frac{s}{\sigma_i^2} e^{-\frac{s^2}{2\sigma_i^2}} \quad (49)$$

where p_i = final proportion of total time spent at RMS level σ_i .

As an example, a series of tests reported in Table 5 had the following average measured values of p_i (where total time is unity)

σ_i	$N_{f_{RCS}}$	p_i	$\left(\frac{A}{N}\right)_r$	σ_i	$N_{f_{RCS}}$	p_i	$\left(\frac{A}{N}\right)_r$	σ_i	$N_{f_{RCS}}$	p_i	$\left(\frac{A}{N}\right)_r$
5.3 ksi	7,000	.139	.0199	7.1	857	.014	.0163	9.0	500	.003	.0060
5.4 "	6,500	.090	.0138	7.3	806	.012	.0149	9.1	490	.017	.0347
5.5 "	6,000	.058	.00966	7.4	780	.009	.0115	9.2	480	.003	.00625
5.6 "	5,500	.034	.00618	7.5	754	.013	.0173	9.3	470	.002	.00426
5.7 "	5,000	.033	.0066	7.6	729	.019	.0261	9.4	460	.005	.0109
5.8 "	4,600	.034	.0074	7.7	703	.021	.0299	9.5	450	.010	.0222
5.9 "	4,200	.028	.00667	7.8	677	.013	.0192	9.6	440	.019	.0432
6.0 "	3,800	.048	.0126	7.9	651	.007	.0117	9.7	430	.002	.00465
6.1 "	3,400	.017	.0050	8.0	626	.002	.0032	9.8	420	.008	.0190
6.2 "	3,010	.027	.0090	8.1	600	.012	.020	9.9	410	.005	.0122
6.3 "	2,600	.029	.0111	8.2	588	.020	.034	10.3	370	.015	.0406
6.4 "	2,190	.027	.0123	8.3	577	.006	.0104	10.4	360	.003	.00833
6.5 "	1,780	.026	.0146	8.4	566	.008	.0141	10.8	320	.014	.0438
6.6 "	1,370	.032	.0234	8.5	555	.006	.0108	10.9	310	.005	.0161
6.7 "	960	.020	.0208	8.6	544	.006	.0110	11.3	270	.005	.0185
6.8 "	934	.019	.0204	8.7	533	.007	.0131	11.6	206	.004	.0194
6.9 "	908	.010	.0110	8.8	522	.012	.0230				
7.0 "	883	.016	.0181	8.9	511	.006	.0107				

A linear summation of fatigue damage was calculated assuming

- Total time 1 million cycles ($5\frac{1}{2}$ hrs.) and
- Using RMS levels as units, with failure times from the Rayleigh (Stationary) curve.

Using this technique, the mean endurance is predicted as 6.6 hours, whereas the average test duration was of the order of 2 hours (see Table 5).

Returning to the more conventional method of life prediction, we can apply the Linear law and Freudenthal's rule to the final distribution of stress peaks as shown in Fig. 21. We obtain, in one million cycles ,

S_{ksi}	$n(s)$	$(N_f)_{\text{ca}}$	$(\frac{n}{N})_{\text{miner}} \times 10^3$	$(N_f)_{\rho=4}$	$(\frac{n}{N})_{\text{Freudenthal}}$
0	0	∞	0	∞	0
2	93,000	∞	0	∞	0
4	159,200	∞	0	∞	0
6	182,200	∞	0	∞	0
8	168,200	∞	0	16,480,000	.0102
10	133,600	∞	0	6,765,000	.0198
12	95,200	∞	0	3,264,000	.0291
14	62,600	∞	0	1,755,000	.0356
16	39,000	∞	0	1,034,000	.0377
18	24,000	12,704,000	1.890	641,600	.0374
20	14,380	4,682,900	3,070	423,300	.0340
22	856	1,845,900	.4640	289,500	.0030
24	502	813,400	.6170	203,800	.0025
26	28	416,000	.0670	147,500	.00019
28	12	247,300	.0485	109,700	.00012
30	6	164,800	.0364	83,500	.00007
32	4	117,800	.0340	64,000	.00006
34	2	87,300	.0229	50,600	.00004
36	0	-	0	-	-
38	0	-	0	-	-
40	0	-	0	-	-

The overall RMS level for these tests was 6.92 ksi.

Using the linear law $(N_f)_{\text{miner}} = \frac{1 \text{ million}}{6.25 \times 10^{-3}} = 150 \text{ million cycles}$
 $\hat{=} 34 \text{ days}$

Using Freudenthal's fictitious S-N curve:

$$(N_f)_{\text{Freud.}} = \frac{1 \text{ million}}{.21} = 4.78 \text{ million cycles}$$

$$\hat{=} 26 \text{ hours}$$

compared with the average experimental life, which was about 2 hours.

A qualitative survey of the secondary cracks in the failed specimens revealed fewer cracks in general than was the case with the Rectangular

distribution. Possibly the relative lack of very low stress cycles, which appears to be the essential difference between the two RMS distributions (see Table 5), would account for this behaviour. The secondary crack population is similar to that for the Stationary Rayleigh results. Indeed, the final peak distribution with the arbitrary RMS history (Fig. 21) is closely akin to a Stationary Rayleigh distribution of the same value as the overall RMS level.

VI. ENDURANCE BEHAVIOR WITH CONSTANT AND RANDOM AMPLITUDE PRELOAD

6.1 Introduction

In this section a study of the effect of preload on Constant Amplitude endurance will be presented, using the test results obtained in this program. The test results involving constant amplitude preload are presented in Ref. 1, while the random amplitude preloading results are contained in Table 7 of this report.

The resulting plots of the Constant Amplitude endurances when given a preload, (either Constant or Random Amplitude) exhibit a truncated-log-normal probability pattern, due to the fact that the extent of fatigue damage due to preload is itself a random variable, rather than being a uniform quantity; as in Fig. 24. The constant amplitude endurances represent an overlapping of the constant amplitude population on the preload population of partially-damaged specimens. The most significant effect of such overlapping is the greatly increased probability of very short and very long constant amplitude endurances due to the cases where preloading causes above-average and below-average damage respectively. Hence the endurance curves show a large drop-off at the low probability endurances. This effect sometimes appears in two-level single-jump constant amplitude tests shown in TN 35 (see for example Fig. 12, Ref. 1) where although the number of cycles of prestress are fixed, damage is still a random variable. Another example of this "asymptotic" behavior of such results in Fig. 14 (b) of Ref. 15.

Of course, the truncation phenomenon complicates the choice of a mean endurance for the test configuration. Keeping in mind the uniform slope of the intermediate probabilities, the natural choice appears to be the intercept with 50% probability, of the best straight line through the endurances which are least affected by truncation.

6.2 Endurance Behavior with Constant Amplitude Preload

The two-level tests reported in TN 35 (Ref. 1) were not analysed in detail in that note. Basically the method employed was that referred to as the Equivalent Fatigue Damage Method (EFD) in Ref. 46, which is itself a generalization of the two-level technique originally used to obtain French's 'Damage line' (Ref. 23).

6.2.1 Low Prestress - High Test Stress Results

In order to establish the statistical significance of these two-level fatigue tests, use is made of the fact that two separate samples were obtained of the single-level endurance at the 'test stress', 34 ksi, and as such constitute two sets of "Stochastically Independent" observations. Since both samples 34 and 34a obviously come from the same population, the F-test for variance (Ref. 47) and the t-test for difference in means (Ref. 48) will be used to assess the significance of these tests.

From Table 3, Ref. 1

<u>Test</u> <u>S_a</u>	<u>Sample</u> <u>number</u>	<u>Sample mean</u> <u>cycles</u>	<u>Log mean</u>	<u>Standard</u> <u>Deviation</u>
34	n ₁ = 9	100,000	$\bar{x}_1 = 5.000$	s ₁ = .179
34a	n ₂ = 9	157,000	$\bar{x}_2 = 5.196$	s ₂ = .273

The variance ratio F is $(.273/.179)^2 = 2.33$. From Fig. 8, Ref. 47, F = 3.4 for 95% significance. Since our value is less, the variances do not differ significantly.

The variance of the S² distribution (using the notation of Ref. 48) is therefore

$$S^2 = \frac{f_1 s_1^2 + f_2 s_2^2}{f_1 + f_2} = .0533 \quad (50)$$

$$s = .231 \quad f_i = n_i - 1$$

The resulting t-distribution is

$$t = \frac{\bar{x}_1 - \bar{x}_2}{s \sqrt{\frac{1}{n_1} + \frac{1}{n_2}}} = 1.8 \quad (51)$$

and f = 16, the degrees of freedom. $f = (n_1 - 1) + (n_2 - 1)$

From Fig. 5, Ref. 47, the significance level is 91% (i. e., less than 95%) hence the difference is not significantly demonstrated. Hence it can be assumed that the samples are from the same population.

However this criterion can also be applied to the two-level results to define the range of the Damage parameter

$$D = 1 - \frac{n_2}{N_2}$$

within which the prestress cycles have been of negligible effect, within the scatter of the test results. Consider the difference in the means of the log-endurances between the prestressed specimens (samples usually contain 9 specimens) and the virgin specimens ($n = n_1 + n_2 = 18$) used at 34 ksi:

$$\log \bar{n}_2 - \log \bar{N}_2 = \log (1 - D)$$

$$\text{Thus if } t = \frac{\log \bar{n}_2 - \log \bar{N}_2}{S \sqrt{\frac{1}{9} + \frac{1}{18}}} = 2$$

Then

$$\log (1 - D) = \frac{2}{\sqrt{6}} S = .815 S$$

From the average standard deviation σ_{est} given in Table 8 of TN 35 (.167), the average value for the pooled standard deviation $S = .212$, approximately.

$$\text{Thus if } \left| \log (1 - D) \right| < .167$$

the results will indicate that the prestressing had very little effect on the test endurance. Since in nearly every case where the prestress level was higher than the test stress level, the prestress cycle ratio was very small, this result would indicate that the linear rule was adequate for the prediction of life for these cases within the scatter of the test results. The condition on $\log (1 - D)$ means that prestress causes no significant damage if $-0.5 < D < 0.33$. Referring to Fig. 19 of Ref. 1, it appears that the majority of the low prestress test results fall within this range. This inability of the low prestress to affect the endurance at a higher test stress significantly not only indicates validity of the linear rule for the small values of cycle ratio used, but also is consistent with the assumptions contained in the Corten-Dolan hypothesis (Ref. 49). Figure 15 of TN 35 shows that the two lowest levels of the high-prestress test results also fall into this category. This latter finding will be confirmed in the following treatment of the high prestress-low test stress test results.

6.2.2 High Prestress - Low Test Stress Results

For the high-stress-to-low-stress tests, there is a possibility that some other rule than the linear rule may be more representative, such as the Corten and Dolan hypothesis. It must be kept in mind in the following that the Corten-Dolan hypothesis was first developed with a repeated two-step load history, whereas the TN 35 tests were concerned with the effects of prestressing at one stress on the subsequent constant amplitude endurance at a second 'test' stress.

The cumulative damage rule put forward by Corten and Dolan is a modification of the linear rule and has the form

$$N_g = N_1 / \sum_1^n \alpha_i (s_i/s_1)^d \quad (52)$$

where N_g = total number of cycles to failure in a variable stress spectrum

$\alpha_i N_g$ = number of cycles applied at stress amplitude S_i

d = reciprocal of the slope of the modified S-N relation (on a log-log plot)

S_1 = maximum stress peak experienced in the test

d is derived from the results of two-step cumulative damage experiments and the stress interaction parameter $R^{1/a}$ is defined as

$$R^{1/a} = \left(\frac{s_i}{s_1} \right)^d \quad (53)$$

Let total number of cycles = $n_1 + n_2 = N_g$

and $\frac{n_1}{N_g} = \alpha$, $\frac{n_2}{N_g} = 1 - \alpha$

Since $N_g = N_1 / (\alpha + R^{1/a} (1 - \alpha))$ (54)

$$R^{1/a} = \left(\frac{N_1}{N_g} - \alpha \right) \left(\frac{1}{1 - \alpha} \right) = \frac{N_1 - n_1}{n_2}$$

Now from TN 35

$$D = 1 - \frac{n_2}{N_2}$$

Thus

$$R^{1/a} = \frac{N_1 - n_1}{N_2(1 - D)} \quad (55)$$

In Ref. 49, Liu and Corten have studied the dependence of $R^{1/a}$ on the stress ratio S_2/S_1 where S_1 is the prestress and S_2 the test stress. From the generally linear log-log behavior they have obtained the relation (their Fig. 9a).

$$R^{1/a} = \left(\frac{S_2}{S_1} \right)^{5.778} \quad (2024-T4 Aluminum wire)$$

In order to assess the corresponding value of the slope for the test results of TN 35, a modified least squares regression of the data was performed utilizing the fact that the limiting point ($R^{1/a} = 1$, $S_2/S_1 = 1$) must be on the regression line. The 59 different values of $R^{1/a}$ and corresponding

S_2/S_1 taken from TN 35 have been tabulated (see Table 6) and the resulting slope value $d = 5.67$. The plot of this relation is given in Fig. 22. Using this relation, the predicted fatigue life ratio under this type of load sequence is given in Table 6, using Eq. 8 of Ref. 8.

i. e.
$$R^{1/a} = \left(\frac{S_2}{S_1} \right)^{5.67} \quad (56)$$

Thus

$$N_g = N_1 / \left[\frac{n_1}{N_g} + \frac{n_2}{N_g} \left(\frac{S_2}{S_1} \right)^{5.67} \right] \quad (57)$$

$$\frac{N_{ge}}{N_{gz}} = \frac{n_1}{N_1} + \frac{n_2}{N_1} \left(\frac{S_2}{S_1} \right)^{5.67} \quad (58)$$

Note that the basis of the method may be taken to be the use of a fictitious S-N curve. It reverts to the linear Law (or Miner Law) if

$$R^{1/a} = \left(\frac{S_2}{S_1} \right)^8 = \frac{N_1}{N_2} \quad (59)$$

A comparison of the Corten-Dolan Life ratio with the linear summation of cycle ratios is also given in Table 6. The test point designations are as given in Tables 5, 8 and 9 of TN 35. It can readily be seen that the linear rule usually overestimates the remaining life, while the Corten-Dolan life prediction is usually conservative for low prestresses and close to correct for high prestresses. (See Fig. 23). There is close qualitative agreement here with the Corten-Dolan results shown in Fig. 8, page 615 of WADC Technical Report 59-507. At low prestress levels there is little to choose between the two methods. The deviation of the Corten-Dolan life ratio at very high prestress levels is to be expected when it is remembered that the theory is limited to the elastic (pure) fatigue area of long lives.

6.3 Constant Amplitude Endurance Behaviour with Random Preload

6.3.1 Introduction

It has been pointed out by many workers that the higher stress levels seem to have the predominant damaging effect in variable amplitude fatigue. Indeed, in the most prominent cumulative damage theories which exist so far (aside from the linear law), such as those of Freudenthal (Section 3.4) and Corten and Dolan (Section 6.2.2) the maximum stress peak of the fatigue history forms the cornerstone of their analyses.

In order to shed more light on the role of the higher stress peaks in damage formation under random loads, a series of tests were conducted in which the Rayleigh fatigue history was interrupted, and the subsequent test pattern made constant amplitude to failure. By varying the runout stress level, randomly - preloaded S-N curves were obtained as shown in Fig. 25. The statistical behavior of the endurance at a given stress level is shown for one of the two pre-stress RMS levels used, in Figure 24. The 50% probability position was usually taken as the mean value. The shape of the curves in Fig. 24 is as expected when one recalls that the damage from the random pre-load will be a random variable.

6.3.2 Evaluation of the Maximum Stress Peak S_1 from the Slope of the $S_2 - N$ Curve

In Ref. 34, Poppleton extended the work of Corten and Dolan to study the Random Load endurance relation. Using Corten and Dolan's notation, their damage equation is:

$$D = m r n^a \quad (60)$$

from which Poppleton uses the derived expression

$$\begin{aligned} \Delta &= D^{1/a} = m^{1/a} r^{1/a} n \\ &= \mu \rho N_f = 1 \text{ at failure} \end{aligned} \quad (61)$$

The value of μ is a measure of the active damage nuclei, while ρ is a damage rate parameter. The maximum of μ appropriate to S_1 is $\hat{\mu}_1$. With a random loading μ_1 and S_1 , will increase on the average to the final values $\hat{\mu}_1$ and \hat{S}_1 dictated by the clipping characteristics of the signal.

If the partial damage due to random preload is designated as $D_1(t)$, then the complete damage equation is

$$D_1(t) + \hat{\mu}_1 \rho_2 n_2 = 1 \quad (62)$$

Since it is assumed that the rate parameter ρ does not vary with cycles, its value at failure in a single level test at S_2 can be substituted in the equation

$$\hat{\mu}_2 \rho_2 N_{f_2} = 1$$

$$\therefore D_1(t) + \frac{\hat{\mu}_1 n_2}{\hat{\mu}_2 N_{f_2}} = 1 \quad (63)$$

Consider the value of μ in the above equation. For the run out history there are two alternatives:

a) If $S_1 < S_2$

$$D_1(t) + \frac{\hat{\mu}_2 n_2}{\hat{\mu}_2 N_{f_2}} = 1$$

or

$$D_1(t) + \frac{n_2}{N_{f_2}} = 1$$

and the $\hat{\mu}_2$ equivalent to the higher S_2 stress achieved, is operative

This is essentially the linear damage hypothesis and gave good agreement for the low CA pre-stress tests discussed in Section 6.2.1.

b) If $S_1 > S_2$

$$D_1(t) + \frac{\hat{\mu}_1 n_2}{\hat{\mu}_2 N_{f_2}} = 1$$

and the higher pre-stress peak S_1 dictates $\hat{\mu}$.

If we introduce a reference stress S_R with damage parameters μ_R, ρ_R and note that:

$$i) \mu_R \rho_R N_{f_R} = \mu_2 \rho_2 N_{f_2} \quad (64)$$

$$ii) \frac{\mu_R N_{f_R}}{\mu_2 N_{f_2}} = \frac{\rho_2}{\rho_R} = R^{1/d} = \left(\frac{S_2}{S_R}\right)^d \quad (65)$$

from the work of Corten and Dolan (Ref. 49), the general equation developed above becomes

$$D_1(t) + \frac{\mu_2}{\mu_R} \left(\frac{S_2}{S_R}\right)^d \frac{n_2}{N_{f_R}} = 1 \quad (66)$$

Taking Logs:

If $S_1 < S_2$

$$a) \log \left[\frac{1}{1-D_1(t)} \right] + d \log \frac{S_2}{S_R} + \log \frac{n_2}{N_{f_R}} = 0 \quad (67)$$

If $S_1 > S_2$

$$b) \log \left[\frac{\hat{\mu}_1}{\hat{\mu}_R} \cdot \frac{1}{1-D_1(t)} \right] + d \log \frac{S_2}{S_R} + \log \frac{n_2}{N_{f_R}} = 0 \quad (68)$$

From these equations it is observed that a fundamental change in the slope of the run-out $S_2 - N_f$ relation will occur, most notably in Log-Log co-ordinates. If the maximum pre-stress S_1 is less than the run-out stress amplitude S_2 the slope will be δ , the same as that of the virgin S-N curve. This is a natural consequence of the application of the linear law (see Section 3.3.1).

If the pre-stress level S_1 is higher than S_2 , the former dictates the slope and it will be d , the value obtained from a consideration of the mixing of the two stress levels S_1 and S_2 according to Corten and Dolan (Sec. 6.2.2).

If the range of stresses used as run-out stress levels are such as to 'bracket' the value S_1 then the $S_2 - N_f$ curve would consist of two straight lines meeting at a 'kink' (at $S_1 = S_2$) such that the higher stress leg would have slope δ while the lower leg would have slope d .

From Section II the regressed slope of the log S-log N curve was

$$\delta = 5.54$$

while from Section 6.2.2

$$d = 5.67$$

The results of the Partial Damage tests are given in Table 7.

Regressing the data, we have:

σ_{P_1}	t_1	CA Levels		Correlation Coefficient
		Used in Regression	Slope	
13.5 ksi	30 minutes	5	-4.96	.994
13.5 ksi	60 minutes	5*	-5.42	.998
16.0 ksi	30 minutes	6**	-5.04	.920
16.0 ksi	15 minutes	5*	-5.68	.999

* lowest (6th) CA level excluded

** lowest (7th) CA level excluded

It is immediately apparent that the scatter in slopes is such as to preclude detecting the small difference in slopes necessary to establish S_1 . It should be noted, however, that the low-stress-level endurance excluded in the above regressions fall generally to the right of the regression line, which would be correct if $d > \delta$. This would suggest that a low value of S_1 fixes the number of active damage nuclei.

To examine this further, we introduce a reference stress level S_R into the Rayleigh-Miner endurance relation:

$$1 = \int_0^{\infty} \frac{N_f}{N_R} \left(\frac{S}{S_R} \right)^{\delta} \frac{S}{\sigma^2} e^{-\frac{S^2}{2\sigma^2}} dS \quad (69)$$

$$= \frac{N_f}{N_R} \left(\frac{\sigma_P}{S_R} \right)^{\delta} \Gamma \left(1 + \frac{\delta}{2} \right) \quad (70)$$

Using the Corten-Dolan framework and writing Eq. 20, Ref. 34 in the simplified form:

$$1 = \frac{\bar{\mu}}{\mu_R} \frac{N_f}{N_R} \left(\frac{\sigma_P}{S_R} \right)^d \Gamma \left(1 + \frac{d}{2} \right) \quad (71)$$

we have the general endurance relation for the Rayleigh distribution of stress peaks.

To obtain an idea of the correct value of $\bar{\mu}$ to use, consider the use of a mean value, $\bar{\mu}$ with the results of the Rayleigh tests (Table 2).

If $S_R = 51$ ksi $N_R = 10^4$ cycles
 $d = 5.67$ and $\Gamma \left(1 + \frac{d}{2} \right) = 4.9$

We have
$$\frac{\bar{\mu}}{\mu_R} = \frac{N_R}{N_f} \left(\frac{S_R}{\sigma_P} \right)^d \left[\Gamma \left(1 + \frac{d}{2} \right) \right]^{-1} \quad (72)$$

Evaluating this expression:

σ_{Pksi}	N_f cycles	$\frac{S_R}{\sigma_P}$	$\left(\frac{S_R}{\sigma_P} \right)^d$	$\frac{\bar{\mu}}{\mu_R}$
9	2,400,000	5.67	18,300	15.5
9.5	960,000	5.37	13,600	28.9
11.5	600,000	4.43	4,600	15.6
13.5	450,000	3.77	1,870	8.5
16.0	270,000	3.19	720	5.4
17.0	120,000	3.00	510	8.7
18.0	58,000	2.83	365	12.8

These results demonstrate unequivocally that a large ratio of $\bar{\mu}/\mu_R$ is needed to make the above equation agree with the experimental results.

Consider the stress peak needed to obtain these ratios of nuclei. From Eq. 12, Ref. 34 we have

$$\frac{\bar{\mu}}{\mu_R} = \left(\frac{S_1}{S_R} \right)^{\delta-d} \quad (73)$$

For the present case

$$S_1 \doteq 51 \text{ ksi} / \left(\frac{\bar{\mu}}{\mu_R} \right)^{7.7} \doteq 0 \quad (74)$$

This result points to an extremely low value of S_1 fixing the nuclei. This confirms the trend exhibited by the slopes of the random preload curves.

6.3.3 Intuitive Values of S_1 from the Probability of Occurrences

Since all these tests were carried out using the single-lever configuration, it is not difficult to estimate the maximum stress peak which is likely to have occurred under conditions of Pure Rayleigh behavior unclipped to 3.6 RMS (see Fig. 8). The value of maximum stress peak depends fundamentally on the duration of the test. The cumulative Rayleigh distribution states:

$$P(s > S_1) = \exp(-S_1^2 / \sigma_p^2) \quad (75)$$

The value of S_1 which is to be used in the cumulative damage theories may be:

- a) Occurrence of a single peak greater than S_1 .

The number of cycles before the maximum stress S_1 is exceeded once is, on the average,

$$N = e^{S_1^2 / \sigma_p^2} \doteq \frac{1}{P} \quad (76)$$

$$\therefore S_1^2 = \sigma_p^2 \ln \frac{1}{P} \quad (77)$$

Assuming 50 cps frequency						
$\sigma_{p \text{ ksi}}$	t_1	N_1	$\ln \frac{1}{P}$	σ_p^2	S_1^2	$S_1 \text{ ksi}$
16.0	15 mins.	45,000	10.71	256.00	2741.76	52.35
16.0	30 mins.	90,000	11.41	256.00	2920.96	54.05
13.5	30 mins.	90,000	11.41	182.25	2079.47	45.60
13.5	60 mins.	180,000	12.10	182.25	2205.23	47.00

Note that all the theoretical values of peak stress S_1 exceed the values of constant amplitude stresses used as run-outs (S_2). It may be argued that to obtain a kink in the Constant Amplitude slope as discussed in the previous subsection it would be necessary to set $S_1 = 28$ ksi, which is about the mid-position of the range of CA stresses (S_2) used as run-outs. For example, using $S_1 = 28$ ksi and $\sigma_p = 9$ ksi, the pre-load test time to obtain $S_1 = 28$ ksi would be about five minutes, and 20 seconds, using the above equation.

b) The stress threshold at which the stress is exceeded only 10 times during the pre-load, on the average;

σ_p ksi	t_1	$(N)_{10}$	$\ln N$	S_1^2	S_1	S_1/σ
16.0	15 mins.	4,500	8.41	2153	46.4	4.10
16.0	30 mins.	9,000	9.10	2330	48.3	4.27
13.5	30 mins.	9,000	9.10	1658	40.7	4.26
13.5	60 mins.	18,000	9.80	1786	42.3	4.45

It appears that this criterion for establishing S_1 will suffer from clipping effects. Also the .2% Proof stress for this material is 52.5 ksi, since these tests are all carried out at $S_m = 16$ ksi (Table 1 of Ref. 1). The fact that the four Partial Damage constant amplitude curves lie close to one another may be the result of all the values of S_1 being equal to 52.5 ksi (Fig. 25).

It has been suggested by Corten in Ref. 30 that the yield stress is too high to use for S_1 , and where possible, an estimate of the "maximum stress encountered" should be employed.

The value Corten suggests is within the range of S_1 specified by the stress peak which is equalled or exceeded once in 1000 cycles down to the S_1 specified by the peak equalled or exceeded once in 100 cycles. This range was obtained from a series of repeated block experiments, and Corten advises that "it is desirable to inspect the final results to determine the reasonableness of the results in relation to the properties of the material and any previous service experience." (SESA Design Clinics, SESA Annual Meeting, Detroit, Michigan, Oct., 1959).

This rather wide range of stress levels from which to specify S_1 , coupled with the method used to establish the slope parameter d has discouraged the use of this hypothesis for predicting the random load test results in this project.

6.4 Discussion of Partial Damage Results

In the equation relating the nuclei ratio to the stress ratio, used in Section 6.4.1, it must be kept in mind that the exponent $\delta - d$ represents the difference between two experimentally obtained slopes, either of which is difficult to determine accurately. The value of this exponent is therefore, subject to sizeable errors, especially when $\delta \approx d$ as in the present case. However, the usual result is that the value of S_1 is very small under these conditions. Such a result would indicate that the conditions fixing the ratio of nuclei are quite different from those suggested by Corten in Section 6.3.3.

Possibly the technique used to obtain d results in a spurious value for this parameter. It was obtained using a single step test, whereas Corten and Dolan used a repeated block program. However, the range of values of d obtained in various experiments (reported by Corten) would suggest that a similar trend would occur frequently, using this approach.

As an incidental observation, it might be instructive to recall the occurrence of a large number of secondary cracks in Random Load testing using load histories which contain a large number of small stress level cycles (the rectangular QS tests in particular). Possibly the very short lives obtained in the QS tests is due to the great increase in the crack nuclei parameter. See Figure 12. If the appearance of secondary cracks is indicative of a large number of crack nuclei available for possible propagation, then the trend exhibited by the above approach may be correct i. e., a large proportion of low stress amplitudes will increase the number of crack nuclei.

However, for a given type of Random Loading, Figure 12 shows that the number of secondary cracks increases with RMS level. This would suggest that within a given type of Random load, the occurrence of the higher stress peaks has the effect of increasing nuclei. However, in this latter case, the reasoning discussed in subsection 6.3.2 would not apply, and indeed is opposite to that which forms the basis of many cumulative damage hypotheses (section 6.3.3).

The Partial Damage test results, when compared with the Rayleigh curve of Section III would lead one to conclude that Random preload will shorten the CA endurance uniformly, without altering the rate of decrease of endurance with stress level. However, continuing the Random loading to specimen failure will produce the interaction effect described by Freudenthal and Heller in Ref. 26, i. e., increase interaction effect at low stress levels, resulting in a clockwise rotation of the S-N curve when moving from CA testing to RA testing.

An examination of the specimens used in the Partial Damage test program for cracks revealed little or no secondary cracks apart from the main crack. A representative group is shown in Fig. 26. From this result it can be concluded that the increased number of nuclei generated by the Random Preload (and probably responsible for the translation of the CA

curves shown in Fig. 25) are not developed under the action of repeated CA stressing.

VII. CONCLUDING REMARKS

- 7.1 The present investigation of fatigue under random loading has been possible through the design and development of an axial load fatigue machine capable of either constant amplitude or random amplitude testing, the latter having the added feature of an adjustable power spectrum. The direct attachment of the shaker to the specimen may account for the lack of progress in random load fatigue testing to date, as this severely limits the load capability of the shaker. The introduction of flexure-pivotted levers presents a versatile load-shaping arrangement to the fatigue test engineer, since the intermediate structure is able to simulate dynamically a wide range of fatigue-sensitive structures.
- 7.2 By inspection of the distribution of constant amplitude fatigue results obtained at low stress levels in this project, it was possible to separate these endurance into two separate log-normal distributions. This discovery has statistically identified the two fatigue mechanisms responsible for the two types of failure previously reported from metallurgical investigations (Section II).
- 7.3 Through the use of the random load fatigue machine developed in this project, it was possible to conduct random amplitude axial load fatigue tests for the first time to the author's knowledge. The application of a non-zero mean stress to random load testing has been a further step to simulate aircraft (and possibly other) service load conditions adequately for the first time (Section III).
- 7.4 With the use of this machine in its two-lever configuration, it was possible to study random amplitude fatigue with a wide-band power spectrum on unnotched specimens for the first time. While the analysis of this type of loading is tractable from the power spectrum point of view (which avoids the 'cycle' concept), the application of cumulative damage rules to this type of loading points to the general inadequacy of such rules at present when applied to complex wave fatigue (Section IV). The test results were of sufficient numbers to state that the introduction of a second degree of freedom results in an altogether different shape to the endurance curve (versus RMS stress or stress peak).
- 7.5 It has been possible through random-number programming of the "short-time" RMS stress level of the Random Amplitude loading to apply experimentally Quasi-Stationary fatigue loads to test pieces for the first time. This type of loading is not only the ultimate simulation of service loading for aircraft, ships and other vehicles, but also is demonstrated in this report to be quite a feasible testing procedure. In principle, Quasi-Stationary random fatigue testing permits the

application of random loads having any reasonable final load distribution whatever. The application of the linear cumulative damage rule, and also Freudenthal's cumulative damage theory, again reveals basic inadequacies in their ability to predict realistic fatigue endurance (Section V). If, as a final refinement, this type of testing is coupled with the two-lever configuration of the test machine a wide variety of structures could be represented dynamically and fatigue tested with loadings closely approximating those encountered in service.

7.6 A series of 'partial damage' tests, involving the determination of the constant amplitude endurance relation for specimens with random amplitude preloading, were carried out to investigate the rate of damage accumulation during fatigue testing at random amplitudes. The analysis of these results has been a formidable problem and, probably, will not be capable of satisfactory study until the development of more satisfactory theories of cumulative damage.

7.7 Throughout this work various cumulative damage rules have been examined in the light of the Random Load Fatigue results from the various load configurations described above. While an attempt has been made to use statistically adequate numbers in these tests, the conclusions enumerated below must, of course, be considered tentative.

a) The Linear or Miner Rule

The linear rule of damage accumulation with the summation of cycle ratios has been shown to be consistently inadequate and indeed dangerous to apply to random amplitude fatigue loadings. The introduction of realistic service loadings (complex wave and quasi-stationary testing) aggravates this inadequacy, with larger and larger proportions of the load spectrum being ignored by this damage calculation.

b) The Linear Rule Applied to Two Distributions

It had been hoped that accurate prediction of the stationary Rayleigh test results would have been possible using the two-distribution interpretation of constant amplitude endurance data. The use of the STF mechanism alone appears entirely inadequate. A more accurate determination of the proportion each distribution contributes to the endurance patterns will be necessary before two-distribution linear damage accumulation can be accurately judged. This is certainly an interesting approach to fatigue prediction since it involves no real stress interaction in the accepted sense, but rather the interplay of two separate fatigue mechanisms.

c) Freudenthal and Heller (Ref. 26)

Freudenthal's rule of cumulative damage, while sensitive to the selection of the maximum stress peak in the load history, nevertheless, gives quite a good representation of endurance for the stationary Rayleigh tests.

For the Quasi-Stationary results, where the linear hypothesis fares badly, the use of Freudenthal's rule, with the marked decrease in endurances associated with the slope of the fictitious S-N curve, provides somewhat better estimates of life although still unconservative.

d) Fuller (Ref. 23)

Fuller's rule, when the procedure for obtaining β is modified from his original criterion of 1000 cycles, to the number of cycles for the single occurrence of the maximum stress peaks, appears to offer an excellent and simple design rule for random amplitude loadings in the intermediate stress regime. This rule need only have accurate STF data and a knowledge of the clipping characteristics of the random signal. Its use with the Quasi-Stationary history points out its main problem area; the establishment of a reliable and unequivocal method for obtaining β .

e) Corten and Dolan (e. g. , Ref. 49)

The establishment of the all-important maximum stress peak S_1 and the derivation of the slope parameter d discouraged the use of the Corten-Dolan Hypothesis, except as a framework to study the active crack nuclei parameter, as it was affected by random preload. This led to the qualitative explanation for the short QS endurances as the result of an increase in active nuclei caused by the large number of small stress cycles prevalent in such tests.

f) Linear Summation of RMS Stress Units

It is suggested in this report that a prediction of endurances under Quasi-Stationary Random Loading may be obtained from the linear summation of the ratios of time spent at a given level of RMS, divided by the Rayleigh Life at that level of RMS. This approach has met with moderate success, but is quite likely a gross oversimplification of the damage accumulation process associated with this type of loading.

7.8 METALLURGICAL FINDINGS

Figure 12 presents a summary of the observations of secondary cracking, which seems to be a feature of random load fatigue. It appears that the mixing of low stress cycles with high stress cycles introduces this phenomenon, and, the greater the proportion of the former, the greater the number of secondary cracks which occur. The only constant amplitude tests to show similar cracking (but in great profusion - see Table 8) were a very large fluctuating compression type of fatigue loading. It has not been determined if a correlation exists between the constant amplitude secondary cracks and the random amplitude cracks. Further study of the effect of random amplitudes on the development of cracks in unnotched specimens under axial loading may shed light on this phenomenon. Studies of the primary (failure) cracks in the present project have been inconclusive and a research program has been initiated at the Institute of Aerophysics into the correlation of two distribution endurance behavior with metallurgical examination of the resulting primary fatigue cracks. Further work along these lines may produce an accurate correlation between number of crack nuclei and stress level to incorporate into a cumulative damage theory such as that advocated by Corten and Dolan.

REFERENCES

1. Swanson, S. R. Systematic Axial Load Fatigue Tests Using Unnotched Aluminum Alloy 2024-T4 Extruded Bar Specimens. UTIA Technical Note 35, May 1960.
2. Laurent, A. G. The Mathematics of Reliability and Life Testing. SAE Paper 453B Automotive Engineering Congress, Detroit Mich. - Jan. 8 - 12, 1962.
3. Weibull, W. Fatigue Testing and Analysis of Results. Pergamon Press (For AGARD) 1961.
4. Swanson, S. R. A Two-Distribution Interpretation of Fatigue S-N Data. Canadian Aeronautical Institute Journal, June 1960.
5. Grover, H. J.
Gordon, S. A.
Jackson, L. R. Fatigue of Metals and Structures. Bureau of Aeronautics, Department of the Navy, 1954.
6. Wallgren, Gunnar Direct Fatigue Tests with Tensile and Compressive Mean Stresses on 24S-T Aluminium Plain Specimens and Specimens Notched by a Drilled Hole. The Aeronautical Research Institute of Sweden, Rep. No. 48, 1953.
7. AGARD Material Properties Handbook, Vol. I Aluminum Alloys.
8. Liu, H. W.
Corten, H. T. Fatigue Damage Under Varying Stress Amplitudes, NASA TN D-647, November 1960.
9. D'Amato, R. A Study of the Strain Hardening and Cumulative Damage Behaviour of 2024-T4 Alum. Alloy in the Low-Cycle Fatigue Range. WADD TR 60-175, April, 1960.
10. Weibull, W. Static Strength and Fatigue Properties of Threaded Bolts, Report 59, The Aeronautical Research Institute of Sweden, 1955.
11. Sinclair, G. M.
Dolan, T. J. Effect of Stress Amplitude on Statistical Variability in Fatigue Life of 75S-T6 Aluminum Alloy, Transactions of the ASME, Vol. 75, P. 867, July, 1953.
12. Lax, L. C.
Reid, D. B. W.
Worsley, B. H. Error Estimation of Fitted Exponential Functions and Transfer Rates of Plasma Constituents Determined by the IBM 650 Computer, Proceedings of the 2nd Conference of the Computing and Data Processing Society of Canada, June 6, 1960.

13. Jones, G. M.
Jones, E. R. W. A Statistical Analysis of the Results of Wohler
Fatigue Tests Made on Material to B. S. S.
6L1 RAE TN Met. 53, May, 1947.
14. Torrey, M. N.
Gohn, G. R. A Study of Statistical Treatments of Fatigue Data.
Page 1091, Proceedings of the American Society
for Testing Materials Vol. 56, 1956.
15. Webber, D.
Levy, J. G. Cumulative Damage in Fatigue with Reference to
the Scatter of Results, S & T Memo No. 15/58
August, 1958.
16. A. M. Freudenthal Fatigue of Materials and Structures under Random
Loading. Page 129 WADC TR-59-676, March, 1961.
17. Wood, W. A. Some Basic Studies of Fatigue in Metals. Fracture-
Published jointly by the Technology Press and John
Wiley & Sons, 1959.
18. International Conference on Fatigue of Metals
Joint I Mech. E. - ASME Conference (London and
New York) 1956.
19. Feltner, C. E.
Morrow, J. D. Micro Plastic Strain Hysteresis Energy as a
Criterion for Fatigue Fracture. Trans. ASME,
J. Basic Engineering, March, 1961.
20. Williams The Extrusion Characteristics and Mechanical
Properties of Alum. Alloy L. 65" A. A. S. U. Rept.
No. 189.
21. Shabalin, V. I. Discontinuity in the Fatigue Curve for Duralumin.
Page 11, Metal Industry (originally reported in
Doklady Akad. Nauk. U. S. S. R. 1958, Vol. 122 4, 600)
2 January 1959.
22. Press, Harry
Meadows, May T.
Hadlock, Ivan A Revaluation of Data on Atmospheric Turbulence
and Airplane Gust Loads for Application in Spectral
Calculations. NACA Report 1272, 1956.
23. Fuller, J. R. Cumulative Fatigue Damage Due to Variable-Cycle
Loading, Noise Control - July-August, 1961.
24. Schelderup, H. C.
Galef, A. E. Aspects of the Response of Structures Subject to
Sonic Fatigue. WADD T.R. 61-187 - July, 1961.
25. Rayleigh, J. W. S. The Theory of Sound. Dover Publications (Original
Publication 1877).

26. Freudenthal, A. M.
Heller, R. A. On Stress Interaction and a Cumulative Damage Rule. J. Aero-Space Soc. July, 1959.
27. Smith, P. W., Jr.
Malme, C. I. Sonic Fatigue Life Determination by Siren Testing. May, 1962. Tech. Report ASD-TR-61-639.
28. Fralich, R. W. Experimental Investigation of Effects of Random Loading on the Fatigue Life of Notched Cantilever-Beam Specimens of 7075-T6 Aluminum Alloy. NASA Memo 4-12-59L. June 1959.
29. Fralich, R. W. Experimental Investigation of Effects of Random Loading on the Fatigue Life of Notched Cantilever-Beam specimens of SAE 4130 Normalized Steel. NASA TN D-663, February, 1961.
30. Freudenthal, A. M. Fatigue of Structural Metals Under Random Loading. Symposium on Acoustical Fatigue, June, 1960, ASTM STP 284.
31. Cartwright, D. E.
Longuet-Higgins, MS. The Statistical Distribution of the Maxima of a Random Function. Proc. Royal Soc. of London Series A, Vol. 237, p. 212, 1956.
32. Schijve, J. The Analysis of Random Load Time Histories with Relation to Fatigue Tests and Life Calculations. N. L. L. Report MP 201.
33. Torbe, I. A New Framework for the Calculation of Cumulative Damage in Fatigue..
Part I. Non-historical Theory U. of Southampton, Report No. 6, April, 1959.
Part II, Historical Theory U. S. A. A. Report No. 1111, July 1959.
34. Poppleton, E. D. On the Prediction of Fatigue Life Under Random Loading. UTIA Report No. 82, February, 1962.
35. Plantema, F. J.
Schijve, J. Full-Scale Fatigue Testing of Aircraft Structures. Pergamon Press (Amsterdam Symposium) 1959.
36. Starkey, W. L.
Marco, S. M. Effects of Complex Stress-Time Cycles on the Fatigue Properties of Metals. Trans. ASME, page 1329, August, 1957.
37. Hald, A. Statistical Tables and Formulas, Wiley Publications, 1952.

38. Games, R. H. Prediction of Aircraft Wing Gust Fatigue Damage by Means of Power Spectral Analysis and Constant Life Curves. SAE Preprint 108, October 1959.
39. Rice, S. O. Mathematical Analysis of Random Noise. (from Bell System Technical Journal, Vols. 23 and 24).
40. Longuet-Higgins, M. S. On the Statistical Distribution of the Heights of Sea Waves. Journal of Marine Research Vol. XI, No. 3, 1952. Bingham Oceanographic Laboratory, Yale University, U. S. A.
41. Press, H.
Steiner, R. An Approach to the Problem of Estimating Severe and Repeated Gust Loads for Missile Operation. NACA TN 4332, September, 1958.
42. Airplane Strength and Rigidity Reliability Requirements, Repeated Loads and Fatigue. U. S. Military Specification MIL-A-8866 (ASG) 18 May, 1960.
43. Raithby, K. D. A Method of Estimating the Permissible Fatigue Life of the Wing Structure of a Transport Aircraft. JRAS 65 November, 1961.
44. Pearson, K. (ed) Tables of the Incomplete Gamma Function. Cambridge University Press (Printing) BIOMETRIKA (Publishers) Re-issue 1951.
45. A Million Random Digits. The Rand. Corp.
46. Douglas Aircraft Co. Inc. Investigation of Thermal Effects on Structural Fatigue. WADD TR 60-410.
47. Section A. 00. 05. Royal Aeronautical Society Data Sheets - Fatigue.
48. Hald, A. Statistical Theory with Engineering Applications. Wiley Publications, 1952.
49. Liu, H. W.
Corten, H. T. Fatigue Damage During Complex Stress Histories. NASA TN D-256. November, 1959.
50. Carr, J. B. Analysis of the Performance of the UTIA Random Load Fatigue Facility. UTIA TN 54. October 1961.
51. Swanson, S. R.
Carr, J. B. A Realistic Approach to Fatigue Testing Under Random Loads.
Part I. MB Vibration Notebook Vol. 8, No. 2, March 1962.
Part II. MB Vibration Notebook Vol. 8, No. 3, August, 1962.

52. Crichlow, W. J.
et al An Engineering Evaluation of Methods for the Prediction of Fatigue Life in Airframe Structures. ASD-TR-61-434, March, 1962.
53. McIntosh, V. C.
Granick, N. Experiments in Random Vibration. WADC Technical Note 56-228, June, 1956.
54. Harris, C. M.
Crede, C. E. Shock and Vibration Handbook Vol. 2 - Data Analysis, Testing and Methods of Control. McGraw-Hill Publications. 1961.
55. Mullinger, D. E. The Development of a Random Motion Vibration System, RAE TN G. W. 571, April, 1961.
56. Stephenson, N. A Review of the Literature on the Effect of Frequency on the Fatigue Properties of Metals and Alloys. NGTE M-320. June, 1958.

APPENDIX A

The Random Load Fatigue Machine

Introduction

Constant-Amplitude fatigue testing machines are almost universally employed in fatigue testing at present. They are not difficult to construct, and have been diligently used over the past 100 years to amass an enormous sufficit of fatigue data based on this somewhat trivial load pattern.

The unfortunate aspect of the almost exclusive use of such fatigue machines which are limited to constant amplitude loading patterns was pointed out by A. M. Freudenthal in 1959. He stated "Since it appeared much more difficult to reproduce the actual variable-load service conditions than to apply constant-amplitude load cycles, this variability was conveniently overlooked as long as this seemed practically feasible, that is, as long as design for fatigue could be either completely disregarded, or based on the results of constant-amplitude tests under the expected maximum load amplitudes". He then asserted "the variability of stress-amplitudes in relation to fatigue can no longer be disregarded in the design of aircraft, ships, motor vehicles, bridges and various other types of structures". (Ref. 16)

Despite the fact that nearly all machinery and structures experience loadings which are usually aperiodic and of variable (random) amplitude, only a half-dozen investigations into actual random load testing have been carried out to our knowledge.

A brief chronological summary of these random fatigue experimental projects up to the present follows. All of these previous projects involve the use of geometric and/or loading stress gradients to obtain reasonably short specimen endurance with small capacity shakers. This introduction of stress gradients not only prevents accurate assessment of the loads or stress levels, but brings into the test an additional factor which has a significant effect on endurance, and even possesses a 'size effect' in the results.

- (1) 1956. Australian tests by A. K. Head and Hooke reported in the 1956 London Conference on fatigue (Ref. 18).

First recorded random load fatigue tests. These tests involved the direct attachment of a small shaker to a 1/2" diameter 2024 aluminium alloy bar as a cantilever loaded in plane bending. A circumferential groove at the root of the cantilever bar formed a stress concentration with $K_t = 1.3$.

- (2) 1956.

American tests by McIntosh and Granick (Ref. 53) in which small unnotched free cantilever beams were loaded at their centres by a

small shaker. This type of bending load introduces resonance difficulties, since the random signal can result in an uncontrolled combination of the fundamental bending mode and higher order modes. The later work in 1961 of Smith and Malme (Ref. 27) was along similar lines.

(3) 1958.

American tests by W. D. Trotter of Boeing Aircraft (Test Report T2-1601) using a shaker to supply bending loads to 0.040" 2024-T3 sheet specimens (unnotched and notched) to establish both random (Rayleigh) and constant amplitude S-N curves.

(4) 1959.

German tests by J. Kowalewski at DVL, Germany, and reported at the 1959 Amsterdam Conference (Ref. 35), in which a cantilever bar of extruded 2024 aluminium alloy with a deep circumferential notch ($k_t = 1.77$) was directly loaded by the vibrator.

(5) 1959 and 1961.

American (NASA) work by Fralich in Refs. 28 and 29, working with 7075-T6 aluminium plate and SAE 4130 normalized steel plate respectively. In these tests the notched plates ($K_t = 4$) act as cantilevers directly loaded by a small vibrator.

(6) 1959.

A testing program carried out by Lockheed Aircraft Corporation (Ref. 52). This project involves the use of an aircraft load history trace, which is followed rapidly by servo-controlled hydraulic jacks (by means of magnetic tape). These actuators axially load 3 inch wide coupons of 7075-T6 aluminium sheet, which have elliptical-hole notches yielding a theoretical stress concentration of 4 or 7. The complex load trace is used in the normal 'forward' sequence for a number of tests and then the sequence is reversed to study the influence of load sequence on the endurance.

(7) In the study described in this report axial loadings of comparatively large magnitude, applied to quite large test specimens, were obtained by placing a lever arrangement between the specimen and a relatively large capacity shaker. A spring device connected to the main lever permits the application of both tensile and compressive mean stresses. Addition of a second lever permits testing with two resonances. The decision to design an axial loading machine is based on the conviction that it is only by knowing accurately the stresses imposed on the specimen during random fatigue tests will a start be made on a fundamental study of fatigue damage accumulation under simulated service conditions.

It will be seen that this facility is of extremely simple design; all the electronic equipment being readily obtained commercially. In fact, the majority of it is commonly available in a modern vibration laboratory. The only special feature is the mechanical load-shaping structure, which can be cheaply and easily made to suit any desired combination of shaker and specimen. However, because of the lack of familiarity with this type of testing to most readers, it was considered desirable to describe its operating principles in this appendix in order to appreciate more fully the test results.

1. Principle of Operation

In Random amplitude testing as in Constant amplitude testing, there are various parameters which may be altered to suit the particular objectives of the experiment. For instance, a choice must be made between the inclusion or exclusion of the phenomenon of resonance. Normally sub-resonant techniques are employed if resonance is to be avoided. Reference 50 describes the performance of the Random Load fatigue machine over the complete frequency range of practical interest (0 - 100 cps). Reference 55 describes the design of a 500 lb. RMS thrust moving-coil vibrator with flat response, and concludes that the adaptation of a vibration system for random motion can be a simple process if the vibrator characteristics are satisfactory.

Since the present project was concerned with the behaviour of aero structures, it was decided to include and exploit the phenomenon of resonance, since in aircraft structures the atmospheric (input) load spectrum is able to excite at least one of the natural frequencies of vibration, and fatigue failure is possible due to the resulting excitation of rigid body and fundamental wing bending modes (. 1 to 5 cps).

The elements of the dynamic system are shown in Figure 28. It consists of the shaker, the levers L_1 and L_2 , the interlever spring, the mean stress spring (S_m), the 'Moving Head' in which one end of the specimen is gripped, the (elastic) specimen, and finally the 'Fixed Head' by which the other end of the specimen is rigidly connected to the foundation of the machine.

By varying the stiffness of the interlever spring and the inertias of the levers about the fulcrum of the lever L_1 , a variety of power spectra between the random (white noise) input and the specimen may be achieved. A general description of this random load test facility has recently been published - see Ref. 51.

The single-degree-of-freedom configuration is obtained when the interlever spring is disconnected from lever L_1 . For the specimen used in this program the resulting resonance occurs at 45 cps (as shown in Ref. 50). When the lever L_2 is connected to L_1 using the interlever spring, a typical power spectrum as shown in Fig. 14 is applied to the specimen, due to the resulting two degrees of freedom for the structure. The location of the input of the exciting force remains a rigid connection between the shaker table and

the lever L_1 for both configurations. The mean stress is applied by means of a yoke or 'C' spring shaped like a 'C' to deflect in a manner similar to the rotation of the lever L_1 . The fixed base of the spring consists of an elevator mechanism operated on two vertical threaded spindles. This elevator platform can be raised or lowered by means of interconnected worm gears. The specimen static mean load and the dynamic loads are measured, calibrated and controlled by a strain gauge bridge located on the flexure plate connecting lever L_1 to the 'Moving Head'. The main structure is made entirely from standard rolled beam sections, and the machine is isolated from the floor (and the electronic equipment) by six seismic suspension springs with telescoping pipes to give lateral stability. All moving parts are mounted on spring steel flexures or flexure pivots. The dynamic component of the strain signal is used to monitor the test. When the specimen breaks, the change in resonance is always such as to reduce this component appreciably. When this happens a photoelectric controller (normalised used to control temperatures in industrial applications) switches off all power. This control is two-sided so that any excursions above the set level of alternating strain will also shut down the machine.

2. Performance of the Machine

While the general operating performance of the machine over the frequency range of interest is described in Ref. 50, the performance at resonance is of interest when considering the capability of the machine over a wide range of lever inertias and specimen resonances. In the following paragraphs this behavior at resonance will be examined in detail. For any given configuration, however, the off-resonance characteristics will be qualitatively similar to those shown in Ref. 50. While the following on-resonance calculations are for the single-degree-of-freedom system, the extension of these calculations to the two-degree-of-freedom system may be obtained using the relevant equations from Ref. 50.

The force applied to the specimen can be considered to arise directly from the position of the shaker head, since the lever L_1 is assumed rigid. Using the notation of UTIA TN 54:

$$|F_{sp}| = \left[\frac{a}{L} \cdot \frac{k_{sp} k_h}{k_{sp} + k_h} \right] x_T \quad (A-1)$$

since the stiffness of the grips is 'in series' with the specimen stiffness. From equations A1 and A2 of UTIA TN 54:

$$\frac{x_T}{I_d} = \frac{K}{\omega_n r_f} \quad \text{since} \quad \omega^2 = \frac{k_f}{M} \quad \text{at resonance}$$

$$\text{and} \quad \frac{x_T}{V_d} = \frac{k_d}{K} \frac{1}{\omega_n} \left[r_f^2 \omega_n^2 + k_d^2 \left(1 + \frac{r_f}{r_d} \right)^2 \right]^{-\frac{1}{2}} \quad (A-2)$$

also
$$x_T = G / \omega_n^2 \quad (A-3)$$

Therefore at resonance:

$$x_T = \frac{|F_{sp}|}{\frac{\alpha \cdot k_p k_h}{L k_p + k_h}} = \frac{k l d}{\omega_n r_f} = \frac{G}{\omega_n^2} = \frac{k_d V_d}{k \omega_n [r_f^2 \omega_n^2 + k_d^2 (1 + \frac{r_f}{r_d})^2]}^{\frac{1}{2}} \quad (A-4)$$

Now by noting the following independent limitations on the shaker operating characteristics:

- a) Table displacement x_T not greater than .0127 meters ($\pm \frac{1}{2}$ "
- b) Amplifier frequency not less than 15 cps
- c) Maximum driver coil current $I_d = 11.3$ amps RMS
- d) Maximum driver coil voltage $V_d = 286$ volts (peak)
- e) Maximum table acceleration $G = 261.8$ meters/sec/sec (26.7 g's)
- f) Maximum rated force = 650 lbs.
- g) Maximum amplifier power = 2 KVA (at present)

an envelope of operating frequency-load combinations can be obtained. This envelope is shown in Fig. 29. It can be seen that any given combination of specimen stiffness and lever inertia automatically fixes both the ordinate and the abscissa and the loading can be easily compared with the capability of the machine at the given frequency.

3. Accuracy of Loading

The 'Moving Head' is supported by four vertical spring steel strips or flexures in a manner similar to that used with the NASA fatigue machine (N. A. S. A. TND-1253). The bending loads due to the 'sink' of the head due to axial movement are negligible (less than 100 psi for the specimen used) for most specimen stiffnesses.

When the 'Moving Head' was positioned during erection of the machine considerable care was taken to remove as much of the bending loads arising from axial misalignment of gripping heads as possible. To measure the bending loads one of the fatigue specimens was fitted with four metal-foil strain gauges in a Wheatstone bridge, such that the active gauges would measure only bending (strain differences). The specimen was gripped in the fixed head and the position of the moving head adjusted to minimize bending strain. Once located vertically, the specimen was rotated through 90 degrees and the procedure repeated. The residual bending stress due to head misalignment was calculated by hanging weights on the end of the instrumented specimen

when held as a cantilever. The corresponding cantilever weight was 30 grams which results in a maximum bending stress of less than 100 psi. (vertical). The horizontal misalignment load was much less than 30 grams. It was found that when the Moving Head was fixed in its final position, that the variation in bending loads due to the collets and the gripping procedure was of the same order as this residual bending. That this bending load has remained negligible is borne out by the Random Amplitude testing, especially with respect to the phenomenon of crack multiplicity. Under random loading, the random nature of these nuclei and the randomness of the final crack position lead us to believe that the residual bending load due to misalignment has not increased significantly.

Since the shaker constitutes a constant-load testing arrangement, monitoring the strain level is sufficient to yield reasonable accuracy in the alternating loading. The mean stress mechanism is essentially a constant-displacement apparatus, and the tensile mean stress usually decreased somewhat in the course of the longer tests. Care was of course taken in the fatigue tests to ensure that the mean stress load remained constant. For the low stress-long life cases, the mean stress was periodically checked at least once every 30 minutes. For higher stress levels, this practise was found unnecessary as very little variation occurred in less than one hour of continuous testing. Also the results of the mean-stress-variation tests described in Section IV. indicate that small inaccuracies in mean stress would have a second order effect on the endurance.

The frequency of testing, being less than 3000 cpm is considered to have an insignificant effect on the fatigue properties as concluded by Ref. 56.

Since the specimen dynamic load was essentially constant to failure, the final cracking of the specimen took place in a very short time. During this period the increased flexibility due to the cracking resulted in a drop-off of the resonant frequency. However the input power spectrum (under Random Amplitude conditions) was always wide enough to maintain the RMS level almost to the minute of failure. Under Constant Amplitude conditions the stress level was effectively maintained right up to failure due to the sudden nature of the failures. In any event the photoelastic strain monitor was set to cut off the main power at quite small drop in stress level merely by positioning the cut-off needle immediately below the RMS needle. This prevented the application of spurious cycles at reduced stress level.

The arrangement for gripping the specimen is similar to that employed by other researchers, (see page 104, 258 and 515 of Ref. 18), and is shown in detail in Fig. 30 and 31 of this report. The gripping jaws are, however, made from standard "rubber flex" collets, (Fig. 31), the smooth faces of which have been specially hook-serrated to give a firm positive grip on the end of the specimen. To insert a specimen in the machine, the sliding block (Fig. 30) holding the compression pin is partially withdrawn from the moving head to allow the specimen to be inserted into the collets. With about 0.1 in. of the specimen protruding from the collet, the locking disk is rotated,

compressing the collet into the hardened steel cone, and causing the internal serrations to grip the end of the specimen. The sliding block is then returned to its central position and a compressive force applied to the end of the specimen by rotating the compression pin. This causes the serrations to "bite" into the specimen while the collet is forced still further into its conical seating. When the compression pin is fully tightened against the 'proud' end of the specimen, it is locked in position by means of a free spinning locknut. Before gripping the specimen in the fixed head, the main pin holding this head to the foundation is loosened to allow it to move freely in the axial direction. The locking procedure described for the moving head may now be used, without any danger of inducing large compressive forces in the specimen.

4. Analysis of the Specimen Strain Traces

Before beginning the analysis of the strain traces obtained on an oscillograph from a Random Noise fatigue test, the accuracy of these traces with respect to the actual loads at the specimen will be discussed. These strain records (shown in Fig. 13) are obtained from a 4-gauge bridge mounted on the steel strip connecting the Moving Head to the Main Lever L_1 . To calibrate these readings, a fully instrumented specimen was inserted into the machine and, using a separate bridge-amplifier circuit the statically-calibrated output from the specimen was then compared with the machine output, using both channels of the Two-Channel Oscillograph. The steps in this static and dynamic calibration are:

1. Statically calibrate the specimen strain bridge by loading the specimen in a commercial tensile test machine of known load accuracy. The strain bridge consists of a) two active gauges mounted on opposite sides of the specimen in the centre parallel section and longitudinally aligned with the axis of the specimen, and b) two dummy gauges also mounted on the waisted parallel portion of the specimen transverse to the specimen axis. The resulting bridge is compensated for temperature, transverse loading and bending effects.
2. Place the calibrated specimen in the fatigue machine, and cross-calibrate the similar 4-gauge bridge mounted on the steel plate connecting the lever L_1 to the Moving Head. This is done by applying various Constant Amplitude levels with an oscillator, and measuring the resulting double amplitudes observed on the oscillograph for both the specimen and the machine.

It was found that the resistance of the moving head to axial movement results in a small (almost negligible) variation in the static strain reading for a given specimen strain depending on the angular position of Lever L_1 . Because of this the test procedure was standardized to always return the lever to a datum angular position at the beginning of each test. It was found that while a small static error resulted from using positions other than the datum position, the actual gradient in strain (slope of the load-strain curve) between the speci-

men load and the transfer plate strain remained the same over a wide range of lever angles about the datum angle. This angle was measured by means of a dial gauge mounted between the shaker casing and the lever L₁. The dial plunger was retracted for all dynamic tests after the static loading is applied.

APPENDIX B

Discussion of Principles and Terminology Used in the Report

Since 1959 a number of technical papers dealing with the fatigue of metals under random loads have appeared in fatigue literature, often with inadequate discussion of the new terminology and principles necessary for a complete description of "random" loads. At the risk of over-simplification the basic ideas will be discussed in this appendix.

To begin with, consider the usual representation of constant amplitude fatigue behaviour of a metal. Wohler observed 100 years ago that when metal experiences sinusoidal stress histories with large amplitude the fatigue endurance was short, while at low amplitudes of stress, the endurances were orders of magnitude longer. Because of this universal characteristic for materials, the usual presentation of endurances is made using a vertical linear scale of maximum stress amplitudes, and a logarithmic abscissa, the number of cycles to failure N .

This semi-logarithmic plot is by far the commonest layout used to present fatigue data and the resulting relation with stress is called the "S-N" curve, although sometimes more properly, it is called the "S-logN" curve. A number of cumulative damage theories presently put forward make use of parameters obtained from a log S-log N presentation of fatigue results with logarithmic scales for both the ordinate S and the abscissa N. However this type of presentation is usually explicitly stated where used.

Fatigue is a 'statistical' phenomenon, at least in all practical cases where it is encountered. This fact is probably largely due to the heterogenous nature of metal on the microscopic scale, where fatigue cracks begin. This characteristic manifests itself immediately when any fatigue test is repeated with exactly identical 'macroscopic' test conditions.

For instance, by continually repeating a test at a given level of stress amplitude S, one obtains a group or sample of endurances with scatter about the mean value. In fatigue analysis it is nearly always the practise to carry out statistical operations on these samples of endurances using their logarithms rather than their actual values. Thus, for instance, the 'mean endurance' nearly always refers to the geometric mean of the endurances, since this is the arithmetic mean of the logarithms. This has become the practise due to early observations of the samples of endurances obtained at the intermediate stress levels (stress levels for which failure occurs between, say, 1000 cycles and 100,000 cycles). While the distribution of sample endurances seemed to represent an underlying skew distribution, the logarithms of endurances exhibited a symmetrical pattern. Indeed this pattern usually could be well represented by the distribution of quantities one obtains from the Law of Errors, or Normal Law or Gaussian Distribution. This is the familiar single-hump bell-shaped distribution (as drawn at several stress levels in

Fig. 6) with the maximum number of quantities falling at the mean value, and only a very small number of quantities exceeding, say, three times the Standard Deviation (The standard deviation is the square root of the mean value for the squares of all quantities involved.). Returning to the case where the quantity in question is the logarithm of the endurance, the endurances are said to form a log-normal distribution.

When one groups the endurances into a histogram over the range of logarithms involved such that all endurances falling within a small log interval are represented by the ordinate, the resulting distribution is usually referred to as the probability density function, representing as it does the density of endurances at every interval of logarithms of cycles to failure.

The probability density function $p(S)$ for a Gaussian distribution is

$$p(S) = \frac{1}{\sqrt{2\pi}} \cdot \frac{1}{\sigma} \cdot \exp\left(-\frac{S^2}{2\sigma^2}\right) \quad (B-1)$$

where

S is the variable involved, such as the logarithm of endurance, and

σ is the root mean square value for all values of S

Since S only appears as a squared term, the distribution is symmetrical about the zero value for S . It can be shown that the variable S has values within unit RMS of the mean (or zero) 68% of the time in a given random history.

Another way to present the distribution of endurances is to consider the cumulative effect of fatigue; e. g., half the endurances will be less than the mean endurance. Two alternative procedures are available using the cumulative approach. For instance in a given sample the endurance level at which 10 percent of the specimens have already failed may be considered the 10% failure probability level, or the 90% survival probability level. There is available cumulative probability paper made to order for various distribution laws. In this report, use is made of log-normal cumulative probability paper. Experimental results, properly sorted or 'ranked' from the lowest endurance to the highest endurance, will exhibit log-normal statistical behaviour only if they plot linearly on such paper. The slope of the straight line representing any log-normal distribution is a direct measure of the scatter or standard deviation or dispersion of the test results.

In order to arrive at some idea of the relation between endurance and stress level, a statistical technique known as Regression Analysis has been applied in this report. It might be intuitive to reason that if one has a sample of endurances at each of a series of stress levels more information may be obtained about the stress-endurance relation by

considering all test results than by merely joining the mean values obtained at each stress level by, say linear segments. .

It must be noted that a sample of test results at a given stress level is only an indication or estimate of the underlying "population". The exact statistical mean values and standard deviation for the underlying "population" could only be obtained by testing an infinite number of specimens. For this reason the mean value from the samples is only an estimate of the population mean.

Regression analysis is the mathematical technique of obtaining the line or curve (with an assumed stress endurance relation) which results in the minimum total deviation from it, for the test results. Since test results usually follow symmetrical distributions, it is necessary to square the deviation, or difference between the test point and the value given by the assumed line or curve. By using the calculus of minima and maxima, a unique line or curve (called the Least Squares curve) can usually be obtained for a family of points. In this report use has been made of a Least Squares Dual Exponential regression for the constant amplitude results plotted on the S-Log N grid, while a Least Squares linear regression has been applied to the same test results when plotted on LogS-logN co-ordinates simply because these were assumed the underlying stress endurance relations in each case. The dual exponential regression assumes the underlying population to be bimodal (i. e. , two humps in the probability density curve).

The random amplitude test results discussed in this report were obtained using a random process, random noise, as the source of the load history. Many processes such as the thermionic electron bombardment which occurs in a thyratron tube, or the flow of air in atmospheric turbulence can be described as random processes. This means that the instantaneous value of the quantity measuring such a process such as voltage or gust velocity is unpredictable (random). However in a manner analogous to a study of the heights of adults in a given group, while the heights are randomly distributed throughout the group, there exists an underlying statistical relation such that there are many heights near the average and few far from the average. Similarly while the load experienced by a structure under loading from a random process is unpredictable at any given moment, over the course of time, the density distribution or histogram of loads experienced, will stabilize to follow a statistical law such as the Gaussian law.

When a Gaussian random process is applied to a linear system, the response of the system will also have a Gaussian distribution of loadings. This refers to the instantaneous values of the input and response quantities involved. In fatigue, fundamental studies have shown that the fatigue process is characterized by the cyclic or to-and-fro action of loads, and dislocations within the metal. While it is outside the scope of this appendix to elaborate on the characteristic, the important fatigue unit is therefore the occurrence of a local reversal in loading during the load history. These

occur, of course, at the maxima and minima of the stress or load history. This is possibly the most difficult point to appreciate in a study of random fatigue loading, because while the distribution of instantaneous stresses in a linear system remain Gaussian when excited by a Gaussian disturbance, the distribution of maxima or peaks will depend on the frequency response characteristics of the system. If the system has a single (lightly damped) degree-of-freedom the density distribution of peaks $p(\hat{S})$ with time will approach the Rayleigh distribution

$$p(\hat{S}) = \frac{\hat{S}}{\sigma^2} \exp\left(-\frac{\hat{S}^2}{2\sigma^2}\right) \quad (B-2)$$

where \hat{S} is the peak value of the variable and σ is the root mean square of the instantaneous value of the variable.

The shape of this distribution is shown qualitatively in Fig. 21. Note that it is not a symmetrical distribution and is positive-valued only. If negative valued or even zero-valued peaks occur in the history the distribution is no longer Rayleigh (see Section IV). Since the distribution is essentially describing the envelope of the signal, it can be appreciated that its statistical parameters will be of greater magnitude than those of the instantaneous values of the signal. For instance, the root mean square of \hat{S} will be $\sqrt{2}$ times the root mean square of the instantaneous values of S , and the maxima \hat{S} will have values less than the root mean square of the instantaneous value of S , i. e., σ only 39 percent of the time. The maximum value of $p(\hat{S})$ will occur at σ , and the mean value of \hat{S} is 1.15σ . This distribution of peaks is also characterized by the zero probability of peaks occurring at the mean (or zero alternating stress level), and as the frequency response of the structure broadens, a second Gaussian distribution of peaks emerges while the Rayleigh distribution recedes. In the limiting case, a structure with an infinitely broad and uniform frequency response will have no effect on the peak distribution of the Gaussian input, and the Rayleigh component will have vanished. Most structures, however, do exhibit the mixed Gaussian-Rayleigh peak distribution obtaining between these two limiting cases.

Since the distribution of peaks is of interest in fatigue, a non-zero measure of the intensity of a symmetrical random process is the Root Mean Square value of the peaks which is exactly analogous to the standard deviation for the Law of Errors in measurement studies. The RMS Peaks, as mentioned earlier, will be $\sqrt{2}$ times the RMS instantaneous stress for a pure Rayleigh distribution. However, as the frequency response characteristics broaden, the factor will, of course, approach unity.

In statistical terminology, a random process whose statistical properties (such as mean value, RMS, etc) remain invariant with time is referred to as a Stationary Random Process. While this assumption of stationarity is good for short durations in random processes occurring in

nature, the intensity level usually will be altered either continuously or discretely over long periods of time, such that while the final overall distributions of loadings approach an invariant form asymptotically, the RMS level at least, will violate the stationarity requirement.

When this happens the process is described as Quasi-Stationary. Certain processes exhibit non-stationary characteristics; for instance, in cases where the RMS level of a random process is either monotonically increasing or decreasing such that the overall RMS is not approached asymptotically. The overall RMS level must, of course, be explicitly related to either the instantaneous stress or to the distribution of peaks when it is used in random load fatigue.

TABLE 1

U. T. I. A. CONSTANT AMPLITUDE TEST RESULTS

Mean Stress = 16 ksi Tension

Spec.	± 34.8 ksi		± 45.1 ksi		± 28 ksi		± 22.5 ksi		± 19.5 ksi				
	Secondary Cracks	Spec.	cycles	Secondary Cracks	Spec.	kcycles	Secondary Cracks	Spec.	kcycles	Secondary Cracks			
F23	43.8 0 - 0	F30	8,003	S - 1	46	72.5	1s - 1s	F43	331.4	0 - 0	132	276.7	1s - 1
F22	46.5 1c - 1	F40	10,980	1c - 1c	51	81.0	1 - 1c	F16	358.9	0 - 1s	137	310.4	0 - 0
F3	48.4 0 - 0	F29	11,266	3+2s-1c	61	81.5	0 - 0	F47	422.6	N.S.-1	136	412.3	0 - 0
F21	53.2 1c - 0	F31	12,008	1c - 0	59	98.1	0 - 0	F11	448.9	0 - 1c	138	507.1	0 - 0
F26	54.7 1s - 0	F32	12,409	1+1c-0	62	106.7	0 - 1c	F34	468.8	N.S.-1	133	655.5	1+1c-0
F5	56.1 0 - 0	F27	13,286	Sevs-1	58	110.1	0 - 1	F37	513.9	0 - 1c			
F1	56.3 0 - 1s	F42	13,510	1+3s-1s	53	114.8	2s-0	64	533.0	0 - 0	135	2,270.2	0 - 0
F20	63.7 0 - 0	F44	13,990	1 - 0.				F46	605.3	N.S.-1	124	4,282.3	1 - 0
F2	65.7 2 - 0	F28	24,900	2s-1				F45	654.4	1c - 0	134	8,537.5	0 - 1c
F10	67.1 1 - 0							F33	665.8	0 - 0	131	12,571.4	0 - 1
F9	71.0 1c - 3s												
F15	71.5 0 - 0							F17	1,150	N.S.-1			
F24	77.4 2 - 1s							F41	1,166	0 - 0			
F7	80.4 0 - 0							F35	1,198	1c - 0			
F18	84.4 0 - 0							F38	1,350	0 - 0			
								F39	1,610	0 - 0			
								F25	1,628	0 - 0			
								F13	1,911	0 - 0			
								F36	3,461	0 - 0			
								F12	3,800	1 - 0			
								F14	4,367	0 - 0			

Legend for Secondary Crack Column:

1c = 1 corner crack (off main crack)

1s = 1 small crack

S = several large cracks

Sevs = several small cracks

N.S. = not severed

TABLE 2
SINGLE LEVEL RANDOM AMPLITUDE
TESTS
(Single Degree of Freedom)

Specimen No.	Duration minutes-secs	$\sigma_p = 18$ ksi		$\sigma_p = 17$ ksi		Specimen No.	Duration hrs-mins-secs	$\sigma_p = 12$ ksi		Secondary Cracks Large-Small	Cycles To Fail	Secondary Cracks Large-Small
		Cycles To Fail	Secondary Cracks Large-Small	Cycles To Fail	Secondary Cracks Large-Small							
194	14:07	42,300	9 - 10	148	26:43	80,150	4 - 1					
3	14:54	44,700	22 - 7	196	34:02	102,100	11 - 6					
2	18:17	54,850	2 - 0	195	34:33	103,700	3 - 3					
5	20:31	61,100	12 - 17	153	41:30	124,500	0 - 1					
4	27:30	82,500	4 - 21	193	51:45	155,300	4 - 2					
6	29:51	89,550	3 - 5	192	59:44	179,200	1 - 1					
Average 8.67 - 10												
Average 3.83 - 2.34												
$\sigma_p = 16$ ksi												
$\sigma_p = 13.5$ ksi												
$\sigma_p = 11.3$ ksi												
$\sigma_p = 9.5$ ksi												
47	0:59:42	179,100	6 - 5	21	2:12:16	396,800	0 - 1					
197	1:10:39	211,950	4 - 1	7	2:17:53	413,650	3 - 5					
55	1:38:00	294,000	0 - 2	9	2:29:19	437,950	1 - 3					
198	1:45:22	316,100	2 - 1	8	2:32:41	458,050	4 - 0					
44	1:51:05	333,250	3 - 7	201	2:55:58	527,900	0 - 1					
10	2:10:57	392,800	1 - 3	1	2:59:50	539,500	4 - 1					
Average 2.67 - 3.17												
Average 2 - 1.83												

TABLE 2 (continued)

Specimen No.	Duration hrs-mins-secs.	Cycles To Fail	Secondary Cracks		Specimen No.	Duration hrs-mins-secs	Cycles To Fail	Secondary Cracks	
			Large-Small	Large-Small				Large-Small	Large-Small
200	2:25:26	436, 300	2 - 2		17	4:00:09	720, 450	0 - 1	
203	2:29:03	447, 000	0 - 4		24	4:28:52	806, 600	0 - 4	
202	2:39:00	477, 000	0 - 0		81	4:30:32	811, 600	0 - 1	
190	3:31:34	634, 700	1 - 0		80	4:33:05	819, 250	1 - 0	
88	5:53:28	1, 060, 400	0 - 0		36	7:24:15	1, 332, 750	0 - 4	
191	6:42:07	1, 206, 400	2 - 3		199	8:04:04	1, 452, 200	2 - 0	
Average .83 - 1.5									
Average .5 - 1.67									
$\sigma_p = 11.5 \text{ ksi}$ $\sigma_p = 9.5 \text{ ksi}$ $\sigma = 8.13 \text{ ksi}$ $\sigma = 6.7 \text{ ksi}$									
204	8:57:15	1, 611, 750	0 - 0						
205	10:07:12	1, 821, 600	2 - 1						
226	11:14:26	2, 023, 300	0 - 0						
206	11:31:03	2, 073, 150	0 - 0						
207	16:15:32	2, 926, 600	1 - 3						
208	20:13:23	3, 640, 150	0 - 0						
209	21:39:22	3, 868, 100	0 - 0						
Average .43 -.57									
$\sigma_p = 9 \text{ ksi}$ $\sigma = 6.35 \text{ ksi}$									

TABLE 3

2-LEVER RANDOM LOAD TEST RESULTS

RMS	σ_p	Sample σ_{trace}	Specimen	kcs (50 cps)	Final Secondary Cracks		
					Large	Small	Total
10.4	12.0		187	88.2	9	8	17
			181	108.0	5	5	10
		10.83	176	146.7	6	2	8
		10.05	179	168.5	10	16	26
		10.36	178	171.6	14	10	24
			180	173.9	8	12	20
			185	253.5	7	2	9
				Average 8.43		7.85	
8.83	10.1		172	307	0	6	
			170	360	1	9	
		8.84	177	399.8	5	2	
		9.06	168	420	0	1	
		8.73	169	481	2	1	
			173	633	0	1	
			174	1013	2	2	
				Average 1.43		3.15	
7.92	9.1		182	791	0	7	
		7.35	186	1064	0	0	
		8.07	188	1073	3	2	
		7.29	175	1293	1	3	
		8.39	184	1405	0	1	
		8.57	183	1530	1	2	
			171	1929	0	1	
				Average .715		2.29	

TABLE 4

SAMPLE OF RANDOM NUMBERS EMPLOYED IN
QS TESTS
Each RMS held for 1 minute before next value set

Number in Sequence	Basic Rectangular set page 93, Ref. 37		Truncated	Truncated
	Rect to 100 $\hat{\sigma} = 10$ ksi	Rect with $\hat{\sigma} = 11.7$ ksi	Normal $\hat{x} = 1.7\sigma =$ 12 ksi	Exponential $\hat{x} = 1.7\sigma$ (σ)max = 12.54 ksi
1	1.5	1.8	6.3	6.1
2	7.7	9.1	4.8	4.4
3	1.8	2.1	5.6	5.3
4	0.8	.9	8.3	8.4
5	1.6	1.9	6.1	5.8
6	5.4	6.4	.7	.6
7	9.5	11.2	9.6	10.0
8	2.2	2.6	4.8	4.4
9	6.9	8.2	3.2	2.8
10	7.5	8.9	4.4	4.0
11	0.8	.9	8.3	8.4
12	0.4	.5	9.7	10.0
13	9.7	11.5	10.5	11.0
14	5.3	6.3	.6	.4
15	2.6	3.1	4.0	3.6
16	4.9	5.8	.1	.1
17	0.3	.4	10.1	10.5
18	2.1	2.5	4.9	4.6
19	5.6	6.6	1.1	.8
20	7.2	8.5	3.8	3.4
21	9.7	11.5	10.5	11.0
22	1.8	2.1	5.6	5.3
23	5.3	6.3	.6	.4
24	6.0	7.1	1.7	1.4
25	0.9	1.1	7.9	8.0

TABLE 5

QUASI-STATIONARY TEST RESULTS

a) Rectangular Distributions

Overall Peak RMS	Speci- men	Life kcs	Overall RMS	Secondary Cracks		
				Total Number	Large	Small
9.63	228	157.5	6.81	6	4	2
9.01	230	313.25	6.37	9	5	4
9.55	231	215.0	6.75	25	5	20
9.05	232	340.75	6.40	28	6	22
9.28	233	359.75	6.56	13	4	9
8.43	234	525.0	5.96	17	7	10
8.19	235	399.75	5.79	3	2	1
8.73	236	516.0	6.17	14	5	9
8.71	237	475.0	6.16	14	3	11
8.37	238	480.0	5.92	15	4	11
7.85	239	704.5	5.55	9	2	7
7.85	240	709.5	5.55	10	3	7

b) Truncated Gaussian Results

Spec	kcycles	Overall RMS	Secondary Cracks
241	653.75	5.66	sevs
242	455.0	5.82	1+sevs
245	540.75	5.80	S

c) Truncated Exponential Results

243	499.25	5.82	1s
246	315.25	5.79	0

d) Arbitrary Distribution

213	268.75	7.02	2+sevs
217	269.5	7.05	S
214	339.75	6.95	1+1c
218	365.5	6.97	1+1c
220	369.15	7.01	S
222	400.75	6.71	S - 3
224	400.95	6.71	3 - 0
223	435.15	6.78	S - 0
215	435.35	6.99	1 - Sevs
219	435.75	6.99	0 - 3s
221	452.50	6.75	S - 2
210	477.4	6.99	2 - 1
216	498.75	7.04	S - 2
212	540.9	6.97	S - 1s
225	541.15	6.79	S - 2+sevs
211	740.0	6.91	1+1s - 1

TABLE 6

REDUCTION OF TN 35 TEST DATA

(Tables 5, 8 and 9, UTIA TN 35)

Test Point	S_z/S_1	$R^{1/2}$	N_{gz}/N_{gz}	$\sum \frac{N}{N}$	Test Point	S_z/S_1	$R^{1/2}$	N_{gz}/N_{gz}	$\sum \frac{N}{N}$
34-10, 000-24	.706	.292	.519	.610	60- $\frac{1}{2}$.567	.0491	.822	.320
40-10, 000-24	.600	.089	.757	.757	60-1	.567	.0491	.822	.320
40-10 ⁴	.850	.410	.977	.913	60-4	.567	.0490	.825	.320
40-20, 000-24	.600	.053	1.078	1.080	60-10	.567	.0558	.726	.290
40-20x10 ³	.850	.315	1.142	1.083	60-40	.567	.0439	.912	.370
44-10, 000-24	.545	.0525	.744	.848	64- $\frac{1}{2}$.532	.0318	.876	.260
44-10 ⁴	.772	.352	.784	.800	64-1	.532	.0374	.756	.220
					64-4	.532	.0316	.868	.260
48-1	.709	.0916	1.548	1.190	64-10-20	.313	.00206	.878	.293
48-4	.709	.0833	1.700	1.310	64-10	.532	.0372	.766	.230
48-10	.709	.0796	1.786	1.370	64-10-40	.625	.0618	1.130	.374
48-40	.709	.0982	1.453	1.110	64-40-20	.312	.004	.448	.181
48-100	.709	.0970	1.473	1.130	64-40	.532	.0294	.947	.310
48-5000-24	.500	.019	1.021	.976	64-40-40	.625	.0768	.915	.324
48-5x10 ³	.709	.108	1.191	1.007	64-100	.532	.0338	.850	.320
52- $\frac{1}{2}$.654	.0859	1.053	.650	67.3- $\frac{1}{2}$.505	.0153	1.401	.20
52-1	.654	.0583	1.548	.960	67.3-1	.505	.0169	1.250	.18
52-4	.654	.0786	1.148	.710	67.3-4	.505	.0126	1.656	.25
52-10	.654	.0725	1.240	.770	67.3-10	.505	.0199	1.053	.18
52-40	.654	.0720	1.250	.780	67.3-40	.505	.0144	1.427	.30
					67.3-7	.505	.0125	1.643	.26

TABLE 6 (con'd)

Test Point	S_z/S_1	$R^{1/2}$	N_{ge}/N_{gt}	$\Sigma \hat{N}$	Test Point	S_z/S_1	$R^{1/2}$	N_{ge}/N_{gt}	$\Sigma \hat{N}$
54- $\frac{1}{2}$.630	.0793	.964	.510	68- $\frac{1}{2}$.50	.0145	1.336	.16
54-1	.630	.0793	.964	.510	68-1	.50	.0138	1.452	.17
54-4	.630	.0723	1.056	.560	68-4	.50	.0122	1.616	.20
54-10	.630	.0735	1.026	.550	68-7	.50	.0104	1.888	.24
54-40	.630	.0691	1.097	.590	68-10	.50	.0120	1.646	.23
56- $\frac{1}{2}$.607	.0679	.874	.430	68-40	.50	.0150	1.267	.26
56-1	.607	.0713	.837	.410	68-100	.50	.0114	1.467	.48
56-4	.607	.0649	.900	.450					
56-10-20	.357	.0058	.502	.362					
56-10	.607	.0678	.867	.430					
56-40	.607	.0723	.818	.410					
56-10-40	.715	.136	1.098	.595					

TABLE 7

SINGLE LEVER RANDOM PRELOAD TEST RESULTS

Prestress RMS = 16 ksi (peak)

t ₁	S ₂	Spec	kcs	Secondary Cracks		t ₁	S ₂	Spec	kcs	Secondary Cracks	
				Large	Small					Large	Small
1/4 hr	34	19	17.1	1	0	1/2 hr	34	85	22.4	0	- sevs
		20	23.3	sevs	- 1			77	26.5	sevs	- 0
		28	25.5	0	- sevs			87	32.2	1s	- 1s
		22	27.1	0	- 0			30	33.9	0	- 1c
		18	30.3	1+1c	- 1c			94	67.6	1+1s+1c	- 0
		Mean	.5P	25.5				152	6.0	S	- 1+1c
	(graph)			.5P	30.0						
1/4 hr	28	49	56.3	1c	- 0	1/2 hr	28	91	18.6	0	- 0
		65	73.4	1s	- 0			151	57.5	1c	1
		66	74.3	1s	- 0			29	67.8	2+sevs	- 1c
		41	75.5	sevs	- 0			42	72.1	1s	- 0
		23	78.5	1+1s	- 0			89	85.2	0	- 0
		.5P	75.0					93	148.7	0	- 0
				.5P	70.0						
1/4 hr	22.5	38	152.1	0	- 0	1/2 hr	22.5	150	24.0	S	- 0
		34	186.3	sevs+1c	- 0			71	158.1	0	- 0
		57	214.6	0	- 1s			33	192.6	0	- 0
		39	226.9	1c	- 0			69	236.0	0	- 0
		43	232.0	2s	- 0			60	332.2	0	- 0
		.5P	210					70	379.5	1s	- 1+1c
				.5P	215						
1/4 hr	.40	164	2.4	1c	- 1c	1/2 hr	16.7	101	262.0	1	- 1
		115	11.5	0	- 0			103	750.4	1s	- 0
		163	11.7	1	- 0			100	825.8	0	- 2c
		165	5.5	2s	- 0			96	1,334.1	0	- 0
		166	16.7	1s	- 1s			108	3,492.2	1c	- 0
		.5P	9.0					149	487.1	0	- 0
				.5P	820						
1/4 hr	19.5	121	431.6	2c	- 0	1/2 hr	40	106	2.3	0	- 1c
		118	584.1	0	- 0			97	4.9	1	- 1
		128	597.8	0	- 0			105	6.6	0	- 0
		140	607.9	1s	- 0			107	10.31	1s	- 1c
		127	674.9	0	- 0			98	21.36	3s	- 1
		.5P	600					.5P	6.6		
1/4 hr	16.7	111	10,024.2	0	- 0						

TABLE 7 (con'd)
 Prestress RMS = 13.5 ksi (peak)

t ₁	S ₂	Spec	kcs	Secondary Cracks		t ₁	S ₂	Spec	kcs	Secondary Cracks																														
				Large	Small					Large	Small																													
1 hr	34	13	4.6	1 - 0	$\frac{1}{2}$ hr*	11.1	102	3,946.6	0 - 0	(not failed)																														
		11	10.9	sevs-0								104	10,000.0																											
		12	11.0	0 - 0																																				
		95	26.0	1+sevs-0										$\frac{1}{2}$ hr*	19.5	146	78.5	0 - S																						
		15	34.7	1+sevs-0															145	136.4	0 - 0																			
		56	52.8	1s - 0																		144	275.1	0 - 1s																
		.5P	21																						147	331.3	0 - 0													
																												142	492.0	0 - 0										
		1 hr	28	76																											50.6	0 - 0	$\frac{1}{2}$ hr	34	73	20.6	0 - 1c			
				32																											53.3	2 - 0							48	28.9
78	58.6			0 - 0	84	30.4	0 - 1s+1c																																	
79	107.8			1 - 0				90	30.9	0 - 1c																														
82	132.5			1 - 2							92	38.2	0 - 1																											
155	107.3			0 - 1										.5P	31																									
156	8.4			1s-1c													$\frac{1}{2}$ hr	28	86	51.1	2s - 1s																			
.5P	69.0																					45	96.1	0 - 1																
1 hr	22.5			40																					236.2	2 - 0	68				124.4	0 - 1								
				52																					251.9	0 - 1s		75	163.6	0 - 0										
		27	270.2	0 - 1																					83	223.1							0 - 0							
		74	323.1	1 - 0																														.5P	(75)**					
		72	443.1	0 - 0	$\frac{1}{2}$ hr	22.5	37																														104.8	1c - 0		
		158	207.7	0-1+2s				25	180.6	2s+1c - 0																														
		.5P	260								16	230.6	0 - 1s																											
		1 hr	16.7	110										7,554.2	0 - 0	26																							261.4	2c - 0
																	35	307.9	0 - 0																					
				1 hr										40	114					4.38	0 - 0	.5P	230																	
112	8.18														1+1c-1c					$\frac{1}{2}$ hr	40						160				3.6	1c - 0								
113	12.60														0-1+1s													154	7.3	1s - 0										
125	14.90														1c-0										159	12.7							2+sevs 1c							
116	17.10														S-0																			109	25.3	1c-1c				
.5P	12.3					161	17.1								2s 1+1c																									
1 hr	19.5				122			373.6	0 - 1c	$\frac{1}{2}$ hr																											19.5	141		
					143			475.7	0 - 0		120	414.2	0 - 0																											
		117	515.3		0 - 0			126	420.7							1c - 0																								
		130	538.3		0 - 0												129	569.8	0 - 0																					
		123	573.1	0 - 1	119									678.0								0 - 0																		
		.5P	510																	157	277.1		0 - 0																	
																								.5P			470													

Note: Legend for Secondary crack column - as Table I

* These tests carried out with prestress RMS = 16 ksi (peak)

** Value used for regression of test results (actual mean appears affected by "discontinuity phenomenon" discussed in Section 2.5)

TABLE 8
 VARIATION OF MEAN STRESS
 ALTERNATING STRESS = ± 34 KSI

Spec	Endurance kilocycles	Secondary Cracks	Spec	Endurance kilocycles	Secondary Cracks	Spec	Endurance kilocycles	Secondary Cracks
M2	62.7	0 - 0	M18	650.9	0 - 2	M24	23.35	2s - 1s
M6	80.0	0 - 1s	M10	708.7	2 - 1	M20	26.51	1 - 0
M1	86.2	1c - 1s	M17	850.0	0 - 11	M27	32.81	1 - 0
M3	107.1	0 - 0	M16	936.0	10 - 10	M25	32.90	2 - 0
M8	107.9	0 - 0	M14	1,122.3	7 - 7	M26	34.00	1c - 0
M7	108.7	0 - 1	M12	1,163.0	0 - 7	M19	35.30	1c+1s-1c
M4	161.5	2c - 2s	M11	1,245.0	5 - 20	M21	35.50	1+2s-1c
M9	186.4	1c - 1	M15	1,306.0	9 - 5	M23	37.71	0 - 0
M5	190.0	0 - 0	M13	1,880.5	6 - 3	M22	44.61	2s - 1s

Mean Stress $S_m = 0$

$S_m = 34$ ksi Compression

$S_m = 34$ ksi Tension

Average Crack number

$$\frac{9}{7} = 1.28$$

$$\frac{105}{7} = 15.0$$

$$\frac{18}{7} = 2.57$$

Note: Secondary cracks described as in Table 1

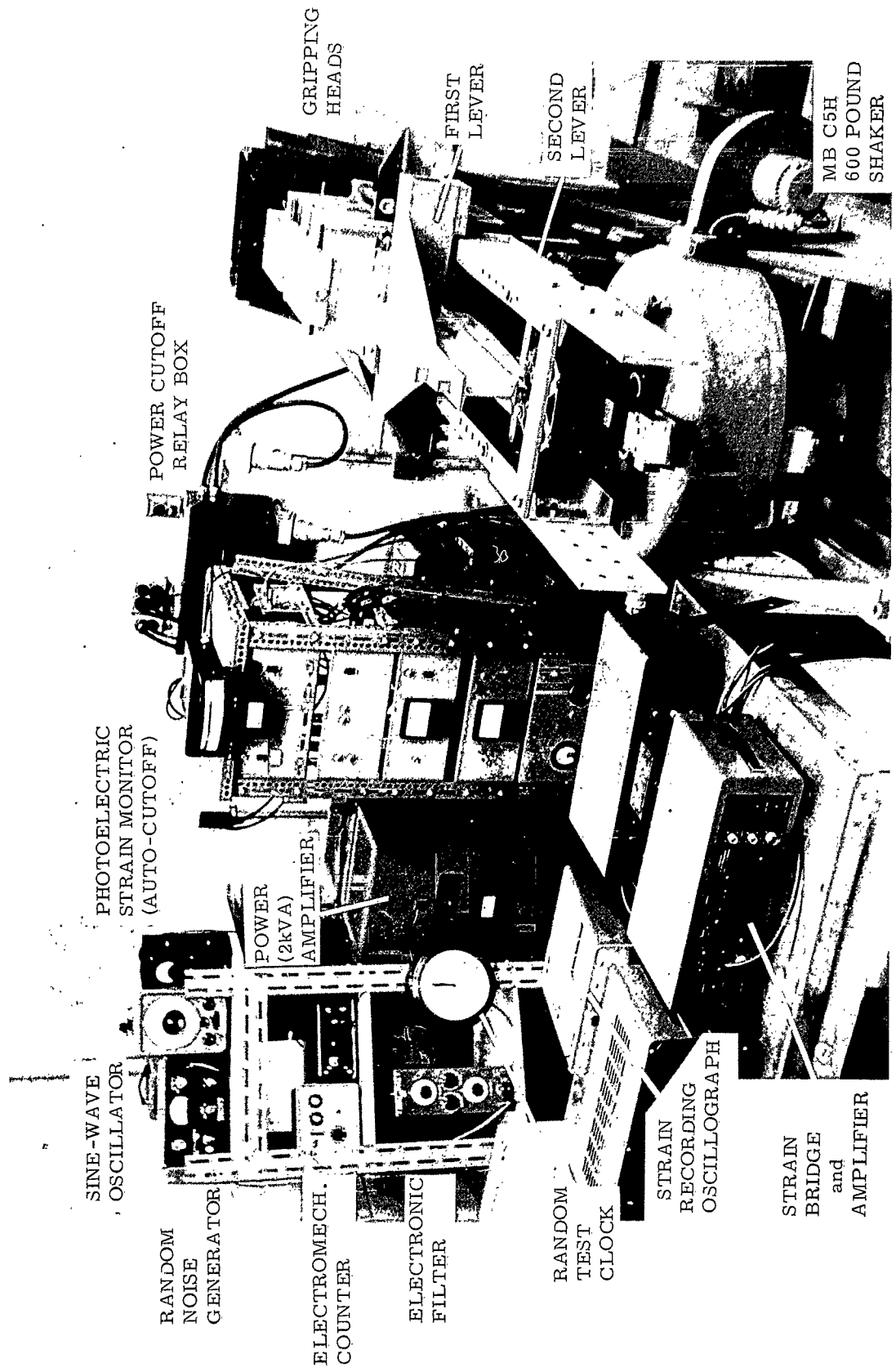
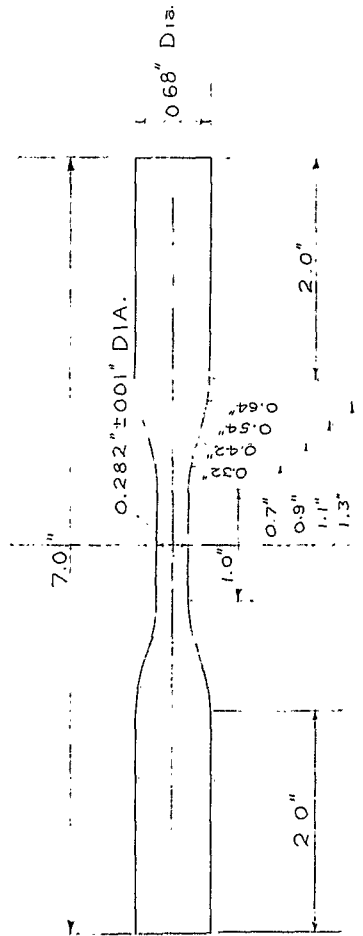


FIGURE 1 LAYOUT OF UTIA FATIGUE TEST FACILITY



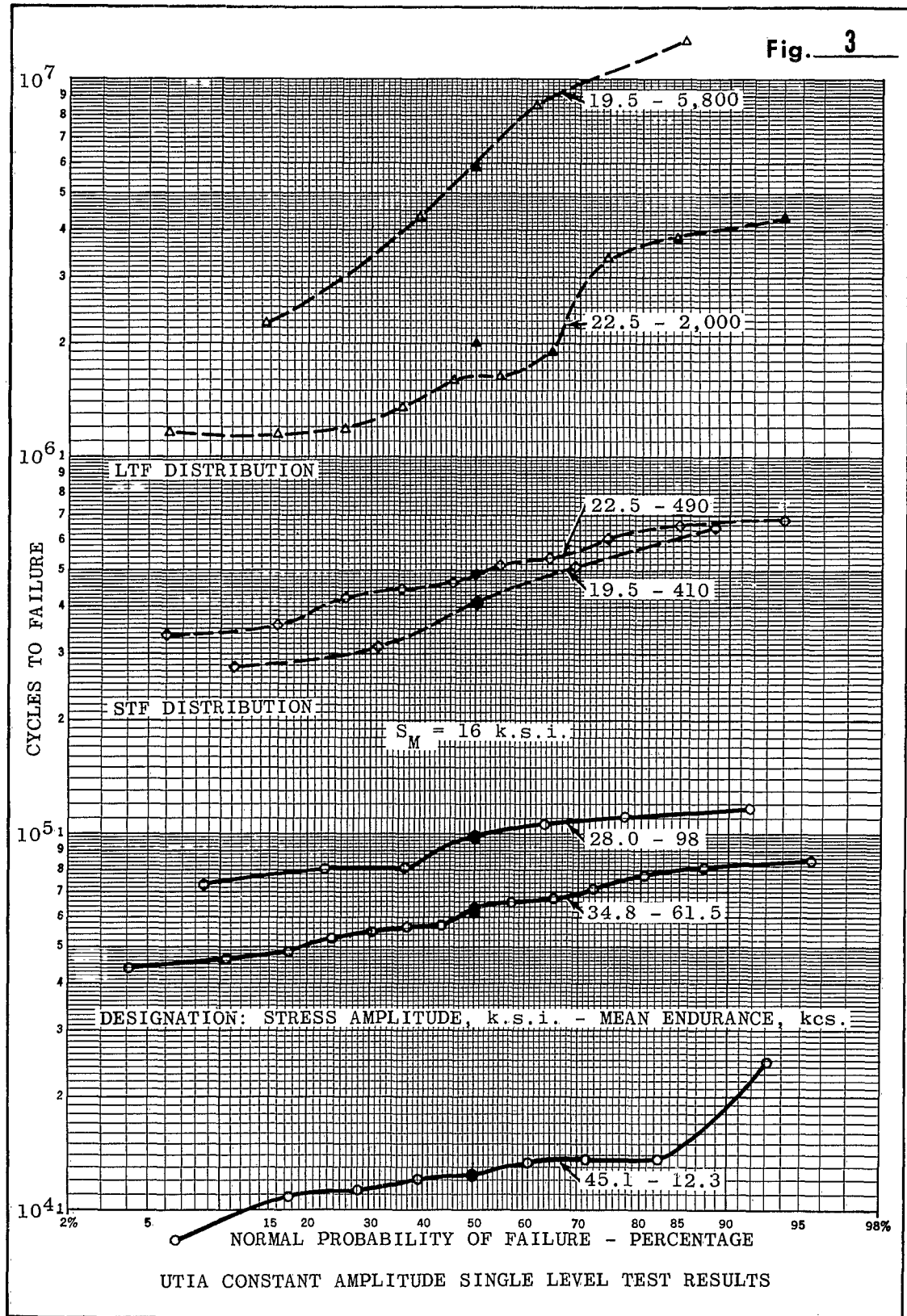
TURN FROM 0.75" EXTRUDED BAR USING STEEL TEMPLATE

TEST SPECIMEN

FIG. 2

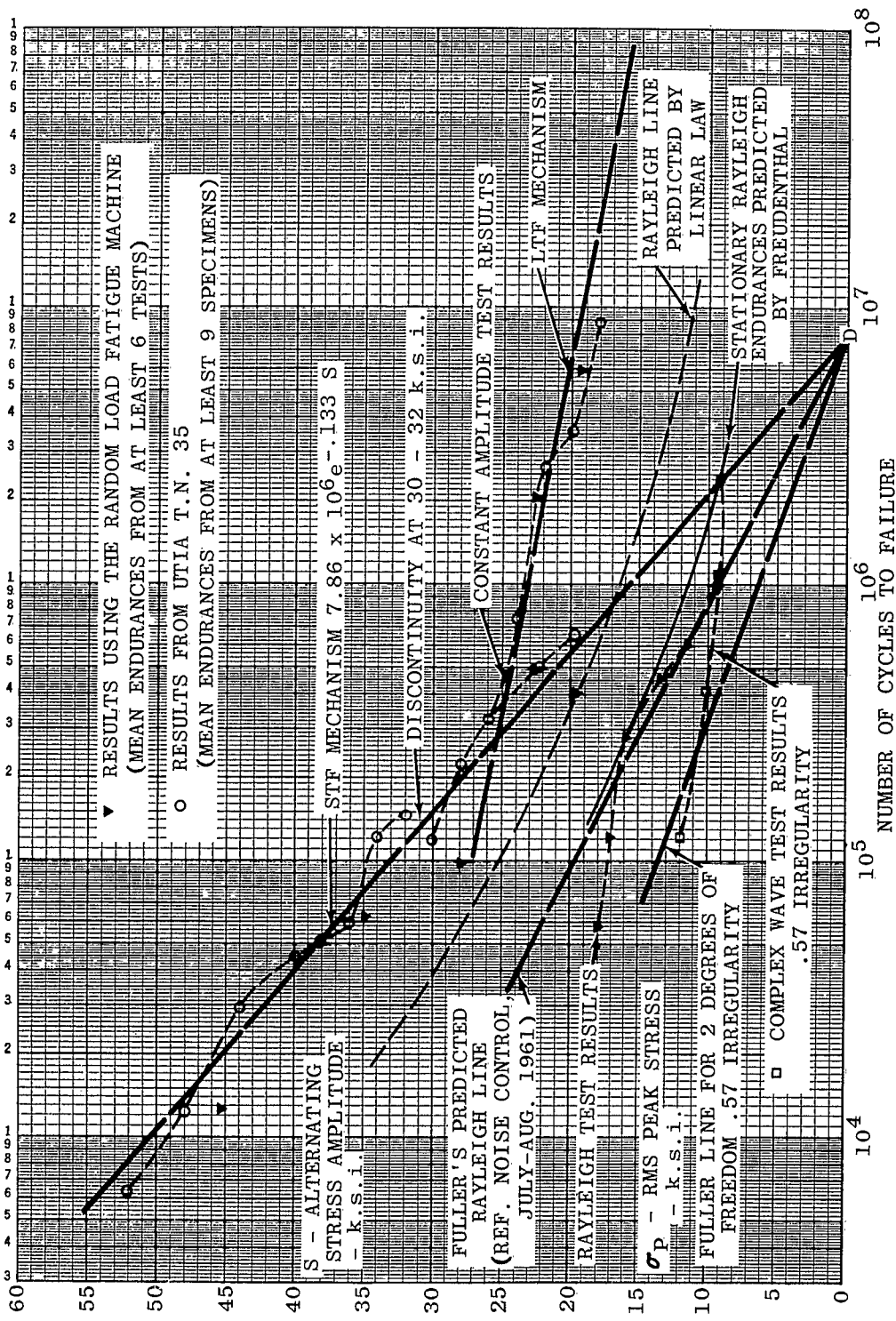
MATL: 2024S-T4 AL. ALY	SPEC. QQ-A-267	No. REQD. 500
FINISH "O" GAUGE (LONGITUDINAL)		
INSTITUTE OF AEROPHYSICS		
UNIVERSITY OF TORONTO		
DWG. TITLE		
FATIGUE SPECIMEN		
NO. 1		
DWG. No. 5/2-60-1		
NEXT ASSY.		
DATE 4/4/60		
SCALE 1:1		
DWG. SIZE A		
DIMENSIONAL TOLERANCES (Unless Otherwise Noted)		
LINEAR DIMENSIONS ±.005		
EXTERNAL DIMENSIONS -.000		
INTERNAL DIMENSIONS +.000		
ANGLE ±1°		
DRAWN BY R. Swanson		
APPROVED BY		

Fig. 3



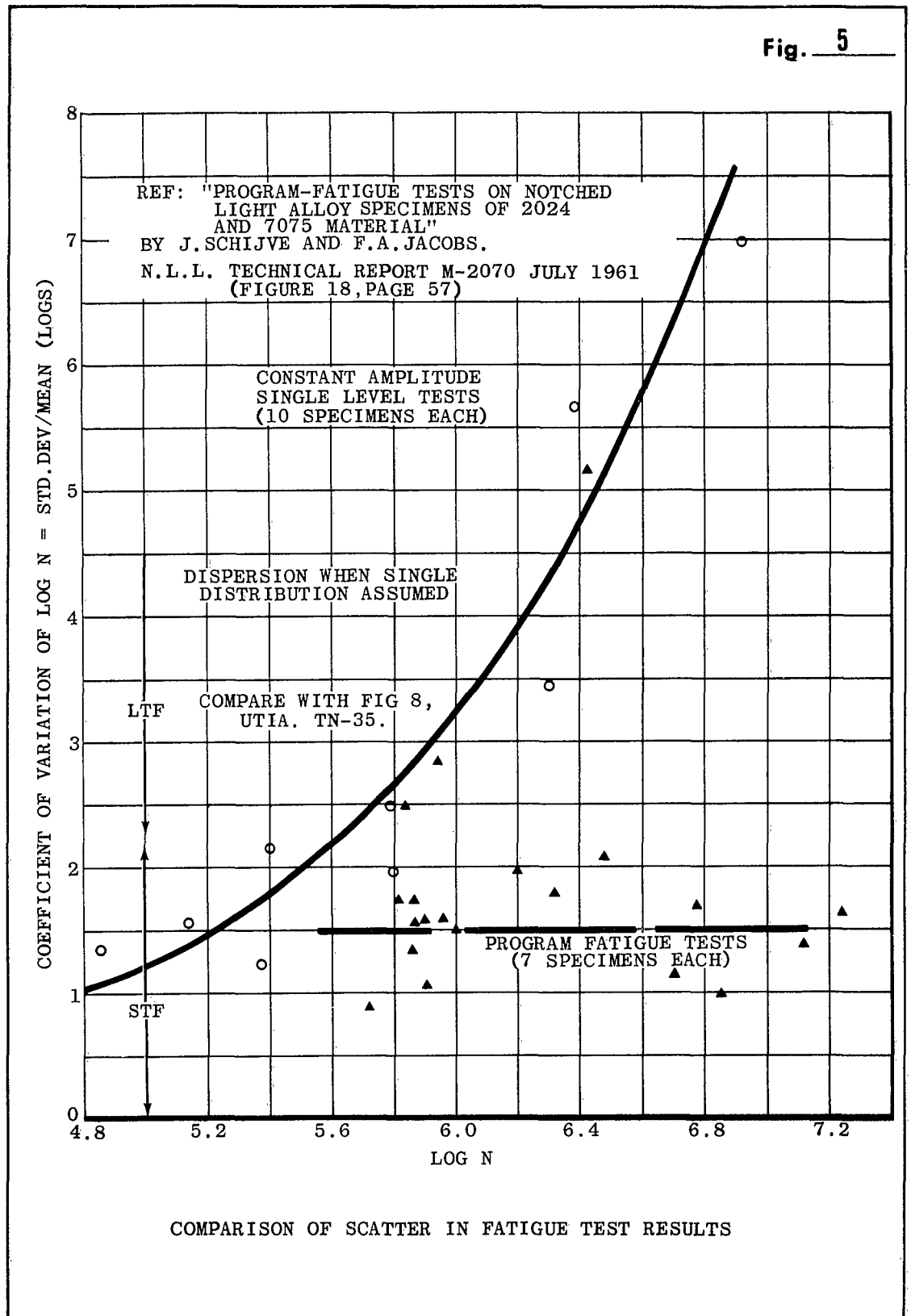
UTIA CONSTANT AMPLITUDE SINGLE LEVEL TEST RESULTS

Fig. 4



PLOT OF MEAN ENDURANCES OBTAINED FROM THE SINGLE LEVEL CONSTANT AMPLITUDE TESTS AND THE STATIONARY RANDOM AMPLITUDE TESTS

Fig. 5



A TWO-DISTRIBUTION INTERPRETATION
OF RESULTS

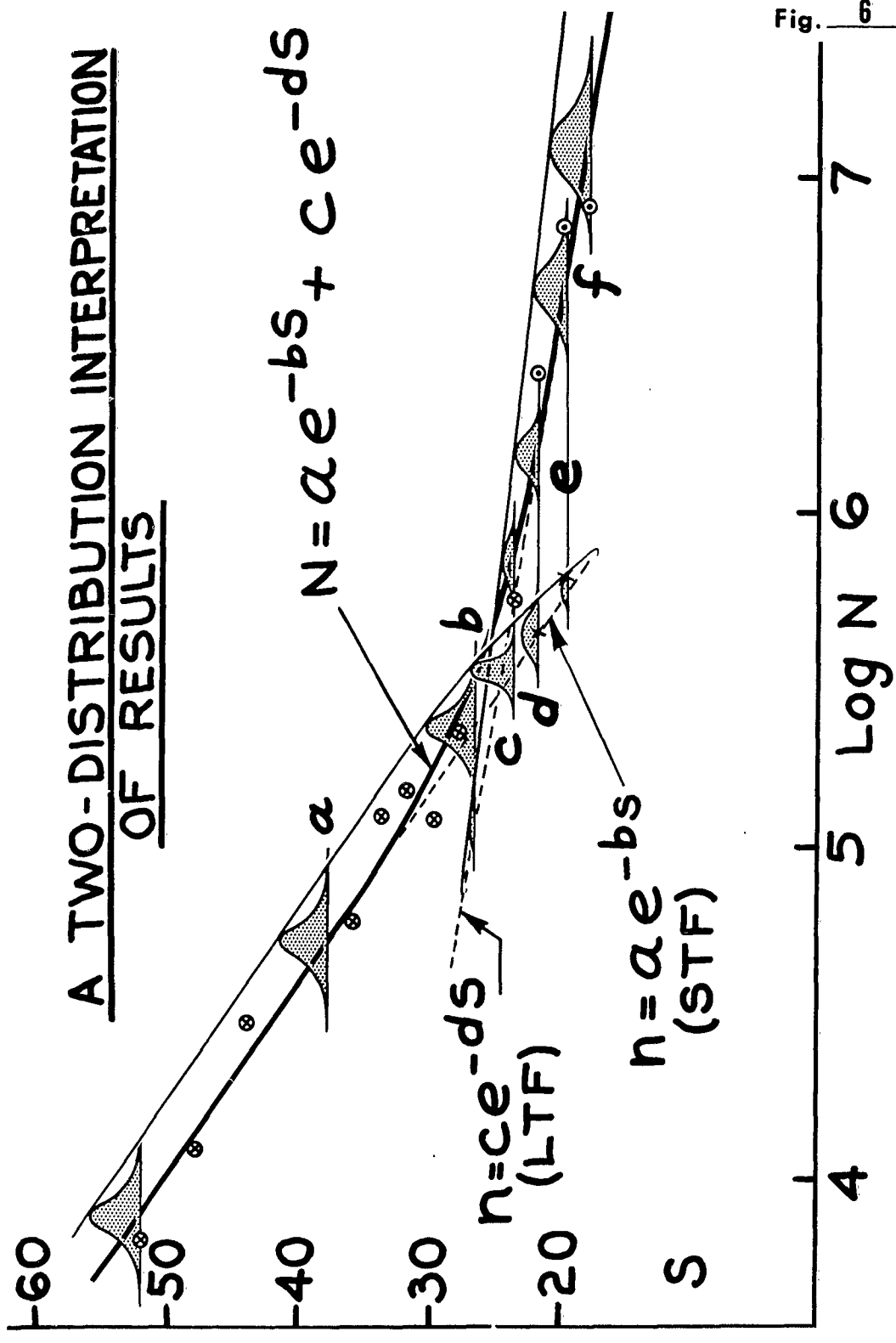


Fig. 6

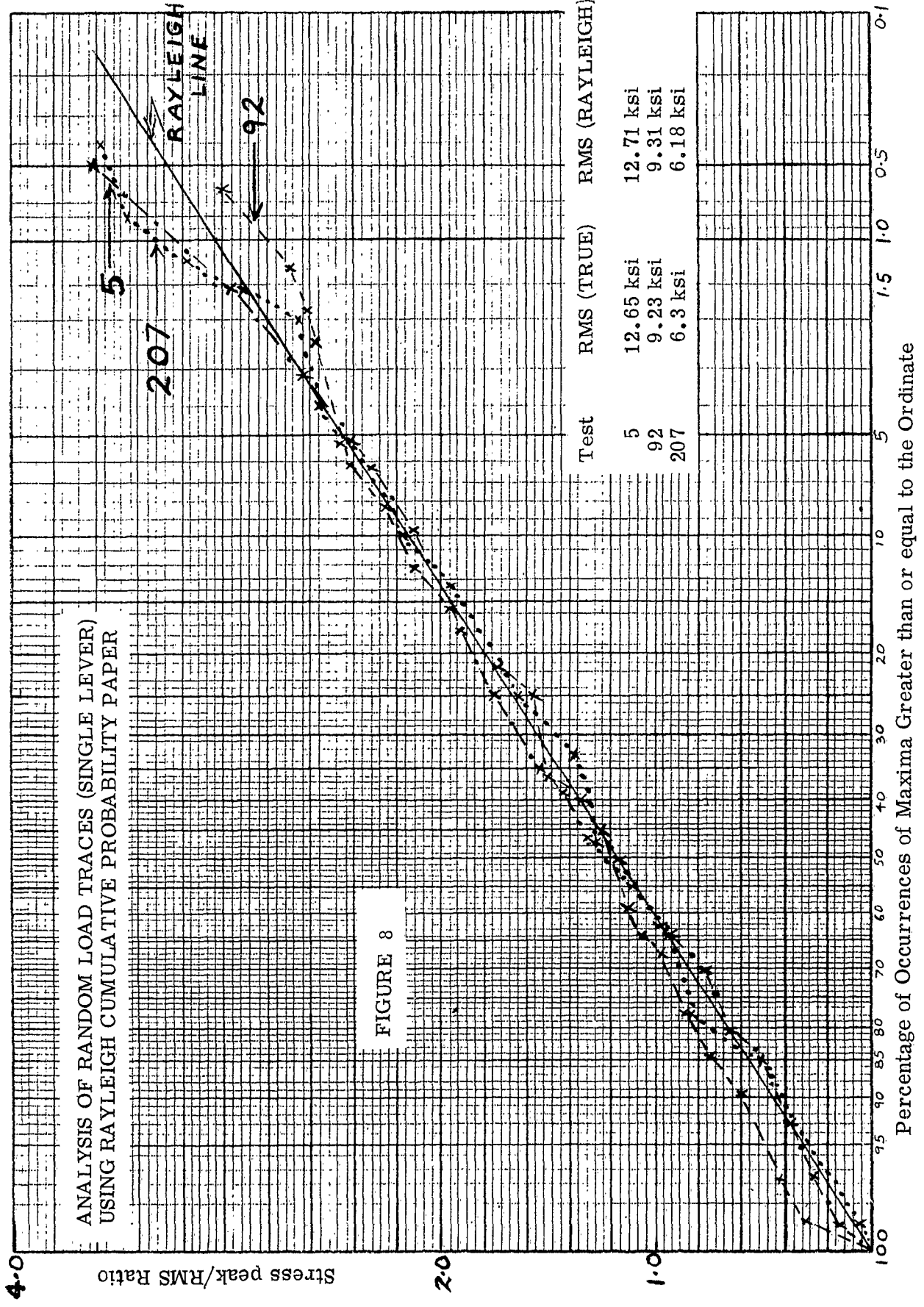
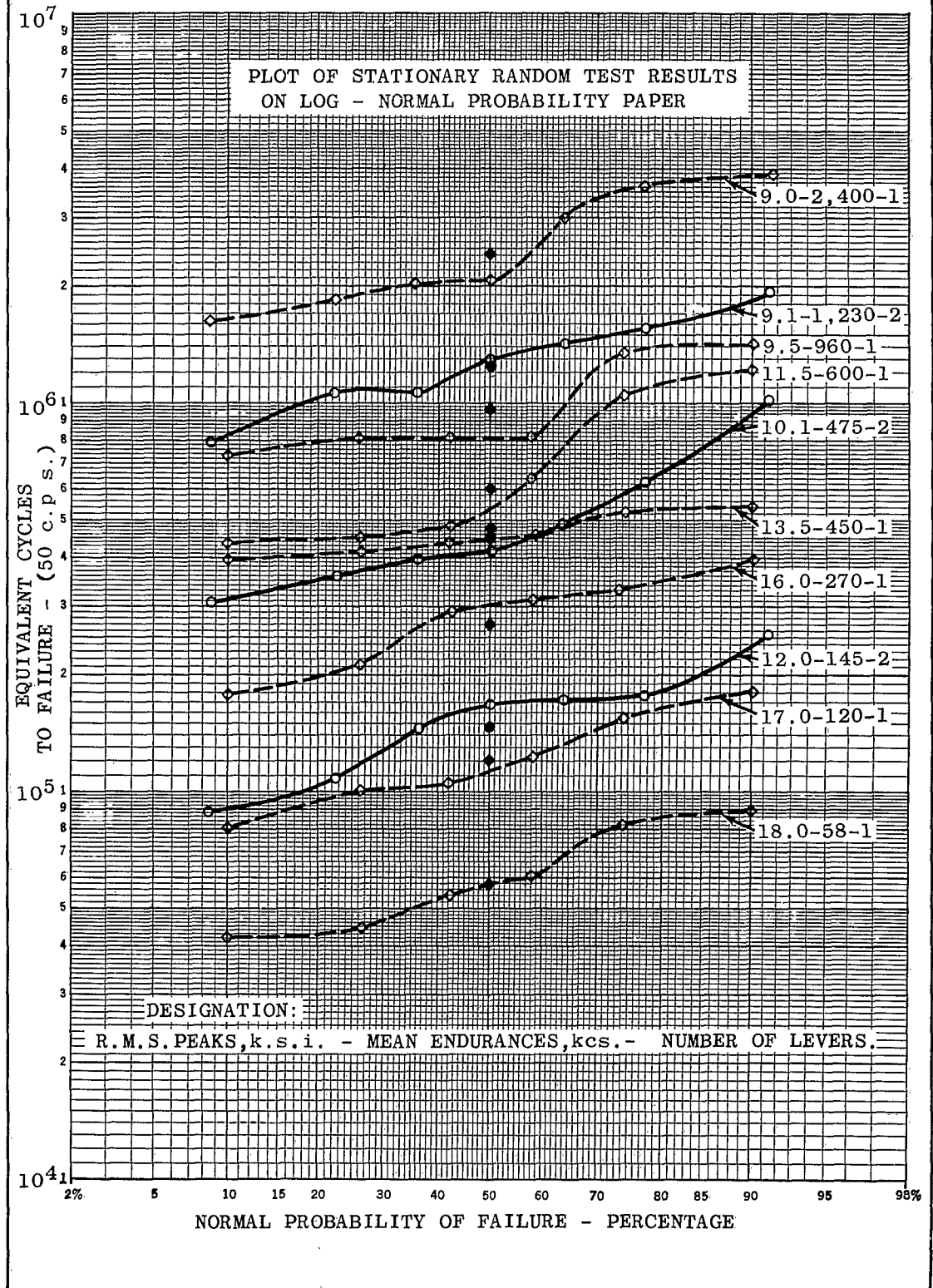


FIGURE 8

Fig. 9



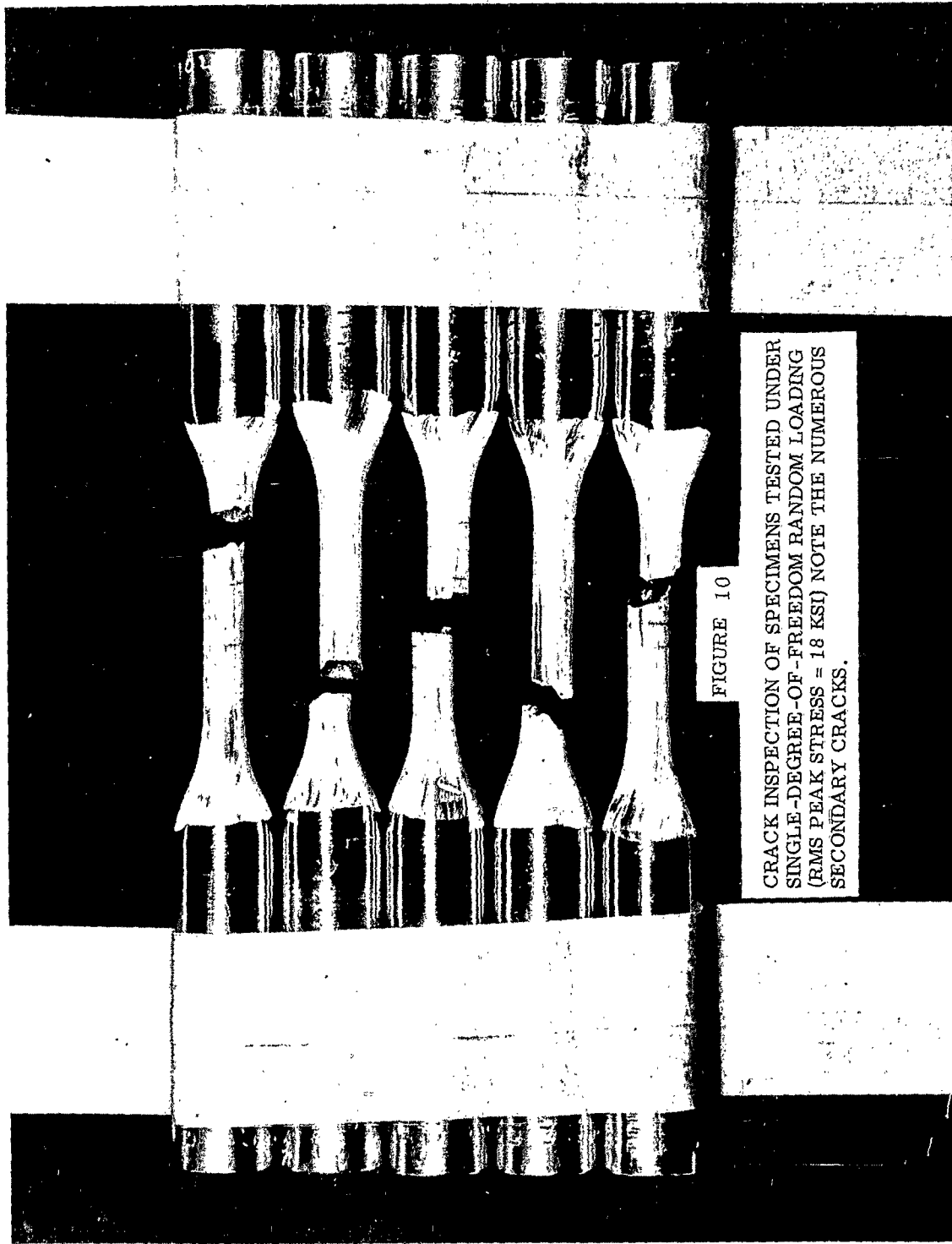


FIGURE 10

CRACK INSPECTION OF SPECIMENS TESTED UNDER
SINGLE-DEGREE-OF-FREEDOM RANDOM LOADING
(RMS PEAK STRESS = 18 KSI) NOTE THE NUMEROUS
SECONDARY CRACKS.

DYE PENETRANT INSPECTION OF A GROUP OF SPECIMENS TESTED AT
CONSTANT STRESS AMPLITUDE (34ksi) WITH A MEAN STRESS CF 16 ksi.
NO SECONDARY CRACKS WERE FOUND.

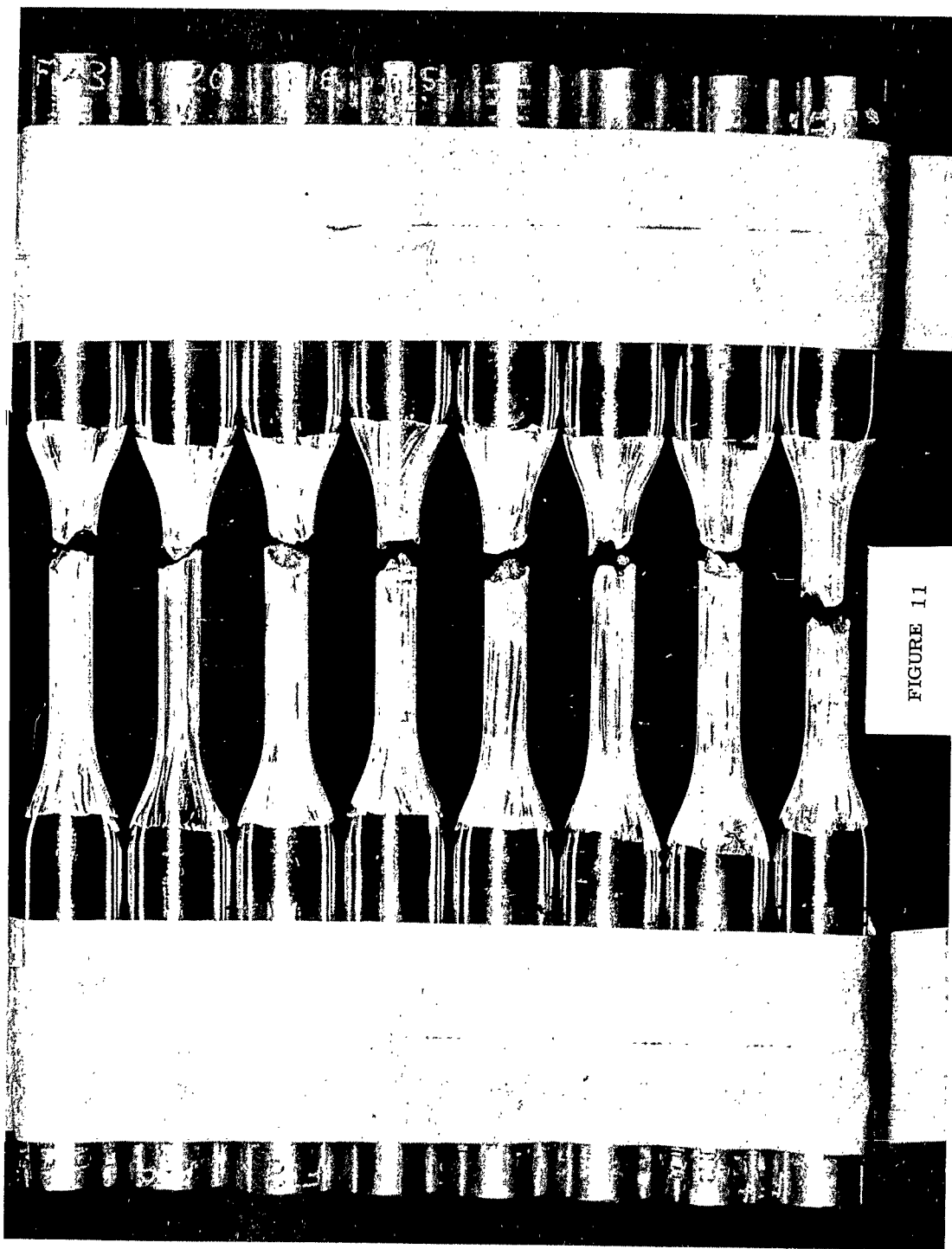
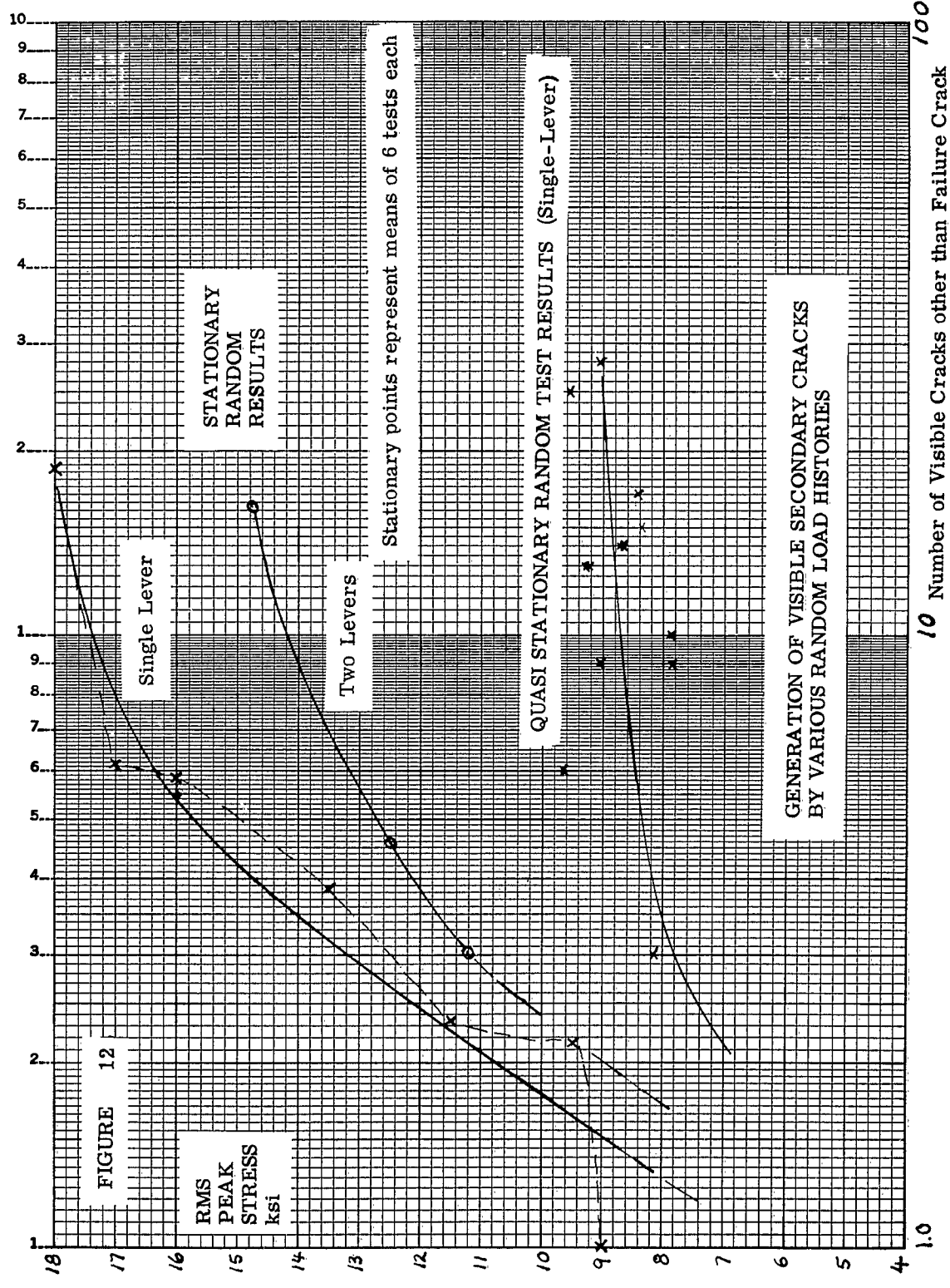


FIGURE 11



COMPARISON OF FATIGUE SPECIMEN STRAIN TRACES

USING A SINGLE LEVER

USING TWO LEVERS

SINGLE RESONANT FREQUENCY
 $f = 45 \text{ cps}$

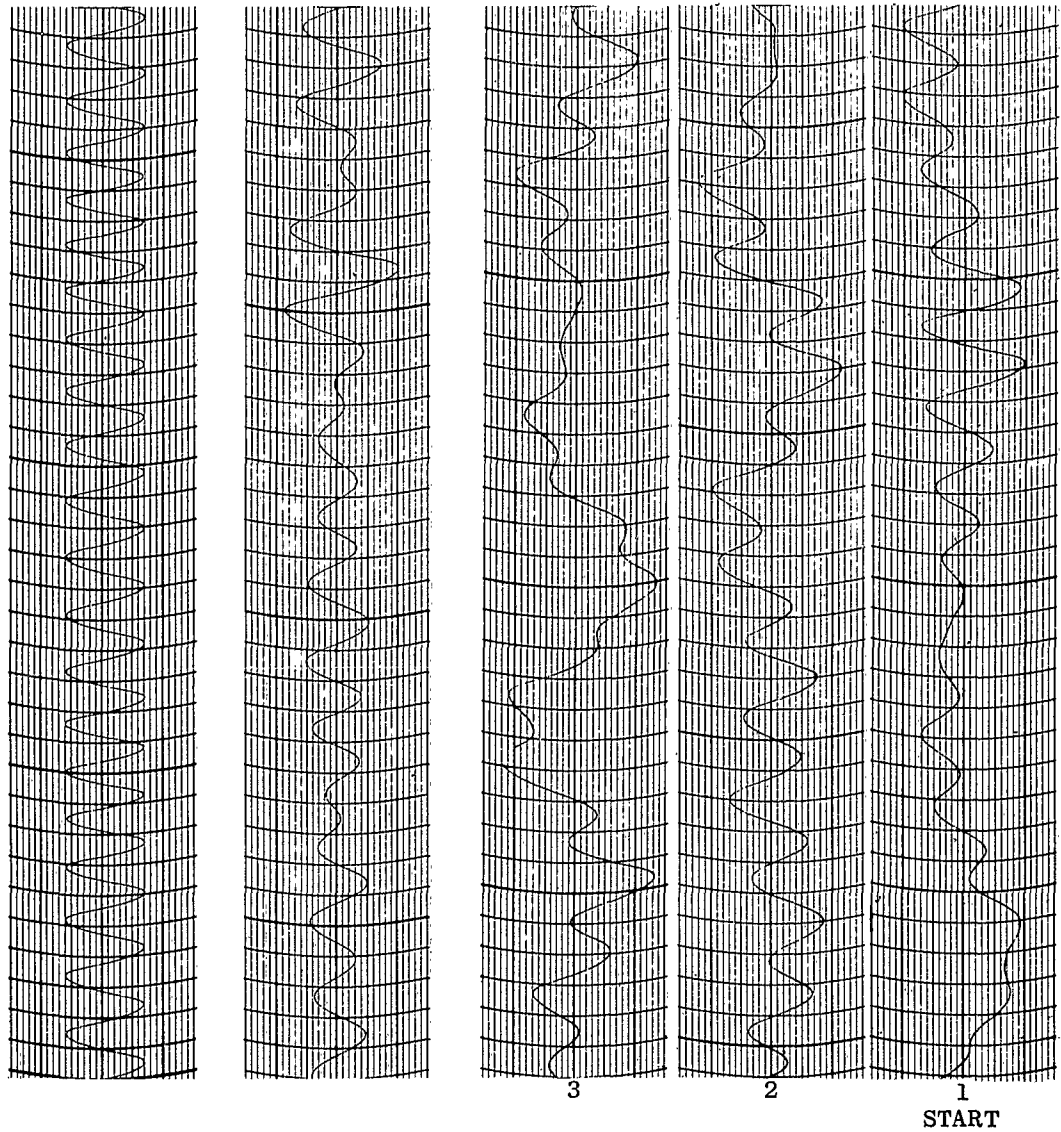
TRACE 178
TWO RESONANT FREQUENCIES
R.M.S. 10.4 ksi

SINE WAVE
INPUT

RANDOM NOISE
INPUT

RANDOM NOISE INPUT
THREE CONSECUTIVE SAMPLES

FINISH



SPEED OF TRACE 62.5 CM PER SECOND
LOAD 1,740 LBS PER CENTIMETER

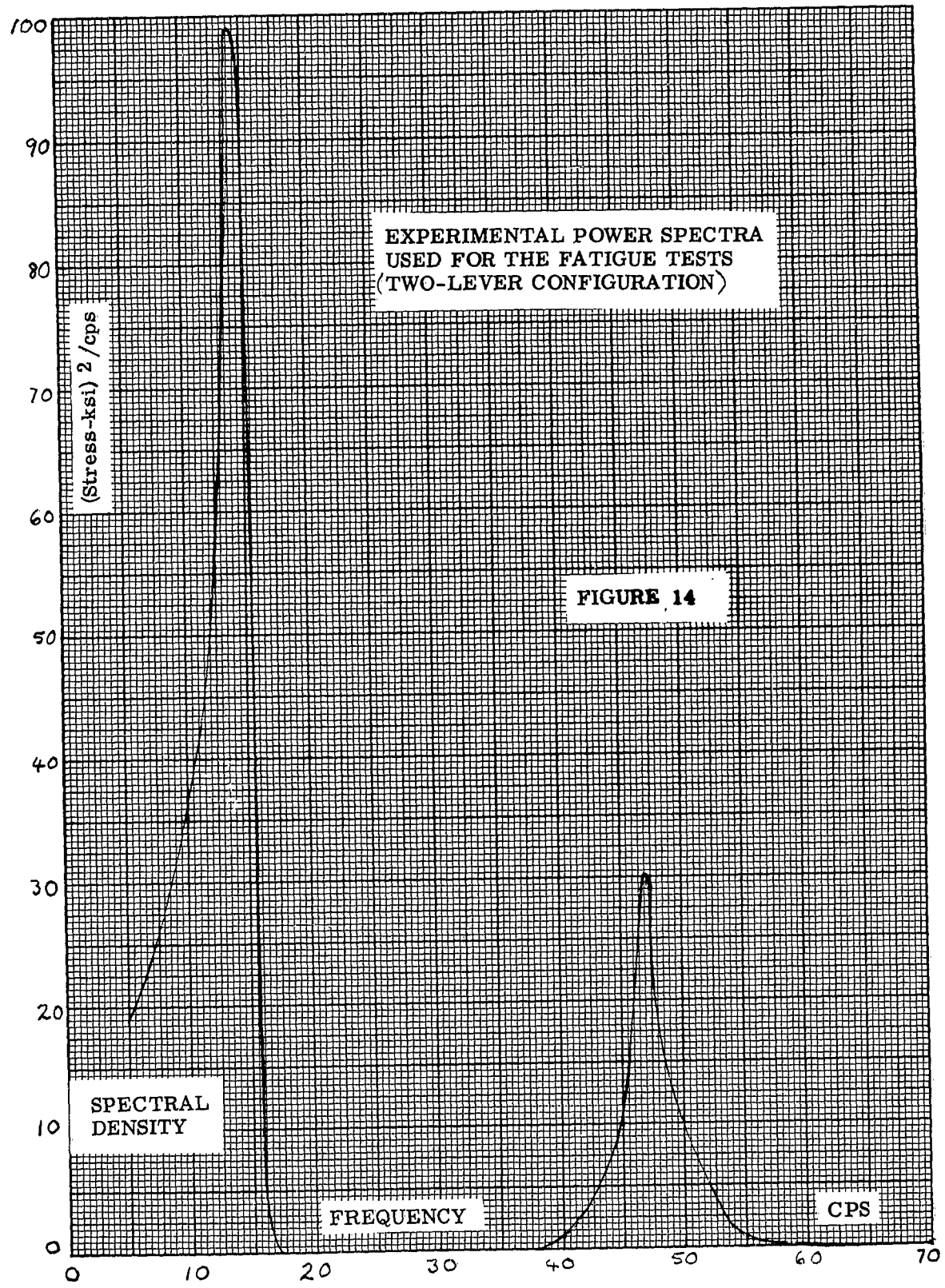
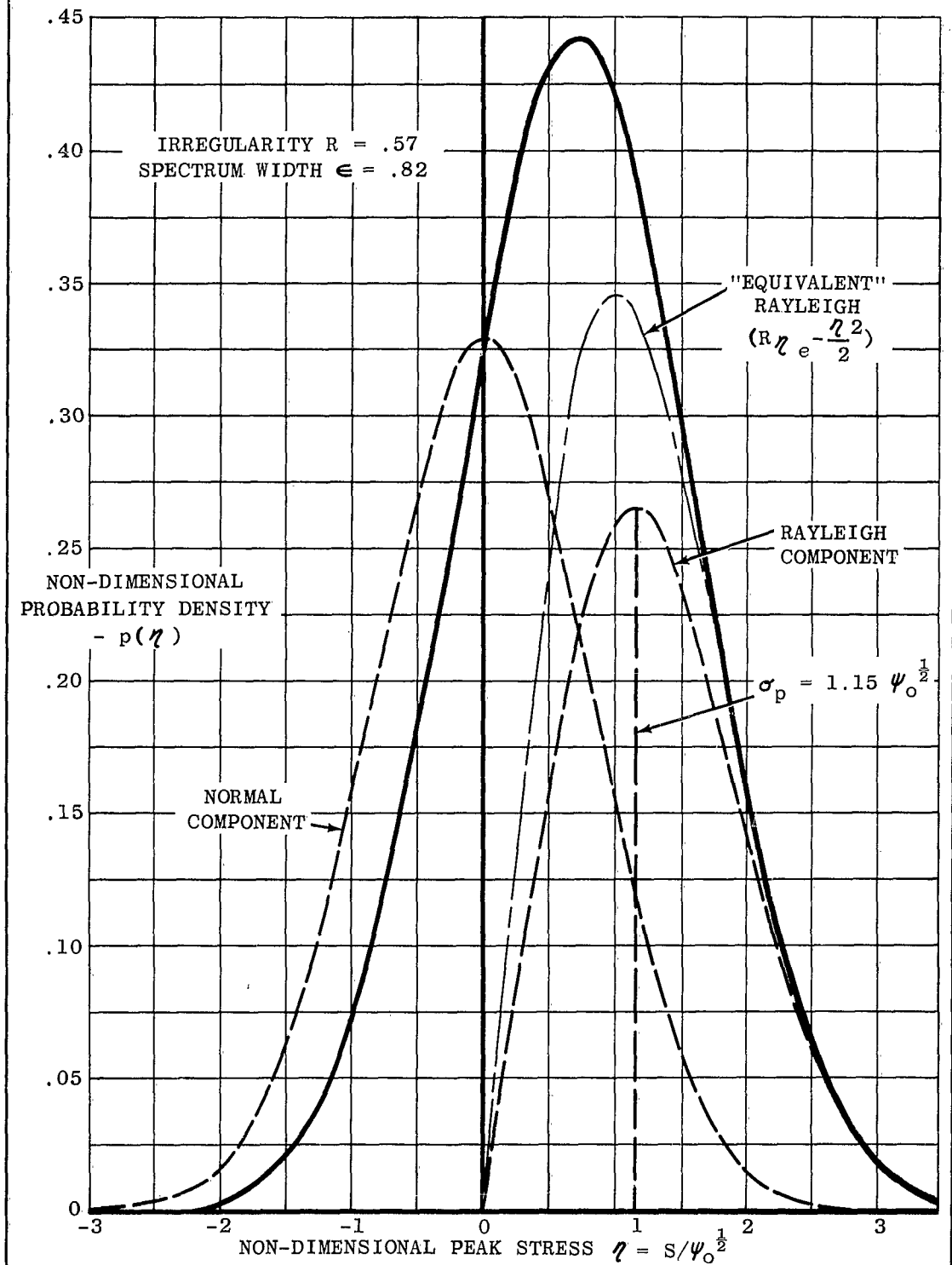


Fig. 15



DISTRIBUTION OF STRESS PEAKS FOR TWO LEVER CONFIGURATION

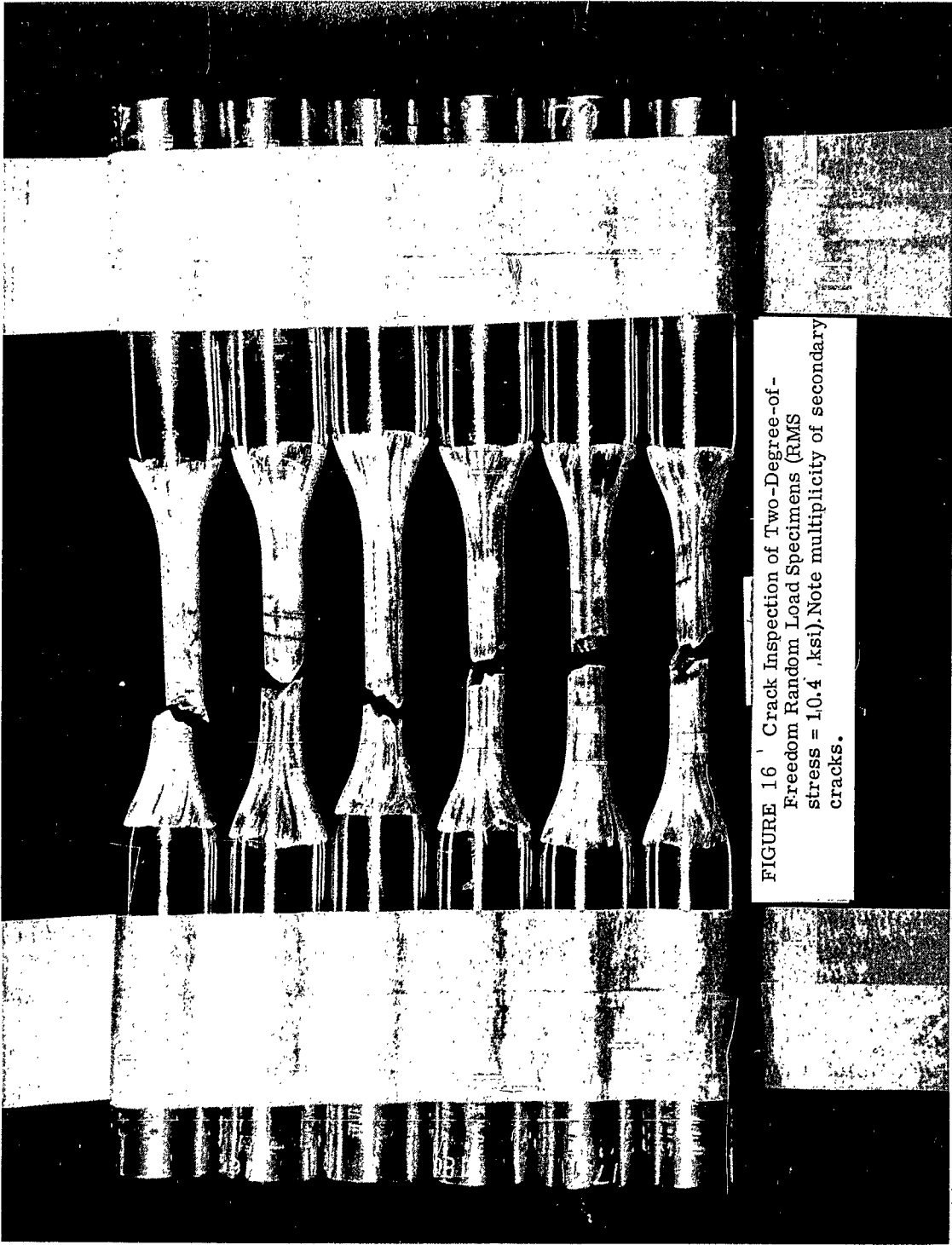
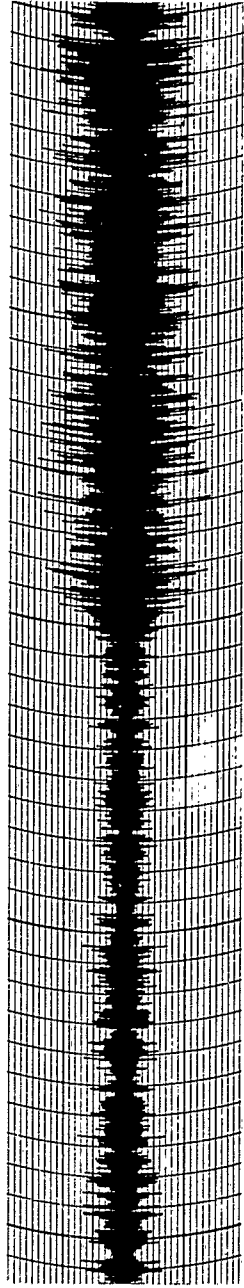


FIGURE 16 Crack Inspection of Two-Degree-of-Freedom Random Load Specimens (RMS stress = 10.4 ksi). Note multiplicity of secondary cracks.

SPECIMEN STRAIN TRACE

TRANSITION IN RMS LOAD LEVEL (MANUAL) 5,300 p.s.i. TO 11,000 p.s.i. RMS



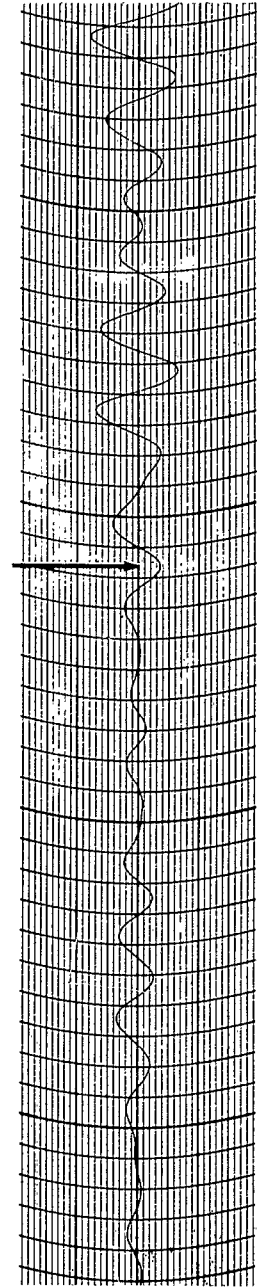
SPEED OF TRACE 5 MM PER SECOND

5.3 k.s.i. RMS

TIME →

11.0 k.s.i. RMS

BEGINNING OF CHANGEOVER



SPEED OF TRACE 625 MM PER SECOND

QUASI-STATIONARY RANDOM LOAD TESTS

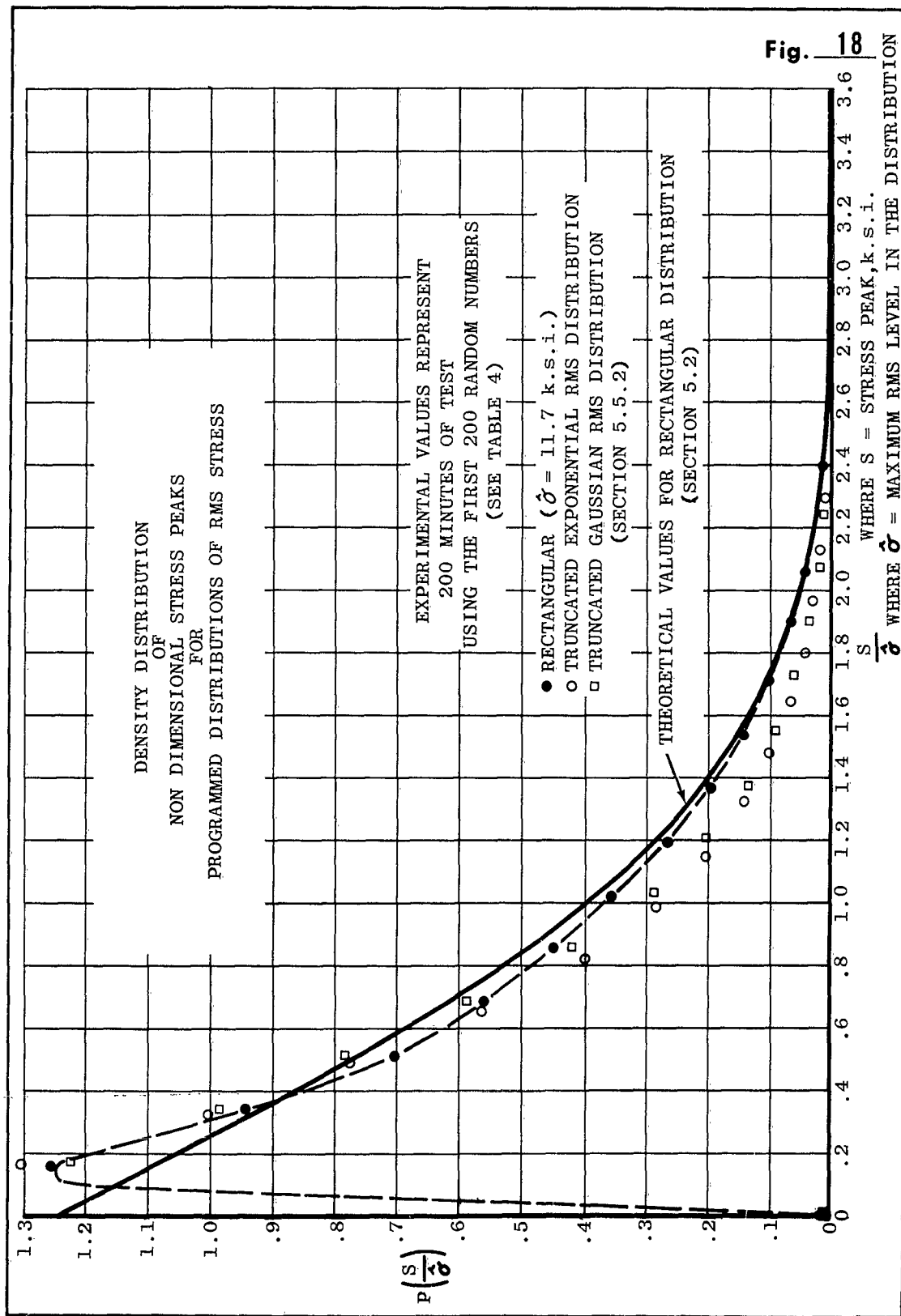
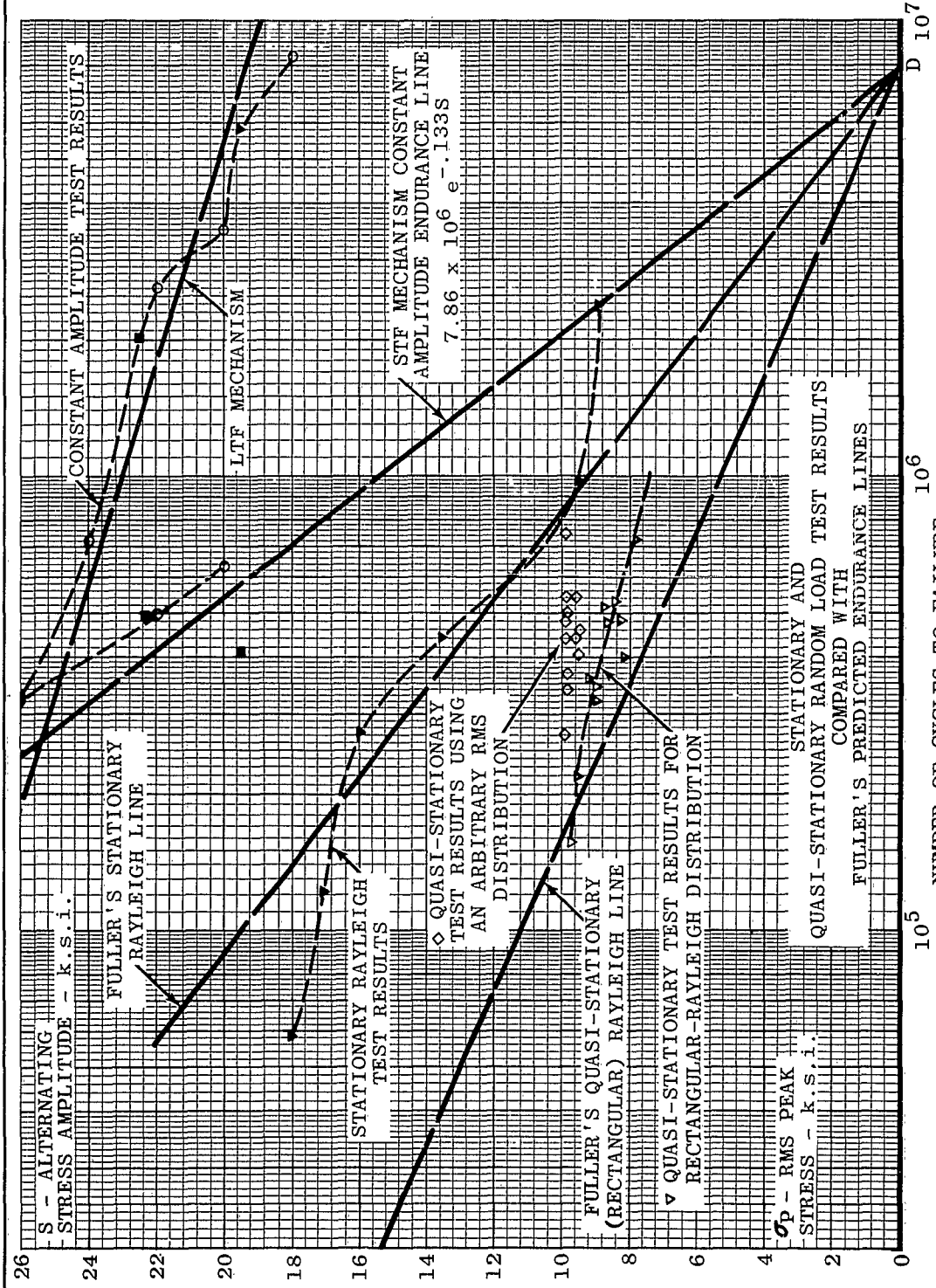


Fig. 18

Fig. 19



10⁵

10⁶

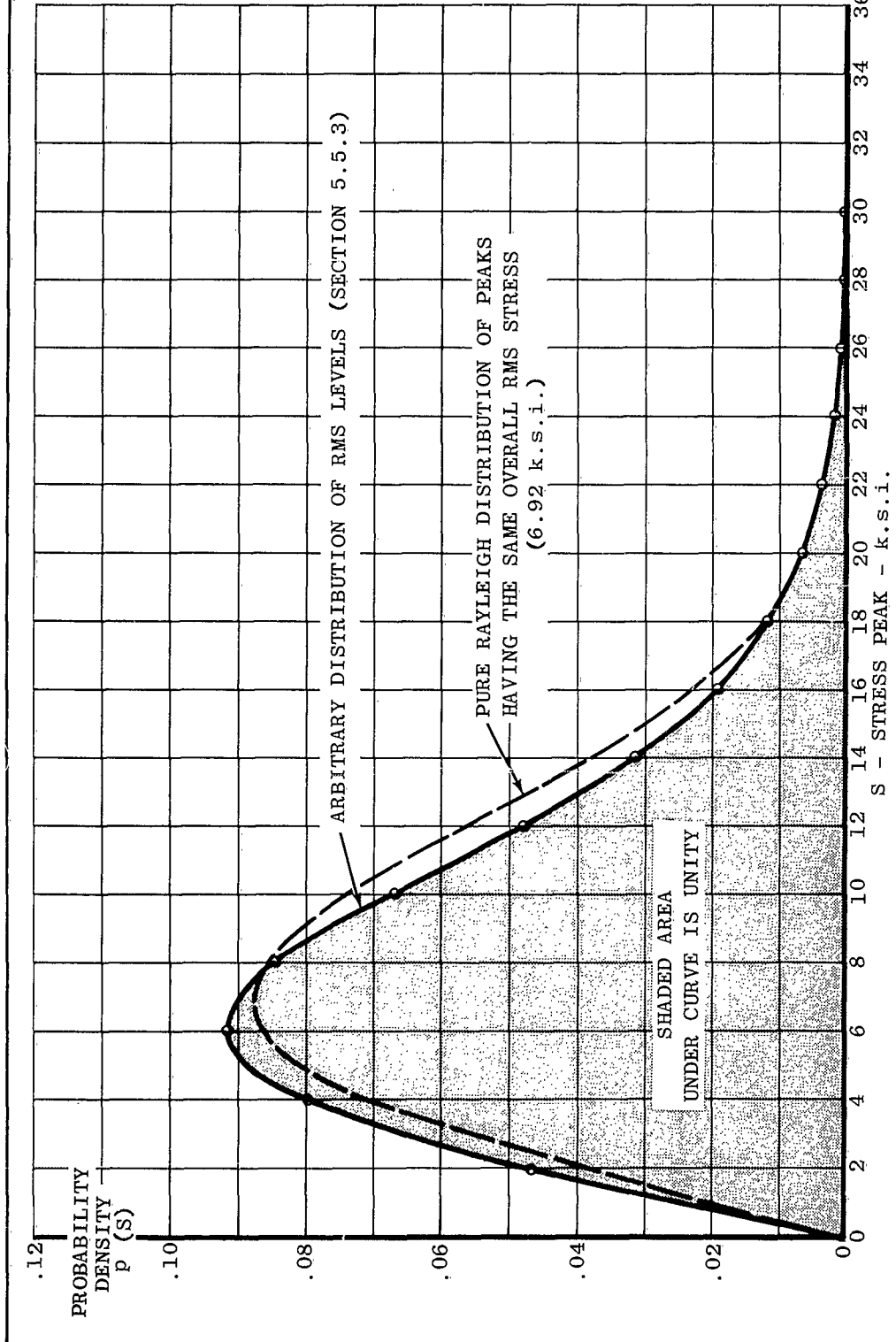
D 10⁷



FIGURE 20

Crack Inspection of Specimens tested with a Quasi-Stationary Random Load History using a Rectangular Distribution of RMS Levels. Overall RMS of these tests 5.5 to 6.8 ksi.

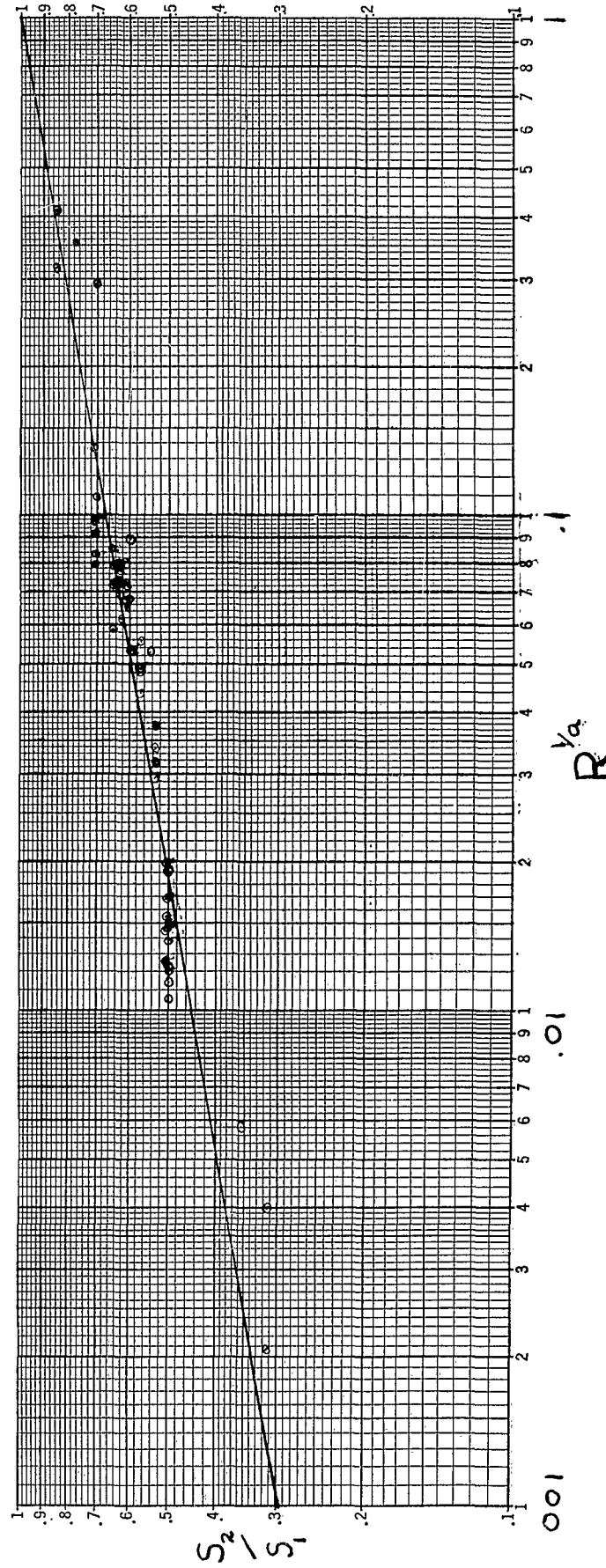
Fig. 21



FINAL PEAK DENSITY DISTRIBUTION $p(S)$ FOR AN ARBITRARY DISTRIBUTION OF RMS LEVELS COMPARED WITH THE EQUIVALENT RAYLEIGH DISTRIBUTION

VARIATION IN THE CORTEN-DOLAN PARAMETER $R^{1/2}$
 WITH STRESS RATIO S_2/S_1 , TESTSTRESS/PRESTRESS

Data Taken from Tables 5, 8 and 9, UT1A T.N. 35



Linear Least Squares Regression Line slope = 5.67

FIGURE 22

The Linear Summation Ratio $\sum \frac{N}{N} \times$
 and
 The Corten - Dolan Life Ratio $\frac{N_c}{N_{fc}}$
 plotted against
 Two -Level (Hi-Lo) Prestress Level

These results (taken from Tables 5, 8 and 9,
 UT1A TN 35) may be compared with those
 obtained by Corten and Dolan for the same
 material Figure 8, Page 615 W.A.D.C.
 TR59-507

FIGURE 23

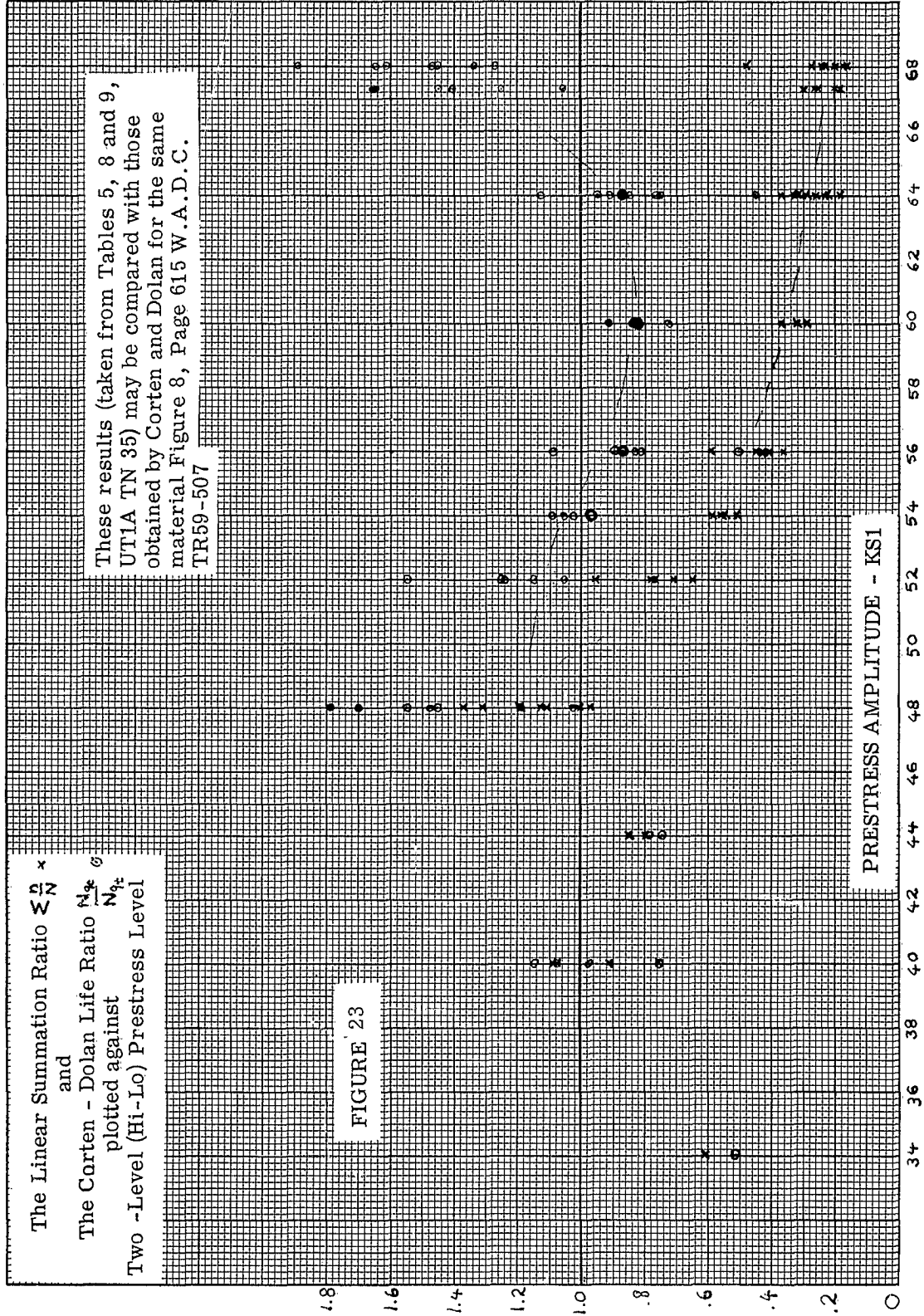
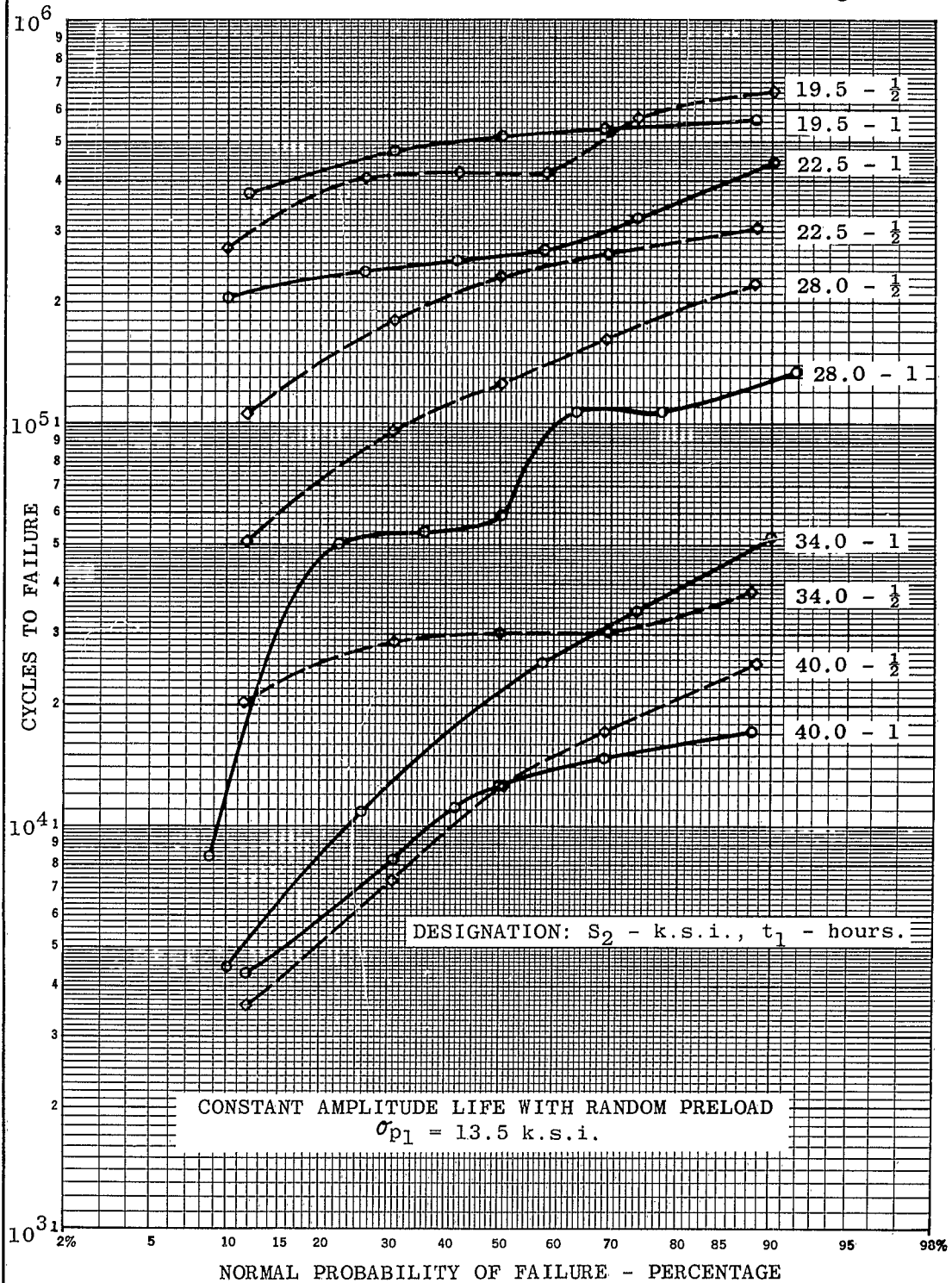


Fig. 24



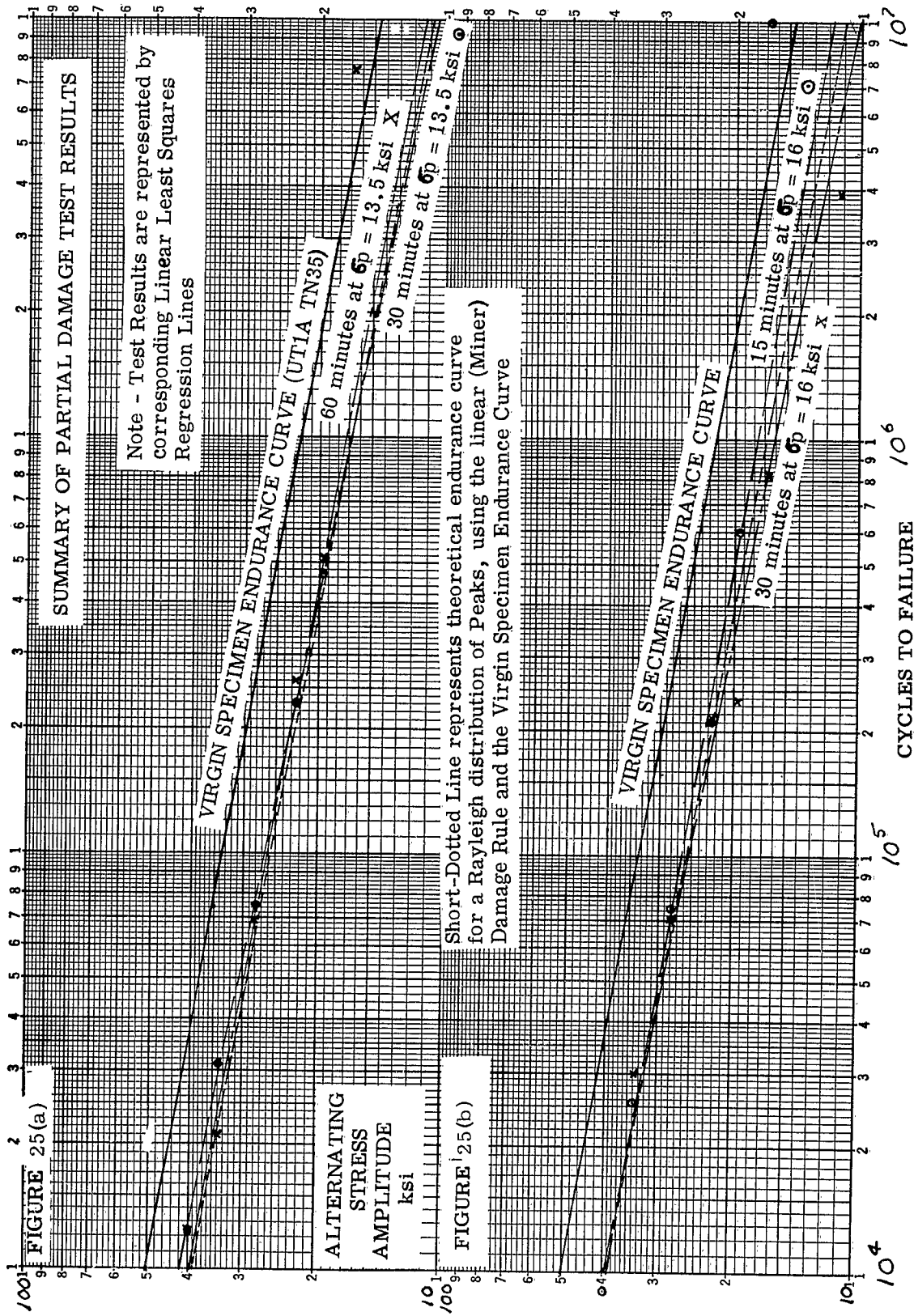




FIGURE 26

Crack Inspection of specimens preloaded with 30 minutes of Random Loads RMS Peaks = 16 ksi followed by Constant Amplitude testing to failure at 22.5 ksi (peak).

Note the absence of any secondary cracks with this test condition

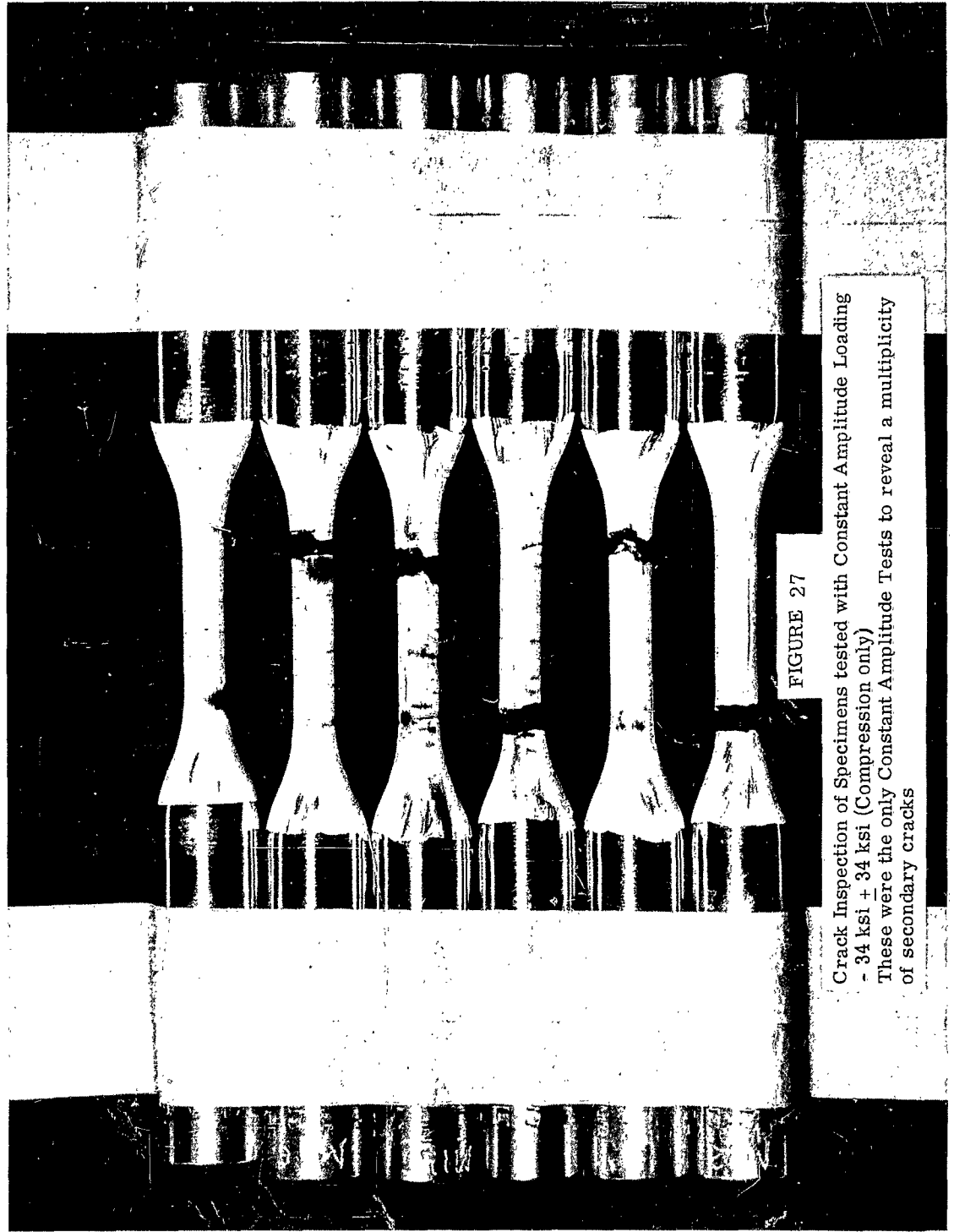
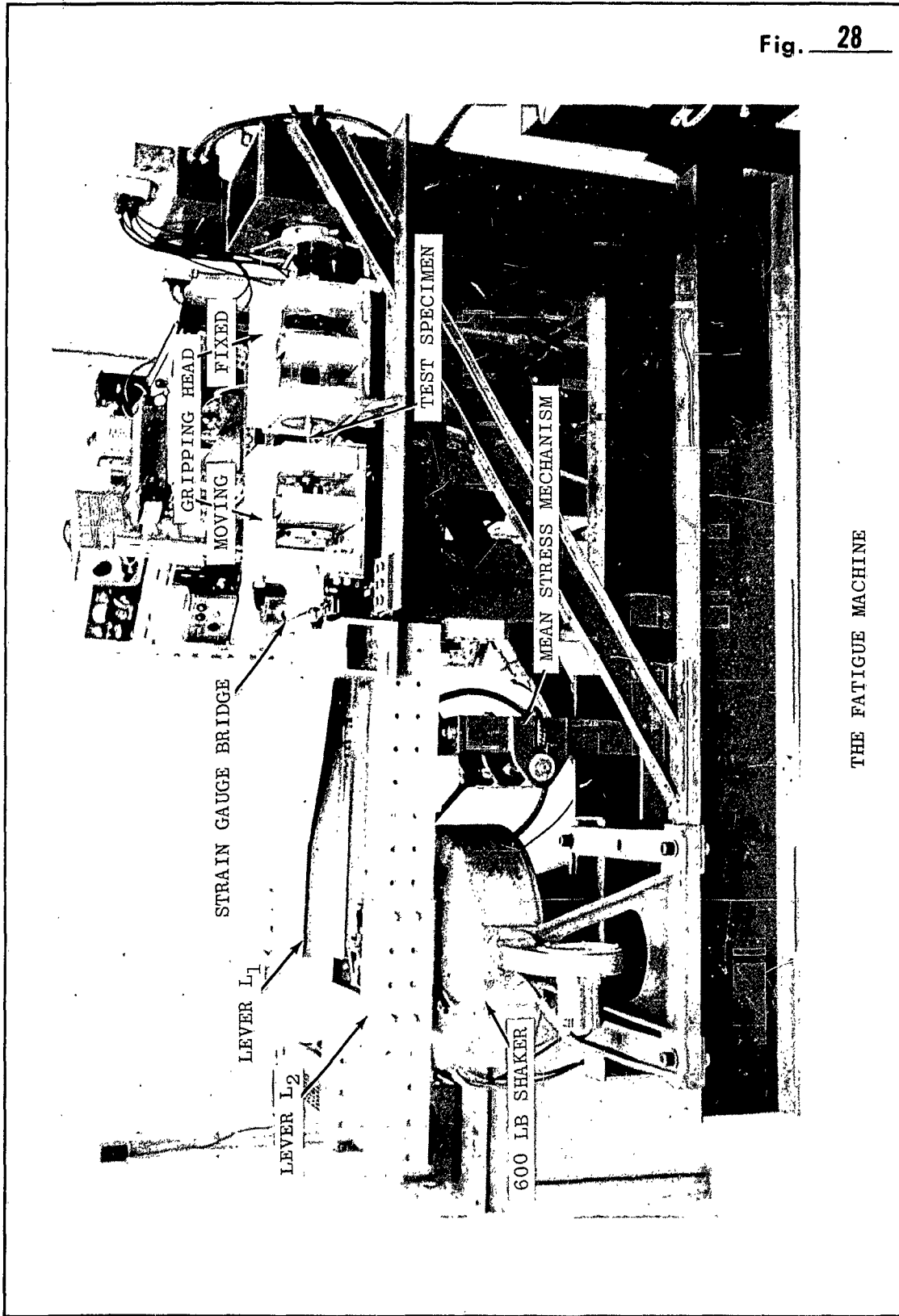
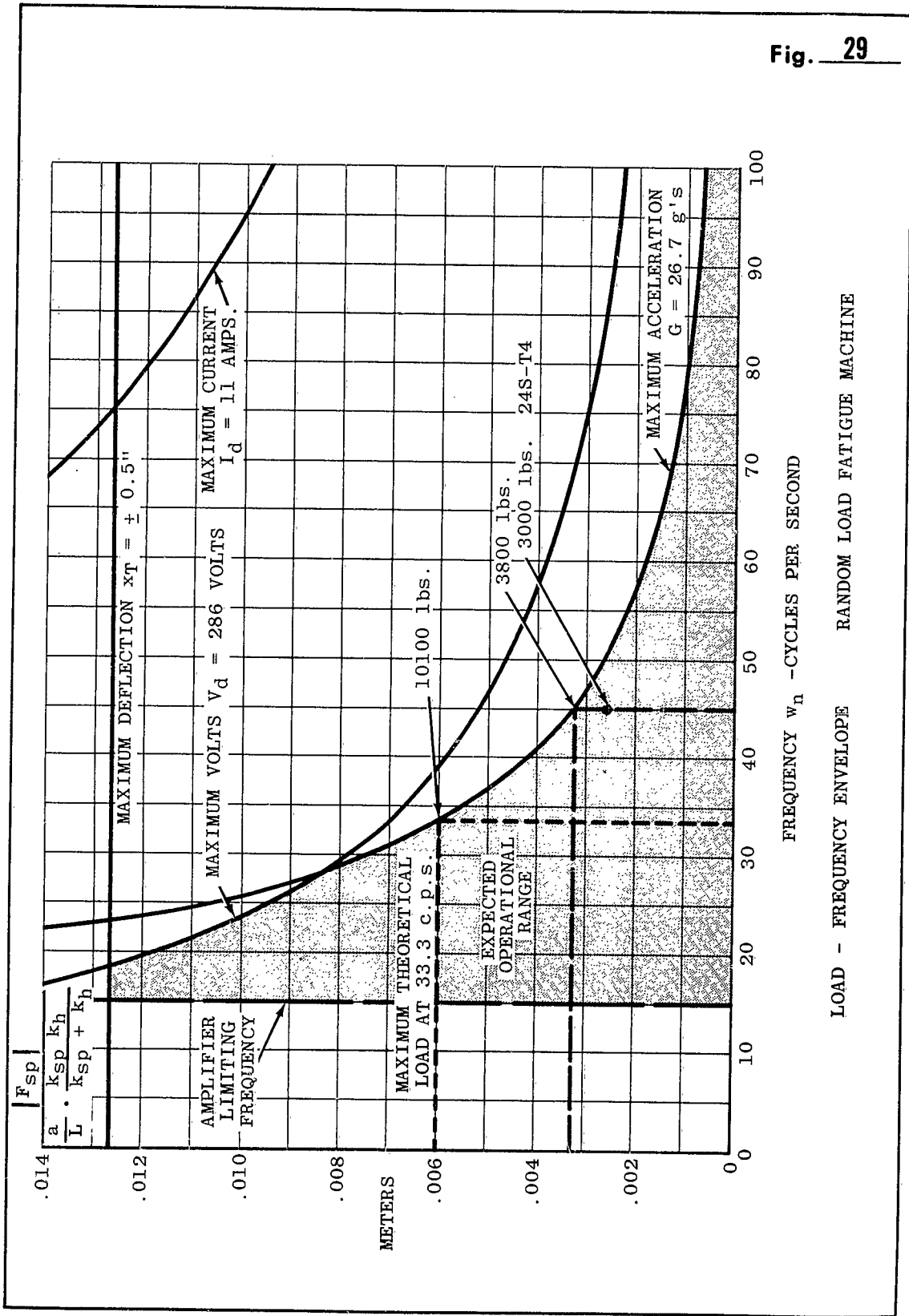


FIGURE 27

Crack Inspection of Specimens tested with Constant Amplitude Loading
- 34 ksi + 34 ksi (Compression only)
These were the only Constant Amplitude Tests to reveal a multiplicity
of secondary cracks



THE FATIGUE MACHINE



LOAD - FREQUENCY ENVELOPE RANDOM LOAD FATIGUE MACHINE

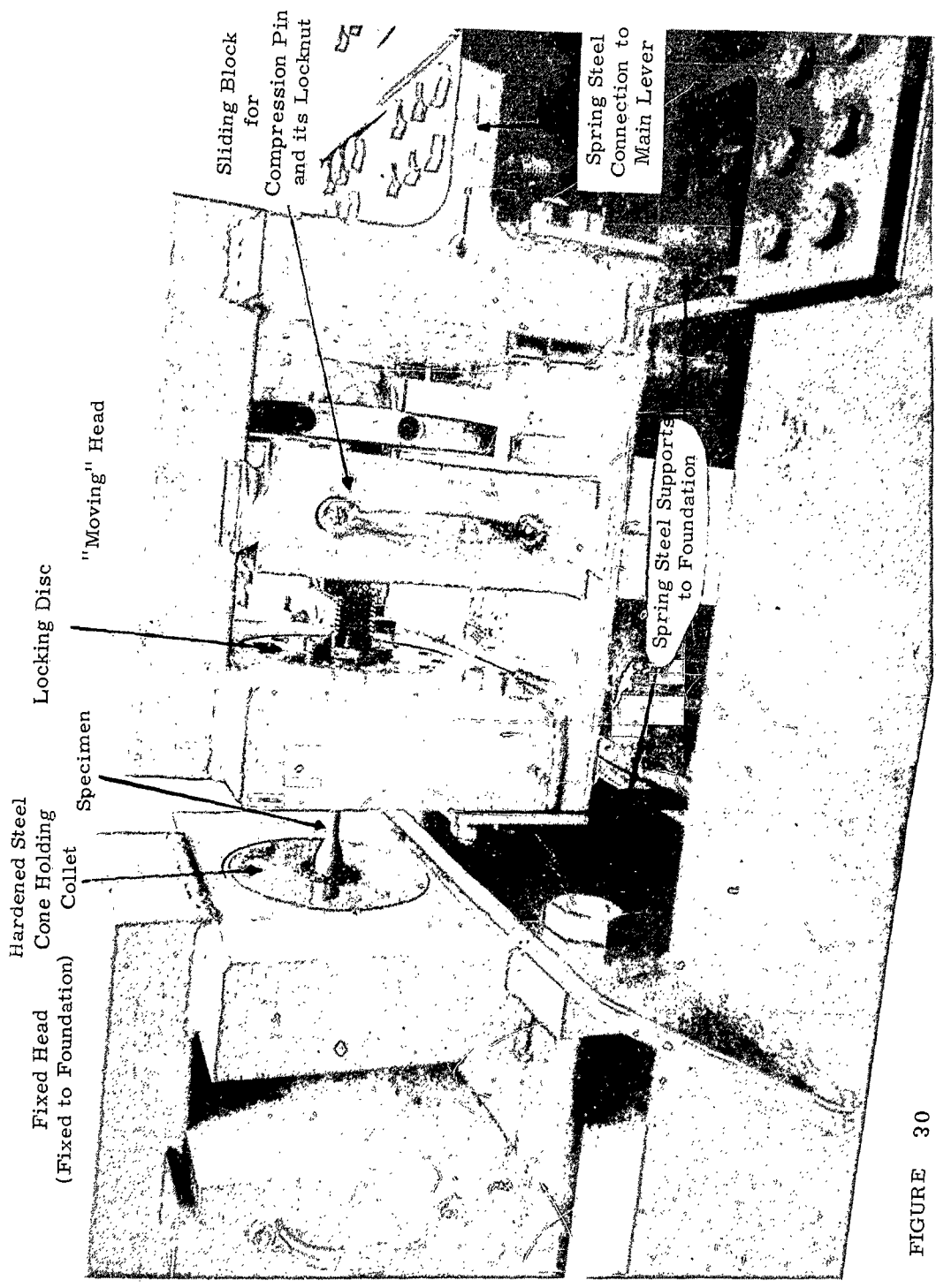
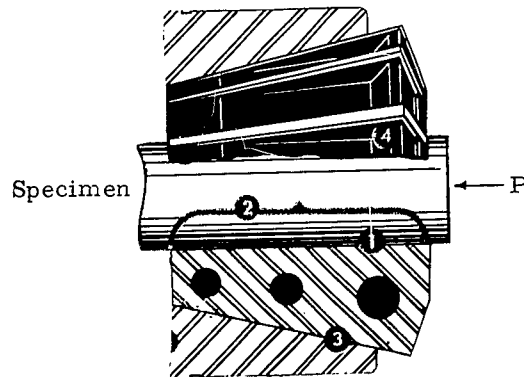
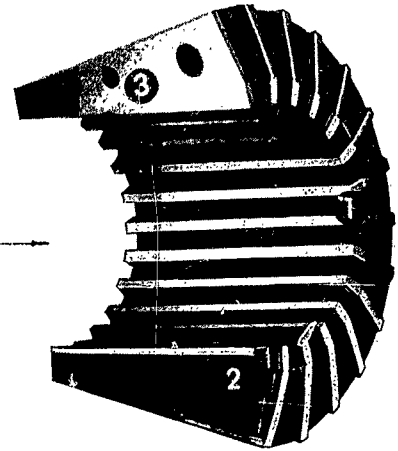


FIGURE 30

SPECIMEN GRIPPING ARRANGEMENT FOR THE UTIA FATIGUE MACHINE

SPECIMEN GRIPPING MECHANISM
 using RUBBER FLEX COLLETS
 with Hook-serrated edges

The standard rubber flex collet is made up of fully hardened alloy steel jaws separated by synthetic rubber, forming an integral mould.



The collet fits into a hardened steel cone and the specimen is positioned to leave about .10 inch clear to apply locking action by means of the compression pin.

The hook serrations shown below pull the collet into the cone when a force is applied by the compression pin.



A variety of collet sizes are commercially available allowing the gripping of specimens from 5/8" to 1 3/8" in diameter



The illustrations are taken from a brochure of The Jacobs Manufacturing Company West Hartford 10, Connecticut U.S. A.

FIGURE 31



UTIA REPORT NO. 84

Institute of Aerophysics, University of Toronto

An Investigation of the Fatigue of Aluminum Alloy Due to Random Loading

S. R. Swanson February, 1963 72 pages 8 tables 31 figures

- 1. Fatigue Life Prediction
 - 3. Random Load Fatigue Testing
 - I. Swanson, S. R.
2. Random Loading of Structures
II. UTIA Report No. 84

A statistical study of the axial-load fatigue behavior of unnotched specimens of 2024-T4 Aluminum alloy has been carried out using both constant amplitude and random amplitude testing. A study of the stress S-log-endurance N relation has revealed the discovery that this relation can be represented by two failure distributions, such that the 'knee' of the S-logN curve is a transition in endurance from the distribution predominant above, to the distribution predominant below this level. A shaker driven fatigue machine was developed employing either constant amplitude sinewave or random noise as the load source, and incorporating lever(s) to shape and magnify the loading at the specimen. Using constant levels of intensity to failure it was found that most cumulative damage rules are unconservative. By programming the intensity level of the signal obtained from random loads, endurance for loadings approximating true service conditions were studied. It was found that for all random load tests, a great number of visible secondary cracks occur on the specimens, which is not observed as a rule under constant amplitude loading.

Available copies of this report are limited. Return this card to UTIA, if you require a copy.



UTIA REPORT NO. 84

Institute of Aerophysics, University of Toronto

An Investigation of the Fatigue of Aluminum Alloy Due to Random Loading

S. R. Swanson February, 1963 72 pages 8 tables 31 figures

- 1. Fatigue Life Prediction
 - 3. Random Load Fatigue Testing
 - I. Swanson, S. R.
2. Random Loading of Structures
II. UTIA Report No. 84

A statistical study of the axial-load fatigue behavior of unnotched specimens of 2024-T4 Aluminum alloy has been carried out using both constant amplitude and random amplitude testing. A study of the stress S-log-endurance N relation has revealed the discovery that this relation can be represented by two failure distributions, such that the 'knee' of the S-logN curve is a transition in endurance from the distribution predominant above, to the distribution predominant below this level. A shaker driven fatigue machine was developed employing either constant amplitude sinewave or random noise as the load source, and incorporating lever(s) to shape and magnify the loading at the specimen. Using constant levels of intensity to failure it was found that most cumulative damage rules are unconservative. By programming the intensity level of the signal obtained from random loads, endurance for loadings approximating true service conditions were studied. It was found that for all random load tests, a great number of visible secondary cracks occur on the specimens, which is not observed as a rule under constant amplitude loading.

Available copies of this report are limited. Return this card to UTIA, if you require a copy.



UTIA REPORT NO. 84

Institute of Aerophysics, University of Toronto

An Investigation of the Fatigue of Aluminum Alloy Due to Random Loading

S. R. Swanson February, 1963 72 pages 8 tables 31 figures

- 1. Fatigue Life Prediction
 - 3. Random Load Fatigue Testing
 - I. Swanson, S. R.
2. Random Loading of Structures
II. UTIA Report No. 84

A statistical study of the axial-load fatigue behavior of unnotched specimens of 2024-T4 Aluminum alloy has been carried out using both constant amplitude and random amplitude testing. A study of the stress S-log-endurance N relation has revealed the discovery that this relation can be represented by two failure distributions, such that the 'knee' of the S-logN curve is a transition in endurance from the distribution predominant above, to the distribution predominant below this level. A shaker driven fatigue machine was developed employing either constant amplitude sinewave or random noise as the load source, and incorporating lever(s) to shape and magnify the loading at the specimen. Using constant levels of intensity to failure it was found that most cumulative damage rules are unconservative. By programming the intensity level of the signal obtained from random loads, endurance for loadings approximating true service conditions were studied. It was found that for all random load tests, a great number of visible secondary cracks occur on the specimens, which is not observed as a rule under constant amplitude loading.

Available copies of this report are limited. Return this card to UTIA, if you require a copy.



UTIA REPORT NO. 84

Institute of Aerophysics, University of Toronto

An Investigation of the Fatigue of Aluminum Alloy Due to Random Loading

S. R. Swanson February, 1963 72 pages 8 tables 31 figures

- 1. Fatigue Life Prediction
 - 3. Random Load Fatigue Testing
 - I. Swanson, S. R.
2. Random Loading of Structures
II. UTIA Report No. 84

A statistical study of the axial-load fatigue behavior of unnotched specimens of 2024-T4 Aluminum alloy has been carried out using both constant amplitude and random amplitude testing. A study of the stress S-log-endurance N relation has revealed the discovery that this relation can be represented by two failure distributions, such that the 'knee' of the S-logN curve is a transition in endurance from the distribution predominant above, to the distribution predominant below this level. A shaker driven fatigue machine was developed employing either constant amplitude sinewave or random noise as the load source, and incorporating lever(s) to shape and magnify the loading at the specimen. Using constant levels of intensity to failure it was found that most cumulative damage rules are unconservative. By programming the intensity level of the signal obtained from random loads, endurance for loadings approximating true service conditions were studied. It was found that for all random load tests, a great number of visible secondary cracks occur on the specimens, which is not observed as a rule under constant amplitude loading.

Available copies of this report are limited. Return this card to UTIA, if you require a copy.